# Downward continuation of Geopotential in Switzerland

Vom Fachbereich Bauingenieurwesen und Geodäsie
der Technischen Universität Darmstadt
zur Erlangung des akademischen Grades eines
Doktor-Ingenieurs (Dr.-Ing.) genehmigte Dissertation

von

**Dipl.-Ing. Perparim Ameti**
**aus**
**Smira**

| | |
|---|---|
| Referent: | Prof. Dr.-Ing. Erwin Groten |
| Korreferent: | Prof. Dr.-Ing. Matthias Becker |
| Korreferent: | Prof. Dr. Zdenek Martinec |
| Tag der Einreichung: | 14.01.2005 |
| Tag der mündlichen Prüfung: | 30.06.2005 |

**Darmstadt im März, 2006**
**D 17**

# Abstract

The main objective of this thesis is the downward continuation of the Geopotential in Switzerland. The downward continuation of the airborne gravity data in Switzerland is a challenging task, due to the well known mountainous topography (Alps). Another interesting factor for the analysis of the downward continuation process is the measurement height (Flight-line altitude), which is about 5000m above sea level. Taking into account these factors, it is convenient to study the downward continuation process using different computation methods as well as different techniques that take into account the topography.

The Principal method proposed in this thesis for the downward continuation of Geopotential in Switzerland is the combination of the Sequential Multipole Analysis (SMA) and Least Square Collocation (LSC) with regularization in the Bjerhammar-Krarup model. This method is then compared with the inverse Poisson's integral method. To improve the stability of the downward continuation process, a number of land (19 GPS/leveling points) data is included in the calculation. The final results from both methods are stored as geoid undulations and are compared with the actual geoid of Switzerland CHGeo98. Since the topography of Switzerland is rough in the south and relative smooth in the north, I propose to use different terrain correction techniques, the second Helmert's condensation technique and the Residual Terrain Model (RTM) technique.

# Zusammenfassung

Die Doktorarbeit untersucht die Möglichkeiten, das Potentials der Erde durch Fortsetzung nach unten zu bestimmen. Als Ausgangsdaten werden Schwerewerte, die durch Fluggravimetrie über der Schweiz beobachtet wurden, benutzt.
Die Bearbeitung der Ergebnisse von Fluggravimetrierungen über alpinen Gegenden stellt wegen der großen Flughöhe und der sehr rauen Topographie sehr hohe Anforderungen an die verwendeten Methoden. Daher werden in der vorliegenden Dissertation verschiedene Techniken benutzt, um den Einfluss der Topographie zu ermitteln.

Die prinzipielle Methode basiert hierbei auf der Kombination einer sequentiellen Multipolanalyse (SMA) und einer kleinsten Quadrate Kollokation (LSC) mit Regularisierung im Bjerhammar-Karup Modell. Diese Methode wird mit der inversen Poisson Integral Methode verglichen. Zur Verbesserung der Lösung der Fortsetzung nach unten werden terrestrisch beobachtete daten (19 GPS/leveling punkte) in der Berechnung eingeführt . Die berechneten Geoidundulationen beider Methoden werden mit dem aktuellen Geoid der Schweiz CHGeo98 verglichen. Da die Topographie der Schweiz im Norden sehr flach, im Süden jedoch sehr rau ist, werden in der Arbeit zwei verschiedene Techniken angewandt, die den topographischen Effekt berücksichtigen; die 2. Helmert Kondensation und die Residual Terrain Model (RTM) Technik.

# Contents

# List of Figures

# List of Tables

# Acknowledgements

This thesis is realized through cooperation between Institute of Physical Geodesy, Darmstadt University of Technology and GeoForschungsZentrum Potsdam. I use opportunity to thank many people who help me to finish this work. Firstly, I want to thank my supervisor, Prof. Dr. Erwin Groten for his help and very patient supervision of my work during all the time. I want to thank Prof. Dr. Mathias Becker from Institute of Physical Geodesy in Darmstadt and Prof. Dr. Zdenek Martinec from GeoForschungsZentrum Potsdam for co-supervision and for their comments and suggestions about this thesis. I also would like to thank very much Dr. Stefan Leinen from Institute of Physical Geodesy in Darmstadt and my research supervisor in Potsdam, Dr. Peter Schwintzer (In Memoriam). He supported and advised me during my four years while I worked in Potsdam and I dedicated him this thesis with great kindliness.

# 1 Introduction

The knowledge of the gravity field of the Earth is an essential item in many disciplines, such as Geodesy, Geology, Geo-Environment etc. Recent achievements in satellite geodesy, especially the CHAMP and GOCE missions, enable the observation of the Earth and its gravity field from space (long-wave components of the gravity field). To study the short-wave components of the gravity field, an approach is needed, which yields an accuracy of about ±1mGal to ±2 mGal within a resolution between 5-10km. Nowadays, this can be achieved using airborne gravity survey. According to Jekeli and Kwon (1999), *"Airborne gravimetry is a proven operation to determine the Earth's gravity field for geophysical applications over remote area"*. Particularly, with the development of the Global Positioning System (GPS) and Inertial Navigation Systems (INS) technology, airborne gravimetry has become a favorite method in the study of regional and local gravity field of the Earth. Application of GPS in airborne gravity surveys allow the determination of the position and velocity of a moving body, as well as the acceleration, by differentiating the position or velocity with respect to time within cm accuracy.

The general objective of this study is the determination of the regional gravity field by means of scalar airborne gravity survey. The scalar gravimetry requires a device that determines the sum of the gravimetric and kinematic accelerations occurring to the airborne platform and a device that determines the vertical acceleration separately. The main objective of this thesis is the downward continuation of the Geopotential in Switzerland. As can be expected, the downward continuation of the airborne gravity data in Switzerland is a challenging task, reason by well known topography (Alps). Another interesting factor for the analysis of the downward continuation process is the measurement height (flight-line altitude), which is about 5000m above sea level. Taking into account these factors, it is convenient to study the downward continuation process using different computation methods as well as different techniques that take into account the topographical impact.

The principal method proposed in this thesis for the downward continuation of Geopotential in Switzerland is the combination of the Sequential Multipole Analysis (SMA) and Least-Squares Collocation (LSC) with regularization in the Bjerhammar-Krarup model. This method is then compared with the inverse Poisson integral method. To improve the stability of the downward continuation process, a number of land data is included in the calculation.

Finally results from both methods are stored as geoid undulations and are compared with the actual geoid of Switzerland CHGeo98. Since the topography of Switzerland is rugged in the south and relative smooth in the north, I propose to use different terrain correction techniques, the second Helmert's condensation technique and the Residual Terrain Model (RTM) technique.

The content of this thesis is divided into nine chapters. The first chapter is the introduction. The second chapter describes the theoretical background of the gravity field of the Earth.

In the third chapter the gravimetric geoid determination is treated, together with the theory of geodetic boundary value problems and airborne geodetic value problems. The definition of the geodetic boundary value problem combining airborne and land gravity data has been also explained in this chapter. The reason for this is that the number of land gravity data is used in the computation of the downward continuation.

Chapter four explains the remove-restore technique for geoid determination using airborne gravity data, as well as the principle of airborne gravimetry. More precisely it comprises the gravity reductions (topographic masses, geopotential model contribution), which are included in the processing of the measured gravity values. A detailed explanation is given to two terrain correction techniques that are used for the gravity data reduction. These are the second Helmert's condensation and the Residual Terrain Model (RTM) method. Both methods are analyzed with the data from the DTM of Aguascalientes-Zacatecas (Mexico) area. The aim of this chapter is to discuss the efficiency of RTM method. This method is based on the definition of the terrain correction in a predefined elevation surface, called *Mean Elevation Surface (MES).* The results presented in this chapter document the efficiency of this method, especially in mountain areas, where the *Mean Elevation Surface (MES)* is defined by filtering of terrain elevations with a resolution of global spherical harmonic potential expansion.

The core of this study has been formulated in the fifth chapter. This is the downward continuation of airborne gravity data and its application to gravity field and geoid analysis. The chapter begins with requirements for the formulation of the problem, which is to find out the best and stable solution for the downward continuation of Geopotential in Switzerland. The solution of the problem which can fulfill the above mentioned requirements for the downward continuation of Geopotential in Switzerland is proposed to be the combination of the Sequential Multipole Analysis (approximation of disturbing potential by potentials of radial multipoles) and least-squares collocation with regularization.

The sixth chapter contains the analysis of the data that has been used to test the proposed method for the downward continuation problem, as well as the comparison of the results with

a standard method for the downward continuation, which is the Inverse Poisson integral method. The main challenge in downward continuation is how to handle topographical effects. The proposed methods for the gravity data reduction, the second Helmert's condensation and RTM method are implemented in the computation procedure. It has been found that the method has both advantages and disadvantages depending on the topography of the area. These terrain correction techniques are first implemented in the combined method of Sequential Multipole Analysis and least-squares collocation (Bjerhammar-Krarup model) and in the iteration solution of the Poisson integral.

The seventh chapter consists of the conclusions and recommendations. Chapter eight consists of the references. A graphical overview of results is presented by annexes in the ninth chapter.

The reduction of airborne gravity data, using Eötvös corrections and the associated separation of vertical aircraft accelerations from gravity variations is not being treated in this study. Moreover, the problems inherent in applying statistical and stochastic techniques, such as LSC method to downward continuation procedure are not discussed in detail here.

Due to the well known topographic structures in Switzerland, neither homogeneity nor "wide-sense stationarity" are guaranteed. Both effects, together with topographic anisotropies may cause errors, which are ignored in this investigation.

Anomalous edge-effects within the flight profiles have been eliminated by simple cut-off technique. Whether or not such procedures led to significant data improvement, has not been tested. The above mentioned cut-off procedure at the end of the flight profiles reduces or eliminates the effects of the distant topography. Otherwise, the improved stability obtained by including surface data and incorporating them in the downward continuation process has not particularly been tested concerning its significance.

In the title of this thesis we speak downward continuation of the geopotential, where we are fully aware of the fact that there are basically two possibilities and it depends on technical conveniences whether gravity anomalies or disturbances are first converted into disturbing potential and then continued analytically down or anomalies in the space are continued down and then converted into potential. From the theoretical point of view, the continuation of the potentials is preferred. In order to facilitate the understanding and comprehension of the thesis, the basic concepts of the various methods applied to airborne data handling are briefly outlined. Numerous references should, in addition, give access to the results of this study even for those who are not familiar with analytical continuation techniques. This is basically an application-oriented investigation focusing on analytical continuation of harmonic functions and reduction of topographic effects for stabilization purposes.

# 2 The Gravity Field of the Earth

## 2.1 Gravity and Gravity Potential

The gravity field of the Earth consists of two parts, the principal one caused by attraction according to Newton's law, the second one caused by the Earth's rotation. The total force, which is the resultant of gravitational force and centrifugal force, is called *gravity* (Heiskanen and Moritz, 1967). These definitions can be formulated in the Earth-fixed rectangular coordinate system as follows:

$$W_P(X,Y,Z) = V_P(X,Y,Z) + \Phi_P(X,Y,Z), \tag{2.1}$$

where $V_P$ is the gravitational potential defined by

$$V_P = G\iiint_{Earth} \frac{dM}{l}, \tag{2.2}$$

where $dM$ is the mass element, $l$ is the distance between the computation point and the moving point, G is the Newtonian gravitational constant: G = 6.672x10$^{-11}$m$^3$s$^{-2}$kg$^{-1}$.
$\Phi_P$ is the potential of the centrifugal force given by (Heiskanen and Moritz, 1967):

$$\Phi_P = \frac{1}{2}\omega^2\left(X_P^2 + Y_P^2\right), \tag{2.3}$$

where polar motion is neglected, $\omega$ is the mean angular velocity of the Earth's rotation. $X_P$ and $Y_P$ are the geocentric coordinates of a given point $P$ in the chosen reference frame (See Figure 2.1):

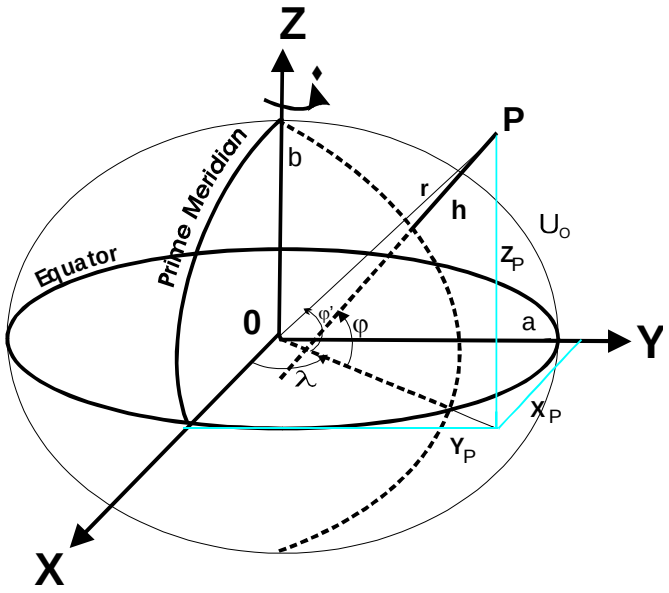


Figure 2.1 Ellipsoidal and geocentric coordinates

The gravitational potential $V_P$ function is expressed by spherical harmonic expansion in the following way (NIMA Report, 2000):

$$V_P = \frac{GM}{r}\left[1+\sum_{n=2}^{n_{max}}\sum_{m=0}^{n}\left(\frac{a}{r}\right)^n \overline{P}_{nm}(\sin\ \varphi')\cdot\left(\overline{C}_{nm}\cos\ m\lambda + \overline{S}_{nm}\sin\ m\lambda\right)\right], \qquad (2.4)$$

where:

| | |
|---|---|
| $V_P$ | - Gravitational potential (m²/s²) at $P(r,\varphi',\lambda)$ |
| GM | - Earth's gravitational constant |
| r | - Distance from the Earth's center of mass |
| a | - Major semi-axis of the reference ellipsoid |
| n, m | - Degree and order, respectively |
| φ' | - Geocentric latitude |
| λ | - Geocentric longitude=geodetic longitude |
| $\overline{C}_{nm,}\ ,\overline{S}_{nm}$ | - Normalized gravitational coefficients |

$\overline{P}_{nm}(\sin\varphi')$ - Normalized associated Legendre function

$$= \left[\frac{(n-m)!(2n+1)k}{(n+m)!}\right]^{1/2} P_{nm}(\sin\varphi')$$

$P_{nm}(\sin\varphi')$ - Associated Legendre function

$$= (\cos\varphi')^m \frac{d^m}{d(\sin\varphi')^m}\left[P_n(\sin\varphi')\right]$$

$P_n(\sin\varphi')$ - Legendre polynomial

$$= \frac{1}{2^n n!}\frac{d^n}{d(\sin\varphi')^n}(\sin^2\varphi'-1)^n$$

$$\left|\begin{matrix}\overline{C}_{nm}\\ \overline{S}_{nm}\end{matrix}\right| = \left[\frac{(n+m)!}{(n-m)!(2n+1)k}\right]^{1/2}\left|\begin{matrix}C_{nm}\\ S_{nm}\end{matrix}\right|$$

$C_{nm}\ , S_{nm}$ - Spherical harmonic coefficients

For m = 0, k = 1
m ≠ 0, k=2

The gradient of *W*, produces the gravity vector $\overline{g}$ ;

$$\bar{g} = grad\ W = \begin{bmatrix} W_X \\ W_Y \\ W_Z \end{bmatrix}, \tag{2.5}$$

The components of this vector are:

$$\left.\begin{aligned} g_x &= \frac{\partial W}{\partial x} = \frac{\partial V}{\partial x} + \frac{\partial \Phi}{\partial x} = \frac{\partial V}{\partial x} + \omega^2 x \\ g_y &= \frac{\partial W}{\partial y} = \frac{\partial V}{\partial y} + \frac{\partial \Phi}{\partial y} = \frac{\partial V}{\partial y} + \omega^2 y \\ g_z &= \frac{\partial W}{\partial z} = \frac{\partial V}{\partial z} + \frac{\partial \Phi}{\partial z} = \frac{\partial V}{\partial z} + 0 \end{aligned}\right\} \tag{2.6}$$

The magnitude of the gravity vector $\bar{g}$ is the gravity *g*.

$$g = \sqrt{g_x^2 + g_y^2 + g_z^2} = \|\bar{g}\|, \tag{2.7}$$

The direction of the gravity vector $\bar{g}$ is the direction of the *plumb line,* or the *vertical.*
The surfaces with the constant potential (*W=Constant)* are called equipotential surfaces. They are everywhere normal to the gravity vector. The surface

$$W(X,Y,Z) = W_0 = Const., \tag{2.8}$$

which approximately coincides with the surface of the oceans is called the *geoid* (Heiskanen and Moritz, 1967).

## 2.2 Normal and anomalous gravity field

Determination of the normal gravity field is closely related to the definition of the reference ellipsoid. A reference ellipsoid is an ellipsoid of revolution with its centre at the geocentre and with its masses equal to the masses of the Earth. One of the most useful reference ellipsoids today is the GRS80 ellipsoid (Geodetic Reference system 1980), which is defined by the following parameters (Moritz, 1992):

| | |
|---|---|
| Major semi-axis | a=6378137.0 m |
| Reciprocal of Flattening | 1/f=298.2572221 |
| Angular Velocity of the Earth | $\omega=7292115 \times 10^{-11}$ rad/s |
| Earth's Gravitational Constant | $GM=3986005 \times 10^{8}$ m³/s² |

With these four parameters it is possible to compute the normal potential U and normal gravity γ on or outside of the surface of the reference ellipsoid (see Figure2.1).
According to Moritz (1980), the gravitational potential $V_{ell}$ of an equipotential ellipsoid of revolution can be developed in a series of zonal spherical harmonics of even degrees (Moritz, 1980):

$$V_{ell} = \frac{GM}{r}\left(1 - \sum_{n=1}^{\infty} J_{2n}\left(\frac{a}{r}\right)^{2n} P_{2n}(\sin\varphi)\right), \tag{2.9}$$

where $P_{2n}(\sin\varphi)$ is unnormalized Legendre polynomial of degree 2n:

$$P_{2n}(\sin\varphi) = \frac{\bar{P}_{2n}(\sin\varphi)}{\sqrt{2n+1}}, \tag{2.10}$$

and $J_{2n}$ are ordinary, i.e. unnormalized, zonal harmonic coefficients

$$J_{2n} = -\sqrt{2n+1}\cdot\bar{C}_{2n,0}. \tag{2.11}$$

Taking into account (2.10) and (2.11) we can write:

$$V_{ell} = \frac{GM}{r}\left(1 + \sum_{n=1}^{\infty} \bar{C}_{2n,0}\left(\frac{a}{r}\right)^{2n} \bar{P}_{2n}(\sin\varphi)\right). \tag{2.12}$$

The coefficients in series (2.9) may be expressed in terms of the coefficient $J_2$ and first eccentricity *e* of the ellipsoid (Moritz, 1980):

$$J_{2n} = (-1)^{n+1}\frac{3e^{2(n-1)}}{(2n+1)(2n+3)}(e^2 - ne^2 + 5nJ_2). \tag{2.13}$$

By entering (2.11) into (2.13) we get

$$\bar{C}_{2n,0} = (-1)^{n}\frac{3e^{2(n-1)}}{(2n+1)^{3/2}(2n+3)}(e^2 - ne^2 - 5\sqrt{5}n\bar{C}_{2,0}). \tag{2.14}$$

The first eccentricity *e* of the reference or level ellipsoid is connected with four defining parameters *a*, *GM*, $J_2$ and $\omega$ by the relationship (Moritz, 1980):

$$e^2 = 3J_2 + \frac{4}{15}\frac{\omega^2 a^3}{GM}\frac{e^3}{2q_0} \ . \tag{2.15}$$

The value $J_2$ is sometimes called the dynamic constant and for the reference ellipsoid, can be expressed by (Moritz, 1980)

$$J_2 = \frac{1}{3}e^2\left(1 - \frac{2me'}{15q_0}\right), \tag{2.16}$$

and constants $e'$ , $m$ and $q_0$ are expressed below. Taking into account (2.10), we can write it as;

$$e^2 = -3\sqrt{5}\bar{C}_{2,0} + \frac{4}{15}\frac{\omega^2 a^3}{GM}\frac{e^3}{2q_0} \ . \tag{2.17}$$

In the expressions (2.15), (2.17) yield to:

$$2q_0 = \left(1 + \frac{3}{e'^2}\right)\arctan e' - \frac{3}{e'} \ , \tag{2.18}$$

where $e'$ is second eccentricity of the ellipsoid

$$e' = \frac{e}{\sqrt{1-e^2}} \ . \tag{2.19}$$

The normal gravity potential at the surface of the reference ellipsoid, being constant for a level ellipsoid, is given by (Moritz, 1980):

$$U_0 = \frac{GM}{\varepsilon}\arctan e' + \frac{1}{3}\omega^2 a^2 , \tag{2.20}$$

where $\varepsilon$ is linear eccentricity of the ellipsoid

$$\varepsilon = \sqrt{a^2 - b^2} \ , \tag{2.21}$$

and $b$ is its minor semi-axis

$$b = a\sqrt{1-e^2} \ . \tag{2.22}$$

The normal potential of the reference ellipsoid (GRS80) is $U_0=6263686.085 m^2 s^{-2}$ (Moritz, 1992). Otherwise the normal gravity γ, can be calculated at the surface of the ellipsoid by the closed formula of Somigliana (Heiskanen and Moritz, 1967):

$$\gamma = \gamma_e \frac{1 + k \ \sin^2 \varphi}{\sqrt{1 - e^2 \ \sin^2 \varphi}} \ , \tag{2.23}$$

where: $k = \frac{b\gamma_P}{a\gamma_e} - 1$, $\gamma_e = \frac{kM}{ab}\left(1 - \frac{3}{2}m - \frac{3}{14}e'^2 \ m\right)$ and $\gamma_p = \frac{kM}{a^2}\left(1 + m - \frac{3}{7}e'^2 \ m\right)$

a, b - Major and minor semi-axes of the ellipsoid, respectively

$\gamma_e, \gamma_p$ - Normal gravity at the equator and poles, respectively

$e^2$ - Square of the first ellipsoidal eccentricity

$\varphi$ - Geodetic latitude

For the calculation of the normal gravity at the points outside the reference ellipsoid, the Taylor series expansion can be used for the upward continuation of the normal gravity from the surface of the reference ellipsoid to the point outside it (NIMA Report, 2000). The normal gravity at height *h* is:

$$\gamma_h = \gamma + \frac{\partial \gamma}{\partial h} h + \frac{1}{2} \frac{\partial^2 \gamma}{\partial h^2} h^2 , \tag{2.24}$$

A frequently used Taylor series expansion for normal gravity above the ellipsoid with a positive direction downward along the geodetic normal to the reference ellipsoid is:

$$\gamma_h = \gamma \left[ 1 - \frac{2}{a}\left(1 + f + m - 2f \ \sin^2 \varphi\right) h + \frac{3}{a^2} h^2 \right], \tag{2.25}$$

Where; $m = \frac{\omega^2 a^2 b}{GM}$ , (for more details see Heiskanen and Moritz, 1967).

### 2.2.1 Disturbing potential

The difference between the actual gravity potential $W$ and the normal gravity potential $U$ at the point $P$ is sometimes called anomalous potential, or in general, disturbing potential $T$ (see Figure 2.2).

$$T(P) = W(P) - U(P)\,, \tag{2.26}$$

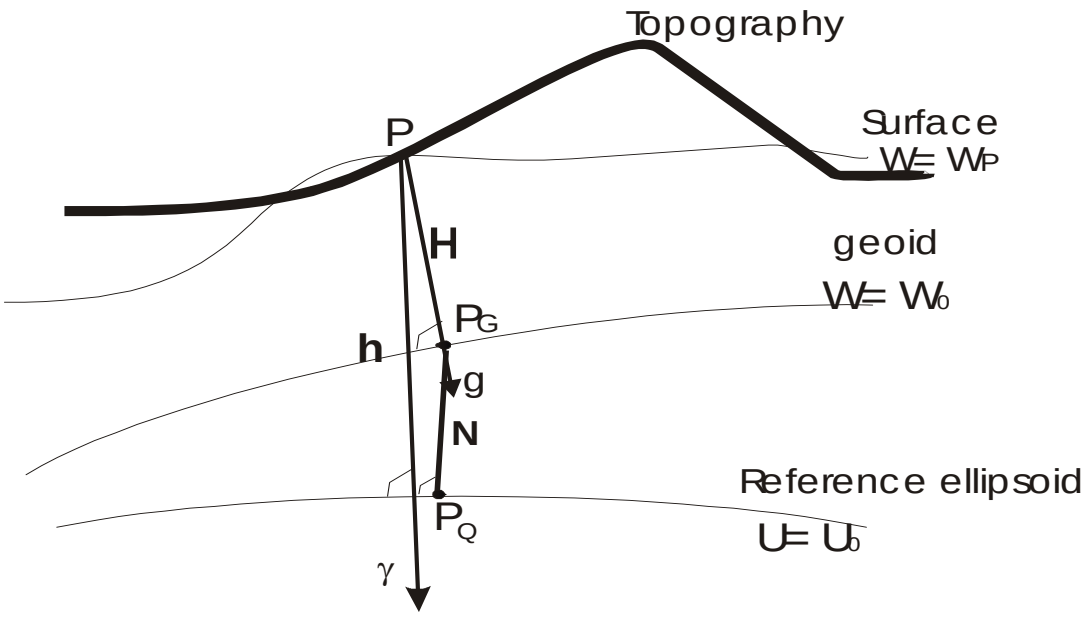


Figure 2.2 Geoid height and height anomalies

### 2.2.2 Gravity disturbances

The gravity disturbance vector is defined as the difference between the actual gravity and normal gravity vector, evaluated at the same location. For the gravity disturbance vector in P with respect to a particular frame we can write:

$$\delta\bar{g} = \bar{g}_P - \bar{\gamma}_P = \begin{pmatrix} g_1 - \gamma_1 \\ g_2 - \gamma_2 \\ g_3 - \gamma_3 \end{pmatrix}, \tag{2.27}$$

where the sub-indices 1, 2 and 3 stand for the respective components in an arbitrary frame. The scalar field of gravity disturbances can be expressed by defining the magnitude of the gravity disturbance vector in the following form:

$$\delta g = \left|\bar{g}_P\right| - \left|\bar{\gamma}_P\right|, \tag{2.28}$$

The relationship between disturbing potential $T$ and gravity disturbances reads:

$$\delta g \cong -\frac{\partial T}{\partial n}, \tag{2.29}$$

where $n$ denotes the ellipsoidal normal direction, or in spherical approximation it reads:

$$\delta g = -\frac{\partial T}{\partial r}. \tag{2.30}$$

### 2.2.3 Gravity anomalies

The gravity anomaly is defined as the difference between the gravity on a geoid and the normal gravity on the reference ellipsoid (see Figure 2.2):

$$\Delta g = g_P - \gamma_Q, \tag{2.31}$$

Equation (2.31) represents the difference of the values in the magnitude between the gravity on the geoid and the normal gravity on the ellipsoid. Otherwise, the difference between their directions is called deflection of the vertical. The deflection of the vertical has two components, a north-south component $\xi$ and an east-west component $\eta$.

$$\xi = \Phi - \varphi, \quad \eta = (\Lambda - \lambda)\cos\varphi, \tag{2.32}$$

where:

$\Phi, \Lambda$ = Astronomical coordinates (plumb line)

$\varphi, \lambda$ = Geodetic coordinates

### 2.2.4 Geoid undulation

The distance between the point $P_G$ on geoid and projected point $P_Q$ on ellipsoid through the normal (vector $\gamma$) is called geoid undulation $N$ (see Figure 2.2). The geoid undulation $N$ is related to the disturbing potential $T$ by Bruns' formula (Heiskanen and Moritz, 1967);

$$N = \frac{T_{(geoid)}}{\gamma_{(Ell)}}, \tag{2.33}$$

And similarly , for the height anomalies $\zeta$ at point $P$:

$$\zeta \doteq \frac{T_P}{\gamma_{Tell}}, \tag{2.34}$$

where $\gamma_{Tell}$ is normal gravity at telluroid. Telluroid is the surface whose normal potential $U$ at every point $Q$ is equal to the actual potential $W$ at the corresponding point $P$, so that $U_Q = W_P$, corresponding points $P$ and $Q$ being situated on the same ellipsoidal normal (see Figure 3.2). The relationship between disturbing potential $T$ and gravity anomaly $\Delta g$ results in (Moritz, 1980):

$$\Delta g = -\frac{\partial T}{\partial h} + \frac{1}{\gamma}\frac{\partial \gamma}{\partial h} T\,. \tag{2.35}$$

This formula is sometimes called the *fundamental equation of physical geodesy*. It is, however, a boundary value for the geodetic boundary value problem. In spherical approximation, this formula can be written in the following form:

$$\Delta g = -\frac{\partial T}{\partial r} - \frac{2}{R} T\,, \tag{2.36}$$

where $R$ is the mean radius of the Earth. The meaning of the spherical approximation should be properly understood. It does not mean that a sphere in geometrical sense replaces the reference ellipsoid, so that a sphere, instead of an ellipsoid, would be used as a reference surface for the geoid (Moritz, 1980). It only means that the errors of the order of the flattening (~1/300) are neglected.

# 3 Gravimetric geoid determination

## 3.1 Introduction

Geoid determination is one of the major tasks of geodesy. Currently this is gaining even more importance due to the development of Global Navigation Satellite Systems (GNSS), like the GPS. These systems offer three-dimensional positioning all over the world. However, GPS offer ellipsoidal heights, which are geometric heights, instead of orthometric heights, which have physical meanings. According to Bruns' Theorem, orthometric heights can be calculated from the potential difference of the reference equipotential surface (the geoid) and the actual point, while the potential difference can be determined with the combination of spirit leveling and gravity measurements. In order to convert the ellipsoid height into a more useful orthometric height we need to know the geoid undulation at the station (see Figure 2.2). The geoid itself can be calculated using different types of input data. The simplest method is to use GPS/Leveling points, where both the ellipsoidal and leveling heights are given. From these data the geoid height can be calculated with a simple subtraction. Unfortunately this solution cannot provide a high-resolution geoid, due to the sparse distribution of the GPS/Leveling points in particular in areas difficult to access. The solution should be sought through gravimetric methods, which include the physical information of the gravity field of the Earth. One way to compute a local geoid is by the establishment and densification of gravimetric networks (e.g. by airborne gravimetry) over a particular area. These networks aim to provide information about the gravity field with high frequency, from which the geoid can be determined with the desired high resolution. One of the biggest achievements in the last decade is the use of the global geopotential models (e.g. EGM96, see Lemoine et al., 1998), which provide us with the information about long wavelength components when using the remove-restore technique for geoid determination. The relationship between geoid heights (undulation) and reference ellipsoid heights (or GPS derived heights) can be written in the following form (see Figure 2.2):

$$H=h-N \tag{3.1}$$

where H is the orthometric height of the actual point, h is the ellipsoid height (which is usually determined directly by using GPS). The gravimetric solution of the geoid is based on gravity data conducted or referred to the geoid, and the solution to the geodetic boundary-value problem can be represented by Stokes' integral formula (Heiskanen and Moritz, 1967), whenever $W_0$ at the geoid is equal $U_0$ at the ellipsoid, see Eq. (2.8) and (2.20):

$$N = \frac{R}{4\pi\gamma}\iint_{\sigma}\Delta g \cdot S(\psi)d\sigma \tag{3.2}$$

where:

| | |
|---|---|
| R | - Mean Earth's radius |
| $\gamma$ | - Normal gravity |
| $\Delta$g | - Gravity anomaly |
| S($\psi$) | - Stokes' function ($\psi$ - Spherical distance) |
| $\sigma$ | - Integration area |

## 3.2 Geodetic Boundary Value Problems

According to Moritz (1980), the geodetic boundary value problem is the determination of the Earth's physical surface from the values of gravity and gravity potential given on it. In modern geodesy, when dealing with measurements that can be outside and/or on the Earth's surface, geodetic boundary value problems deal with the determination of gravity potential on and outside the Earth's surface from the data preformed on and outside Earth's surface. The given boundary data can be linear or non-linear functionals of the unknown gravity potential. An example of a non-linear functional of the Earth's gravity potential is the gravity; defined as the magnitude of the gradient of the gravity potential. Alternatively, there are gravity anomalies and gravity disturbances. An example of a linear functional is the gravity potential itself or the gravity vector, i.e. the gradient of the gravity potential. In Stokes' and Molodensky's approach to the BVP, the geometry of the boundary surface is not known. The missing information about the geometry must then be determined from the boundary data. Therefore, more than one functional must be given on the boundary to uniquely determine geometry and potential. If, however, the boundary surface is assumed to be given, e.g. for the fixed gravimetric BVP, one functional is sufficient. Formulation of the BVP depends on the choice of the boundary surfaces. The surface can be a sphere, an ellipsoid of revolution, a telluroid, or even the Earth's surface. For a better understanding, it should be noted that both Stokes' and Molodensky's vector and scalar BVP lead formally to the same linear BVP (Klees, 1997). However, the definition of the boundary surface and the unit vector field are different. In the case of linearized BVPs, in Stokes' approach the boundary surface is the ellipsoid, whereas in Molodensky's approach it is the telluroid (Moritz, 1980).

### 3.2.1 Stokes' approach of the boundary value problem

The scalar geodetic boundary value problem was first formulated by Stokes in 1849. The formulation of the Stokes approach is based on the partial differential equation valid for the gravity potential *W* (Vanicek and Janak, 2000);

$$\nabla^2 W(r) = -4\pi G\rho(r) + 2\omega^2 . \tag{3.3}$$

$\rho(r)$ is the mass density of the Earth at, G is the Newtonian gravitational constant:
$G = 6.672\text{x}10^{-11}\text{m}^3\text{s}^{-2}\text{kg}^{-1}$ and ω is the angular velocity of the Earth's rotation.
This is a non-homogeneous elliptical equation of second order, or more precisely known as the Poisson equation. In this way, Stokes applied this formulation to the disturbing potential *T* outside the Earth ($\rho(r)$=0) to fulfill the following expression, for a harmonic function-Laplace equation (Vanicek and Janak, 2000):

$$\nabla^2 T(r) = 0 , \tag{3.4}$$

The assumption $\rho(r)$ =0 (harmonicity) is of course violated by the presence of the topography (and the atmosphere). According to the Helmert's theory, he suggested that this problem could be avoided by transforming the formulation into a space where *T* is harmonic outside the geoid.(Vanicek and Janak, 2000) The actual disturbing potential *T* is transformed to a disturbing potential $T^H$, harmonic outside the geoid, by subtracting from it the potential caused by topography (and the atmosphere) and adding to it the potential caused by topography (and the atmosphere) condensed on the geoid (or some other surface below the geoid). Applying the Laplace equation to $T^H$ we then get:

$$\nabla^2 T^H(r) = 0\,, \tag{3.5}$$

which is harmonic everywhere outside the geoid. This approach is known as the Stokes-Helmert approach of the boundary value problem.

### 3.2.2 Formulation of the Stokes-Helmert boundary value problem

According to Martinec (1998), before dealing with disturbing potential which is generated by the differences between the actual potential and the potential of the reference ellipsoid, this potential has to be corrected by the effect of the topography resulting in the potential known as the *Helmert's disturbing potential* $T^H$.
The aim is to transform the disturbing potential *T* to another disturbing potential $T^H$ , which is harmonic everywhere above the geoid and its boundary value equation can be linked to observations in harmonic space (Vanicek and Janak, 2000);

$$T(\vec{r}) \rightarrow T^H(\vec{r})$$

$$\nabla^2 T(\vec{r}) = 0 \rightarrow Homogeneous \quad equation \quad , \tag{3.6}$$

$$geoid \rightarrow co-geoid$$

The difference between the geoid and the co-geoid is that co-geoid contains the indirect effect caused by the reduction of the topographical effect. The definition of disturbing potential $T^H$ in the Helmert space (see Figure 3.1) can be expressed then by following equation (Vanicek and Janak, 2000):

$$T^H(\vec{r}) = T(\vec{r}) - DTE(\vec{r}) - DAE(\vec{r})\,, \tag{3.7}$$

where

$$T(\vec{r}) = W(\vec{r}) - U(\vec{r})\,, \tag{3.8}$$

$T^H(\vec{r})$ - Disturbing potential in Helmert's space

$T(\vec{r})$ - Disturbing potential in real space

$DTE(\vec{r}) = \frac{\partial}{\partial H}\left(V^T(\vec{r}) - V^{CT}(\vec{r})\right)$ - Direct topographical effect

$V^T(\vec{r})$ - Effect of topographical masses

$V^{CT}(\vec{r})$ - Effect of condensed topographical masses

$DAE(\vec{r}) = \frac{\partial}{\partial H}\left(V^A(\vec{r}) - V^{CA}(\vec{r})\right)$ - Direct atmospheric effect

$V^A(\vec{r})$ - Effect of Atmosphere

$V^{CA}(\vec{r})$ - Effect of condensed Atmosphere

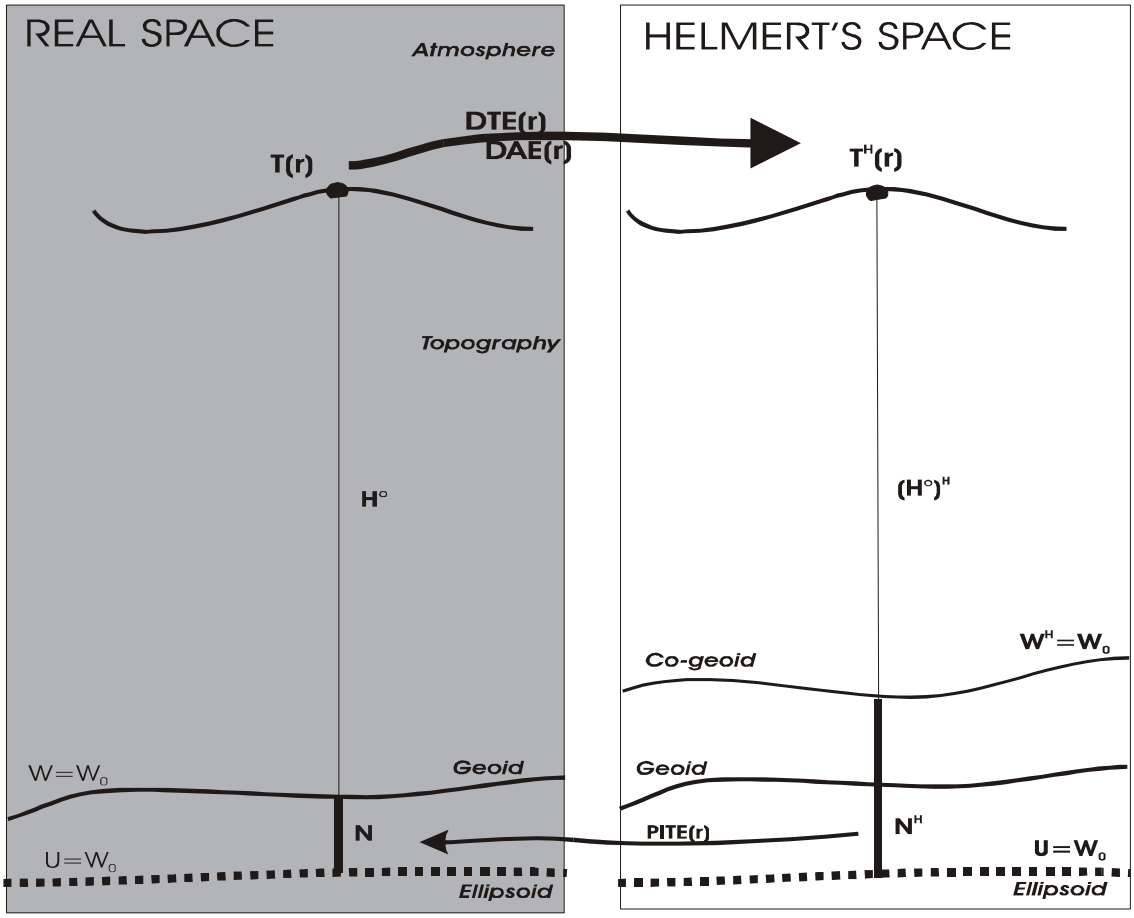


Figure 3.1 Stokes' - Helmert's scheme for geoid determination (Vanicek and Janak, 2000)

In gravimetric geoid determination, the low frequency part of a geoid is usually provided by a geopotential model (e.g. EGM96, Lemoine et al. 1998) in terms of spherical harmonic coefficients, complete up to degree and order $n_{max}$ (e.g. 360 for EGM96). The medium frequency band is covered by Stokes' integration of residual gravity values (e.g. gravity anomalies). The high frequency band is covered by the effect of a high-resolution digital terrain model (DTM). Thus the geoid height is split into three components (Forsberg, 1994):

$$N = \delta N^{GM} + \delta N^{Stokes} + \delta N^{DTM} . \tag{3.9}$$

Before applying the Stokes integration, gravity anomalies must be reduced due to the geopotential model contribution and due to the topographical effect.

$$\Delta g = \Delta g^{GM} + \Delta g^{Stokes} + \Delta g^{DTM} . \tag{3.10}$$

The final solution of the Stokes BVP is given by the expression for geoid undulation (see Eq. 3.2)

$$N = \frac{R}{4\pi\gamma} \iint_{\sigma} \Delta g \cdot S(\psi) d\sigma , \tag{3.11}$$

where $R$ is the mean Earth radius, $\gamma$ is the normal gravity, $\sigma$ is the area of integration, $\Delta g$ is the gravity anomaly on the geoid and $S(\psi)$ is the Stokes function given by:

$$S(\psi) = \frac{1}{\sin(\psi/2)} - 6 \cdot (\sin\frac{\psi}{2} + 1 - 5 \cdot \cos\psi - 3 \cdot \cos\psi \cdot \ln(\sin\frac{\psi}{2} + \sin^2\frac{\psi}{2}) , \tag{3.12}$$

where $\psi$ is the angular distance.

### 3.2.3 Ellipsoidal corrections

In the determination of the geoid with high accuracy, a spherical approximation can no longer be tolerated, in general, (spherical approximation causes geoid errors of 20cm in a global average) and ellipsoidal corrections must be applied. The derivation of these corrections is based on the following considerations (Sanso and Rummel, 1997) :

a) A position on ellipsoid is mapped one-to-one onto a corresponding position on a mean sphere.

b) The mean sphere ( $\varepsilon = 0$ ) represent a "Taylor point" for a Taylor series of a function F defined on the ellipsoid ( $\varepsilon > 0$ ).

Identifying the ellipsoidal coordinates φ,λ with spherical coordinates on the mean sphere it follows:

$$F(\varphi,\lambda) = F_0(\varphi,\lambda) + \varepsilon \cdot F_1(\varphi,\lambda) + \varepsilon^2 \cdot F_2(\varphi,\lambda) + \ldots\ldots\ldots , \tag{3.13}$$

with $F_0(\varphi,\lambda)$ corresponding to $\varepsilon = 0$ (mean sphere). Due to the smallness of the flattening parameter, that is expressed by linear eccentricity of the ellipsoid $\varepsilon = \sqrt{a^2 - b^2}$ (see Eq. 2.21); it suffices to use spherical expressions for $F_i(\varphi,\lambda), i = 1,2,\ldots\ldots$ (For more details see Sanso and Rummel, 1997).

Considering that $F_0$ on the mean sphere corresponds to $F$ on the ellipsoid. Beginning with the Bruns formula for the geoid undulation that reads (see Eq. 2.33);

$$N = \frac{T}{\gamma}, \tag{3.14}$$

$$\gamma = \gamma_0\left[1 - \frac{1-3\sin^2\varphi}{4}\cdot\varepsilon\right], \tag{3.15}$$

where γ is the normal gravity on the ellipsoid and $\gamma_0$ is the mean gravity. For the geoid undulation we then obtain:

$$N = \frac{T}{\gamma_0}\left[1 + \frac{1-3\sin^2\varphi}{4}\cdot\varepsilon\right] = N_0 + N_1\cdot\varepsilon, \tag{3.16}$$

with

$$N_0 = \frac{T}{\gamma_0}\ , \quad \text{(on the sphere)} \tag{3.17}$$

and the first order correction term for the geoid undulation follows:

$$N_1 = N_0\left(\frac{1-3\sin^2\varphi}{4}\right). \tag{3.18}$$

### 3.2.4 The Molodensky approach

While the problem of Stokes' may be formulated as: Determination of the geoid based on the gravity potential $W=W_0=const$ (see Figure 3.2) . and gravity g given at all points of the geoid, the problem of Molodensky is based on the determination of the physical Earth's surface *S*, from the gravity potential *W* and gravity vector *g* given on it (Sünkel, 1997). In space both the gravity potential *W* and gravity vector *g* are spatial functions, depending on three space coordinates. At the Earth's surface *S*, the gravity potential and the gravity vector are restricted to $W_S$ and $g_S$, respectively. Following the Dirichlet solution of the boundary value problem, the gravity potential *W* outside *S* can be uniquely determined if the gravity potential $W_S$ is given on *S (see Figure 3.2)*. Then the gravity vector $g_S$ can be represented as a function of *S* and $W_S$ (Sünkel, 1997):

$$g_S = F(S, W_S). \tag{3.19}$$

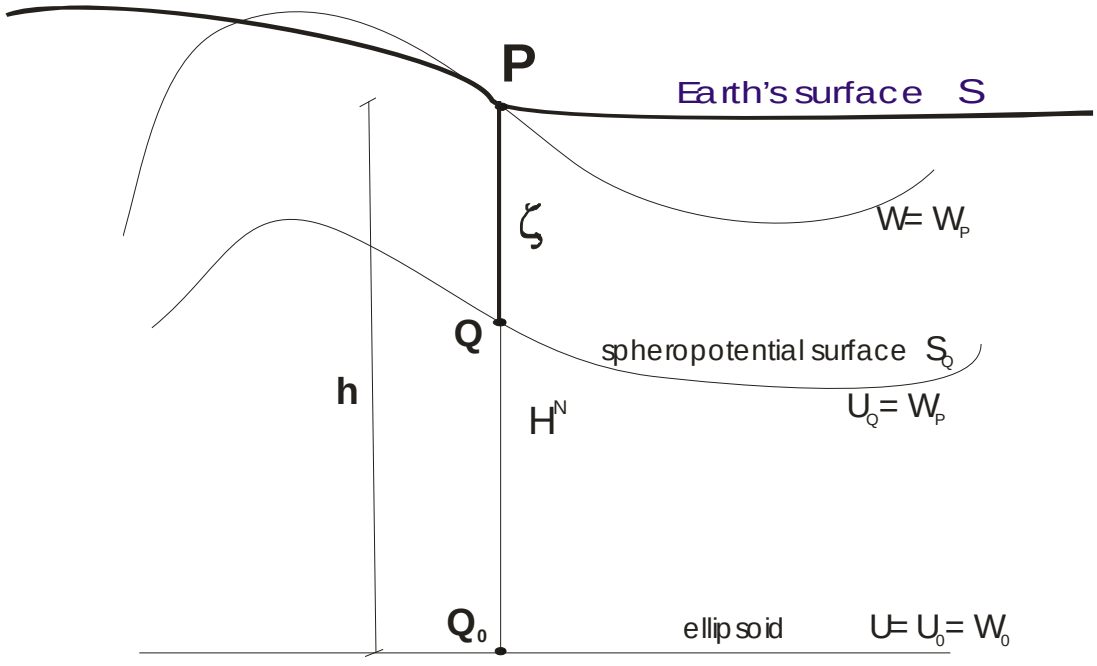


Figure 3.2 Molodensky's scheme and its relation to the telluroid

Compared to this direct approach, The Molodensky problem can be conceptionally formulated as an inverse problem:

$$S = \Phi(W_S, g_S). \tag{3.20}$$

The Molodensky's operator $F$ is a complicated nonlinear operator and may be solved by proper linearization. Since $W_S$ is given, we may consider $g_S$ as a function of $S$ only, and vice versa, we may express the surface $S$ as a function of the gravity vector on the surface $g_S$:

$$g_S = f(S) \text{ and } S = f^{-1}(g_S). \tag{3.21}$$

If we introduce an approximation $S_Q$ to the Earth's surface (Taylor point) and denote the gravity vector at surface $S_Q$ with $\gamma_Q$, then we obviously have:

$$S = S_Q + \zeta \ , \tag{3.22}$$

$$g_S = \gamma_Q + \Delta g \ , \tag{3.23}$$

$$\gamma_Q = f(S_Q), \tag{3.24}$$

Where:

$S_Q$ - Spheropotential surface (telluroid)

$\zeta$ - Height anomaly

$\Delta g$ - Gravity anomaly

$\gamma_Q$ - Normal gravity on the telluroid

Then a Taylor series, terminated after the linear term, yields:

$$\gamma_Q + \Delta g = f(S_Q + \zeta) = f(S_Q) + f'(S_Q)\zeta \, . \tag{3.25}$$

Expressing the gravity anomaly with:

$$\Delta g = f'(S_Q)\zeta \, , \tag{3.26}$$

and formally we obtain the solution

$$\zeta = [f'(S_Q)]^{-1}\Delta g = M \cdot \Delta g \, , \tag{3.27}$$

$$\zeta = M \cdot \Delta g \, , \tag{3.28}$$

where, $M$ is the linear Molodensky's operator.

The telluroid (spheropotential) surface $S_Q$ is chosen such that the normal potential at the telluroid point $Q$ coincides with the actual potential at the corresponding Earth's surface point $P$. The ellipsoidal height of the point $Q$ is called *normal height* $H^N$ and the distance between points $P$ and $Q$ is called *height anomaly* $\zeta$ (see Figure 3.2) and they are presented below by following expressions:

$$U_Q = W_P, \tag{3.29}$$

$$\zeta = h - H^N. \tag{3.30}$$

## 3.3 Boundary value problems of airborne gravimetry

From the given airborne gravity data at a flight surface $F$, the gravity field between the Earth's surface $S_T$ and the flight surface $F$ is to be determined. Mathematical representation of the BVP reads (Schwarz and Li, 1997):

$$\begin{cases} \Delta T(x, y, z) = 0 \quad for \quad 0 \le z \le H \\ A_i T\big|_F = g_i \\ (i = 1,2,.....,n) \end{cases}, \tag{3.31}$$

where $T$ is the disturbing potential; $A_i$ is a linear functional relating T to the measurement $g_i$; n is the number of measurement types; $x, y, z$ are the coordinates in a local coordinate system, the origin of which is in the centre of the area of interest, as shown in Figure 3.3

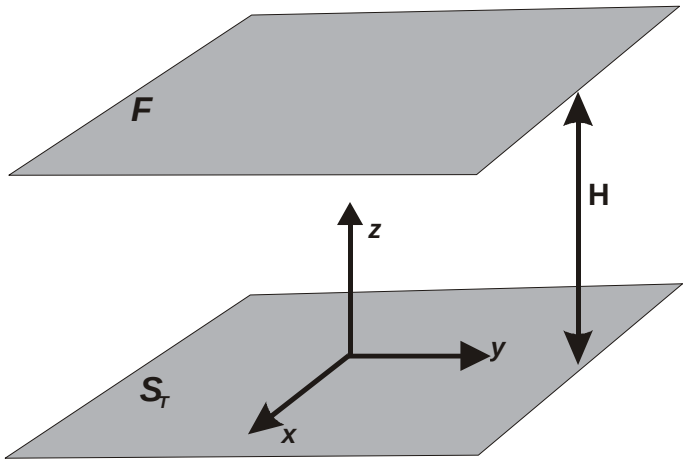


Figure 3.3 The local coordinate system in airborne gravimetry

### 3.3.1 Scalar BVP of airborne gravimetry

In airborne gravimetry, different to conventional cases, the boundary conditions are given on the flight surface *F* and can be formulated as (Schwarz and Li, 1997):

$$\begin{cases} \Delta T(x,y,z) = 0 \quad for \quad 0 \le z \le H \\ \\ \dfrac{\partial T}{\partial z}\Big|_F = -\delta g^H \end{cases}, \tag{3.32}$$

where $\delta g^H$ is the gravity disturbance at flight level.

### 3.3.2 Vector BVP of airborne gravimetry

In the case of vector gravimetry, the boundary value problem can be formulated as follows (Schwarz and Li, 1997):

$$\begin{cases} \Delta T(x,y,z) = 0 \quad for \quad 0 \le z \le H \\ \dfrac{\partial T}{\partial x}\Big|_F = \delta g_x^H \\ \\ \dfrac{\partial T}{\partial y}\Big|_F = \delta g_y^H \\ \\ \dfrac{\partial T}{\partial z}\Big|_F = -\delta g^H \end{cases}, \tag{3.33}$$

where $\delta g_x^H$ and $\delta g_y^H$ are the two components of the gravity disturbance vector along the x-axis and y-axis measured at flight level.

### 3.3.3 BVP of Airborne Gradiometry

Formulation of the BVP of airborne gravimetry can be expressed as follows (Schwarz and Li, 1997):

$$\begin{cases} \Delta T(x,y,z) = 0 \quad for \quad 0 \le z \le H \\ \dfrac{\partial^2 T}{\partial x \partial x}\Big|_F = g_{xx}^H \,, \quad \dfrac{\partial^2 T}{\partial x \partial y}\Big|_F = g_{xy}^H \quad , \quad \dfrac{\partial^2 T}{\partial x \partial z}\Big|_F = g_{xz}^H \\ \dfrac{\partial^2 T}{\partial y \partial x}\Big|_F = g_{yx}^H \quad , \quad \dfrac{\partial^2 T}{\partial y \partial y}\Big|_F = g_{yy}^H \quad , \quad \dfrac{\partial^2 T}{\partial y \partial z}\Big|_F = g_{yz}^H \\ \dfrac{\partial^2 T}{\partial z \partial x}\Big|_F = g_{zx}^H \quad , \quad \dfrac{\partial^2 T}{\partial z \partial y}\Big|_F = g_{zy}^H \quad , \quad \dfrac{\partial^2 T}{\partial z \partial z}\Big|_F = g_{zz}^H \end{cases} , \quad (3.34)$$

where $g_{xx}, g_{xy}, ....., g_{zz}$ are the tensor components of second derivatives of the disturbing potential at flight level, see Schwarz and Li, (1997) for details, i.e.

### 3.3.4 Boundary value problem combining airborne and ground gravity data

The determination of the gravity field between the flight surface and the Earth's surface using only airborne gravity data is a downward continuation process, i.e. it is inherently an unstable process (Schwarz and Li, 1997). In order to stabilize the downward continuation process, the combination of airborne gravity data together with terrestrial gravity and other data needs to be considered. The boundary value problem combining airborne and ground data can be formulated as follows: Given airborne gravity data at flight surface *F* and gravity field related data on the Earth's surface *S*, the gravity field between the Earth surface S and the flight surface F is to be determined. The mathematical formulation reads:

$$\begin{cases} \Delta T = 0 \quad for \quad 0 \le z \le H \\ A_i T\big|_F = g_i \quad i = 1,2,....,n \\ B_j T\big|_S = f_j \quad j = 1,2,....,m \end{cases} , \quad (3.35)$$

where $A_i$ and $B_j$ are linear functionals relating gravity disturbing potential $T$ to airborne data $g_i$ and ground data $f_j$. $n$ and $m$ are the number of measurement types for airborne data and ground data respectively. The solution of the BVP combining airborne and ground gravity data, can be carried out by using a planar harmonic expansion, see Bian and Zhang (1993) for details, i.e.

$$T(x,y,z)=\sum_{i=0}^{\infty}\sum_{j=0}^{\infty}e^{-z\omega_{ij}}[\cos(i\omega_1 x)\cdot\sin(i\omega_1 x)]\begin{bmatrix}A_{ij} & B_{ij}\\ C_{ij} & D_{ij}\end{bmatrix}\begin{bmatrix}\cos(j\omega_2 y)\\ \sin(j\omega_{2y})\end{bmatrix}+ \sum_{i=0}^{\infty}\sum_{j=0}^{\infty}e^{z\omega_{ij}}[\cos(i\omega_1 x)\cdot\sin(i\omega_1 x)]\begin{bmatrix}E_{ij} & F_{ij}\\ G_{ij} & H_{ij}\end{bmatrix}\begin{bmatrix}\cos(j\omega_2 y)\\ \sin(j\omega_2 y)\end{bmatrix}, \quad (3.36)$$

where; $\omega_{ij}=\sqrt{i^2\omega_1^2+j^2\omega_2^2}$ .

$\omega_1$ and $\omega_2$ are circular frequencies in the direction of the x or y-axis, respectively. The coefficients $A_{ij}, B_{ij}, \ldots\ldots, H_{ij}$ are to be determined using the boundary conditions. In this chapter we should illustrate some special cases of boundary value problems combining airborne and ground data.

Neuman Problem

$$\begin{cases}\Delta T=0 \quad for \quad 0\le z\le H\\ \dfrac{\partial T}{\partial z}\Big|_F=\delta g^H\\ \dfrac{\partial T}{\partial z}\Big|_S=\delta g^0\end{cases}, \quad (3.37)$$

Mixed Neuman-Dirichlet Problem

$$\begin{cases}\Delta T=0 \quad for \quad 0\le z\le H\\ \dfrac{\partial T}{\partial z}\Big|_F=\delta g^H\\ T\big|_S=T^0\end{cases}, \quad (3.38)$$

Mixed Gradiometry-Neuman Problem

$$\begin{cases}\Delta T=0 \quad for \quad 0\le z\le H\\ \dfrac{\partial^2 T}{\partial z\partial z}\Big|_F=\delta g_{zz}^H\\ \dfrac{\partial T}{\partial z}\Big|_S=\delta g^0\end{cases}, \quad (3.39)$$

Mixed Gradiometry-Dirichlet Problem

$$\begin{cases}\Delta T=0 \quad for \quad 0\le z\le H\\ \dfrac{\partial^2 T}{\partial z\partial z}\Big|_F=\delta g_{zz}^H\\ T\big|_S=T^0\end{cases}, \quad (3.40)$$

# 4 Remove-restore technique for geoid determination using airborne gravity data

## 4.1 Introduction

In recent years, airborne gravimetry has become a very useful tool in many fields of geosciences, such as geodesy, geology, geophysical exploration etc. In geodesy the airborne gravity measurements are used for the determination of a precise local or regional geoid (Forsberg and Brozena 1997, Kearsley et al. 1998, Wei and Schwarz 1998). Thus, the accuracy of a 5-10cm airborne gravity derived geoid can be used as a precise vertical reference of orthometric height. This provides an efficient way to determine orthometric height without traditional leveling which is a very expensive and slow process for present developments. The application of airborne gravimetry shows its efficiency, which is basically due to its advantages in the determination of gravity by the combination of kinematical GPS, INS (Inertial Navigation System) and gravity meters with stabilized platforms. In general airborne surveys are treated as very good tools to cover large scale and mountain areas, which are difficult and expensive to cover with traditional land surveys. These areas require a large survey altitude, causing problems in the downward continuation process, which is the main topic of this study.

## 4.2 Principle of Airborne Gravimetry

In principle, airborne measurement techniques can be divided into three main groups (Hein, 1995):

- Scalar Gravimetry,
- Vector Gravimetry and
- Gravity Gradiometry

We shall focus our attention on the first group, which is the most developed and useful technique today. The most extended system used in scalar gravimetry consists of damped two-axis platform systems (e.g. LaCoste & Romberg sea/air gravity meter system), GPS, Inertial Navigation System and optionally, altimetry system (Bastos et al. 2000). We also identify two main effects in gravity surveys performed on such moving platforms: one caused by the motion of the aircraft and the second due to the attraction of the mass of the Earth. In practice, the major problem is the separation of the gravitational acceleration from the non-gravitational accelerations that are occurring to the aircraft.
As is mentioned above, scalar gravimetry requires both, a system that determines the sum of the gravimetric and kinematical acceleration occurring to the airborne platform, plus a vertical positioning system (e.g., GPS receiver or/and an altimeter), that determines the kinematical accelerations alone. The resulting gravity vector is determined by the difference between the two (Meyer et al. 2003). The most common implementation of this technique is based on the installation of damped two-axis platform sea-air gravimeters, mounted in either a helicopter or an aircraft (e.g., LaCoste & Romberg or Bodeseewerk KSS-31) that is oriented in a vertical

direction. It is the implementation of scalar gravimetry that has seen significant advances in accuracy in the last decade. According to Salychev (1998), an improvement in accuracy can be achieved by using an inertial navigation system (INS) both as a stabilizing mount for a separate gravimetric sensor and as the gravimetric sensor itself. Initial test results showed that accuracies of 1 mGal with a spatial resolution of 2-3 km can be achieved over a profile length of 50km in areas with medium gravity field variability. These results were achieved at a 500 m flight altitude with a speed as low as 50 m/s and maximum change in gravity over a test area of 30 mGal.

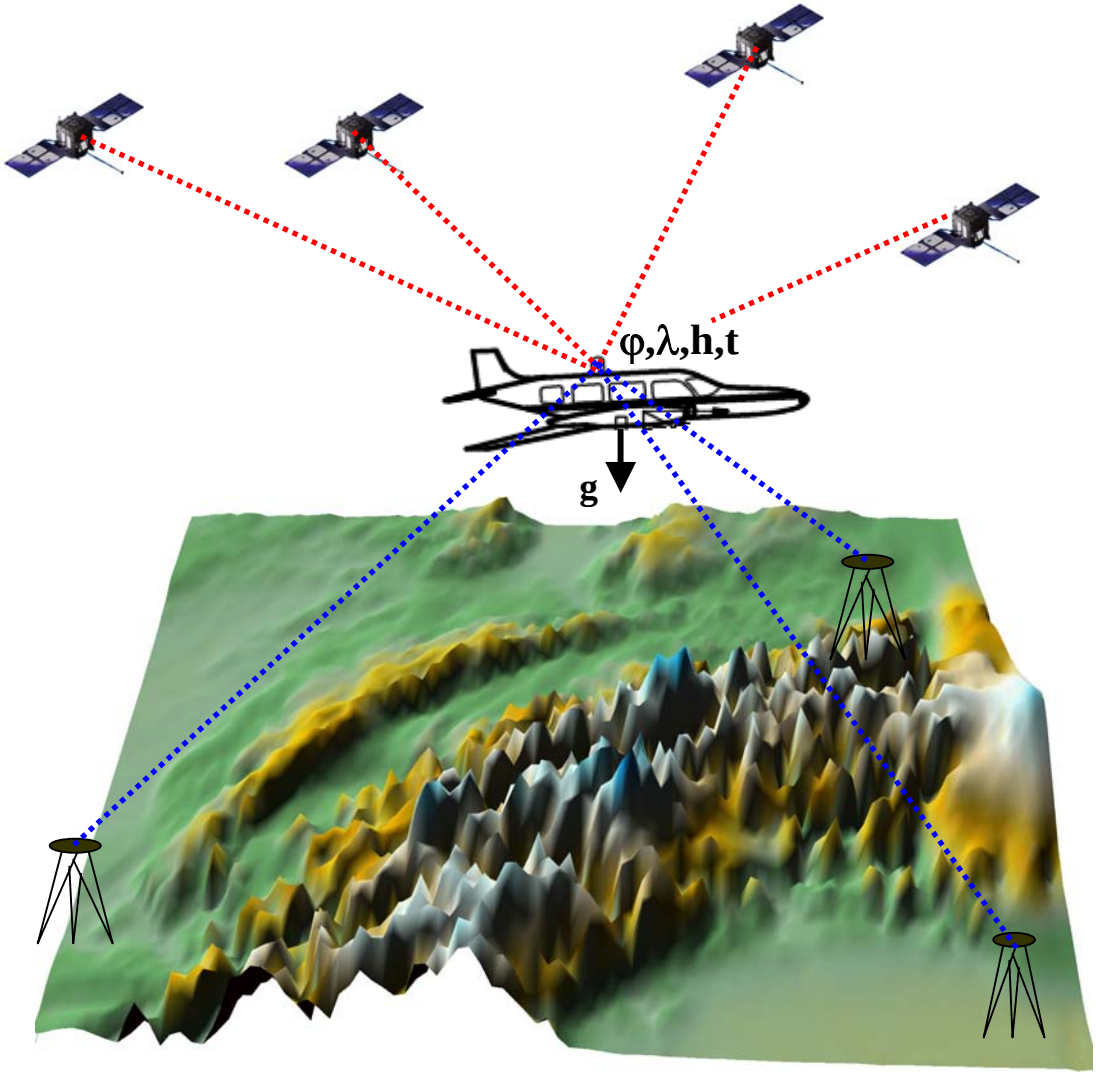


Figure 4.1 Principle of the airborne gravity surveys

A simple measurement model of airborne scalar gravimetry is given by following expression: (Hein, 1995):

$$g(h) = \delta a_E - \frac{g}{2}\left(\varepsilon_x^2 + \varepsilon_y^2\right) + a_x \sin\varepsilon_x + a_y \sin\varepsilon_y + a_z + \Delta g + \gamma + \Delta g(t), \tag{4.1}$$

where:

$g(h)$ - Gravity observation at height h

$\delta a_E$ - Eötvös effect

$\frac{g}{2}\left(\varepsilon_x^2 + \varepsilon_y^2\right)$ - Initial misalignment

$\varepsilon$ - Off-vertical tilt error in horizontal plane (x, y)

$a_x \sin\varepsilon_x + a_y \sin\varepsilon_y$ - Mislevelling

$a_x$ - Acceleration in horizontal x-direction

$a_y$ - Acceleration in horizontal y-direction

$a_z$ - Vertical (aircraft) acceleration

$\Delta g$ - Gravity anomaly

$\gamma$ - Normal gravity

$\Delta g(t)$ - Tidal variation

The Eötvös effect can be calculated in spherical approximation as follows (Hein, 1995):

$$\delta a_E = 2\omega\cos\phi\sin A \cdot v + \frac{v^2}{\left(R + h\right)}, \tag{4.2}$$

where:

$\omega$ - Angular velocity of the Earth's rotation (see Eq. 2.3)

$v$ - Horizontal velocity of the aircraft

$A$ - Azimuth

$\phi$ - Geographical latitude

$R$ - Mean Earth's radius

$h$ - Height above sphere (ellipsoid)

Geodetic developments that were achieved in recent years, especially the launching of artificial satellites (e.g. Global Positioning System [GPS]), permits the determination of positions on and around the Earth extremely accurately. These coordinates obtained by the GPS refer to its geocentrical reference frame (WGS84 ellipsoid) and can be determined within a centimeter of accuracy or better. Determination of positions with such accuracy (kinematical DGPS) can be regarded as the major achievement in the philosophy of local-regional geoid determination from airborne gravity data. Application of GPS improves the determination of the major first-order noise sources in airborne gravity, namely aircraft vertical accelerations and the Eötvös effect. With these effects removed, it is easy to concentrate on modeling and removing subtler effects, such as horizontal acceleration and long period cross coupling.

## 4.3 Gravity reduction in remove-restore technique

According to Heiskanen and Moritz (1967), the Stokes integral and similar formulas presuppose that the disturbing potential $T$ is a harmonic function outside the geoid, which implies that there are no masses outside the geoid. This assumption that there are "no masses outside the bounding surface" is necessary to solve any problem of physical geodesy as the boundary value problem of the potential theory. This is because the boundary value problems of potential theory always involve harmonic functions that satisfy Laplace's equation ($\Delta T = 0$). Since realistically, there are masses outside the geoid, they must be removed or moved (compensated) inside the geoid before applying the Stokes approach of geoid determination (Stokes' integral). The resulting geoid is called a co-geoid and can be converted to the geoid by adding the indirect effect. There are many methods for the reduction of gravity observation caused by topographical masses outside the geoid. In this study we will examine two of them; First, the second Helmert's condensation method and second, the Residual Terrain Model (RTM) method.
The remove-restore technique for the geoid determination can be formulated as follows (see Eq. 3.9):

$$N = \delta N^{GM} + \delta N^{RES} + \delta N^{DTM}, \tag{4.3}$$

where:

| | |
|---|---|
| $N$ | Total geoid undulation |
| $\delta N^{GM}$ | Contribution of global geopotential model |
| $\delta N^{RES}$ | Contribution of residual field |
| $\delta N^{TOP}$ | Contribution of topographic effect |

The major contribution to geoid undulation gives the geopotential part $\delta N^{GM}$ (EGM96, Lemoine et al. 1998), which approximates the geoid in most areas of the world with an accuracy of $\approx \pm 1$m at wavelengths down to 100 km.

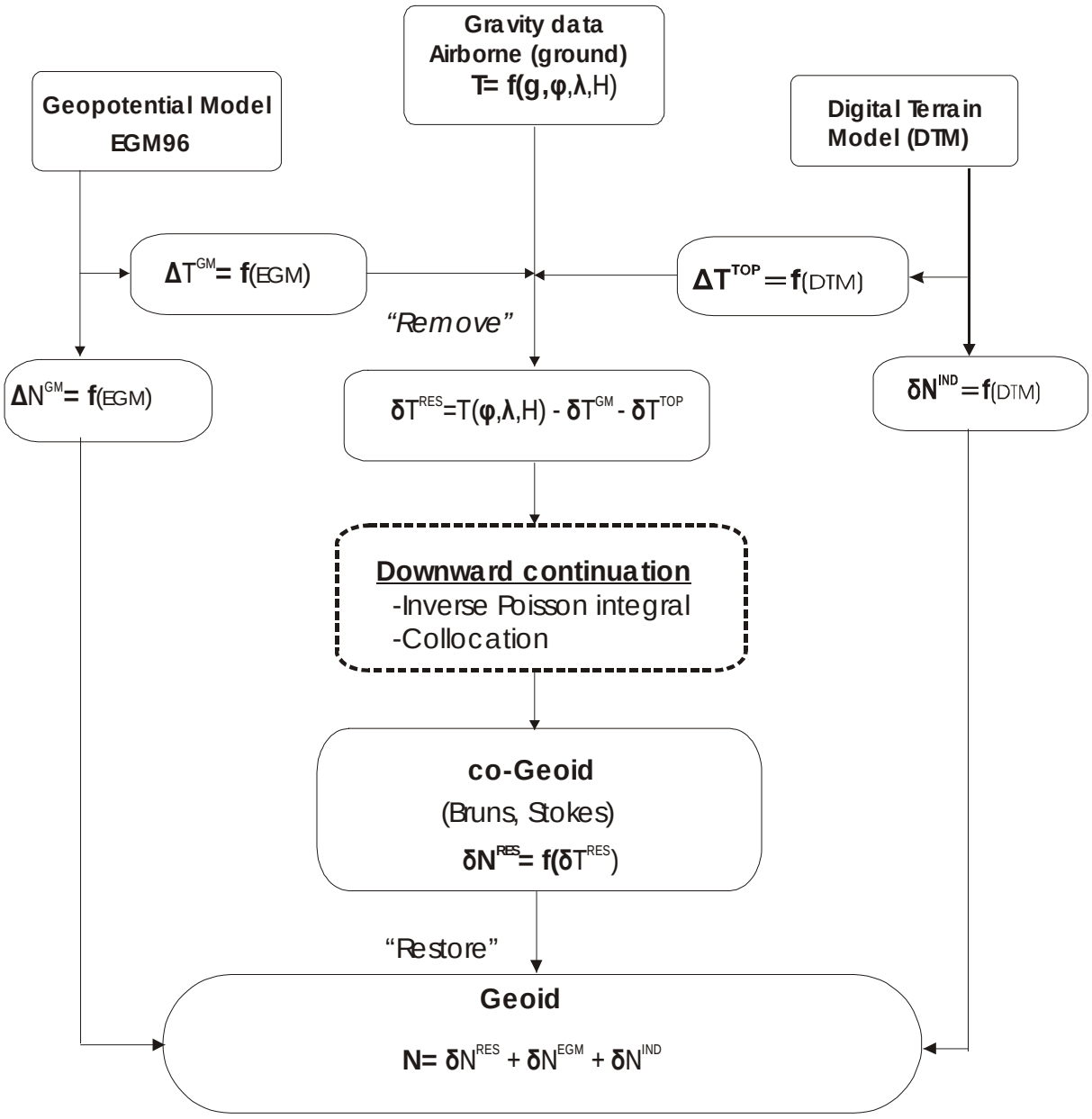


Remove-restore scheme for the geoid computation

### 4.3.1 Contribution of the Geopotential Model

The spherical harmonic representation of the Earth's gravitational potential $V$ is given (NIMA Report, 2000):

$$V = \frac{GM}{r}\left[1+\sum_{n=2}^{n_{\max}}\sum_{m=0}^{n}\left(\frac{a}{r}\right)^n \overline{P}_{nm}(\sin\phi')\cdot\left(\overline{C}_{nm}\cos\ m\lambda + \overline{S}_{nm}\sin\ m\lambda\right)\right], \qquad (4.4)$$

The potential of a rotational reference ellipsoid is represented by the expansion

$$U(r,\phi,\lambda) = \frac{GM'}{r}\left[1+\sum_{n=2}^{n_{\max}}\sum_{m=0}^{n}\left(\frac{a}{r}\right)^n \overline{P}_{nm}(\sin\phi)\cdot\left(\overline{C}'_{nm}\cos\ m\lambda + \overline{S}'_{nm}\sin\ m\lambda\right)\right], \qquad (4.5)$$

*with* $\overline{S}'=0$ *and* $\overline{C}'_n \cong \overline{C}'_{n0} \neq 0$ *for n=2,4,6,… and M'* is the mass of the reference ellipsoid. The disturbing potential of a geopotential model is given by:

$$T_{GM}(r,\phi,\lambda) = V_{GM} - U = \frac{GM}{r}\sum_{n=2}^{n_{\max}}\left(\frac{a}{r}\right)^n \sum_{m=0}^{n}\left(\Delta C_{nm}\cos m\lambda + \Delta S_{nm}\sin m\lambda\right)\overline{P}_{nm}(\sin\phi), \quad (4.6)$$

where $\Delta C_{nm}$ and $\Delta S_{nm}$ are the differences between the fully normalized coefficients of the geopotential model and ellipsoid potentials (the difference $M$-$M'$ is assumed to be negligibly small) and $M'$ can be replaced by $M$. Taking into account the boundary condition of physical geodesy, we get the following expansions:

for *gravity anomalies*, it reads

$$\Delta g_{GM}(r,\phi,\lambda) = \frac{GM}{r^2}\sum_{n=2}^{n_{\max}}(n-1)\left(\frac{a}{r}\right)^n \sum_{m=0}^{n}\left(\Delta C_{nm}\cos m\lambda + \Delta S_{nm}\sin m\lambda\right)\overline{P}_{nm}(\sin\phi), \qquad (4.7)$$

and, with the Bruns equation, for *geoid undulation*

$$\delta N_{GM}(r,\phi,\lambda) = \frac{GM}{r\gamma}\sum_{n=2}^{n_{\max}}\left(\frac{a}{r}\right)^n \sum_{m=0}^{n}\left(\Delta C_{nm}\cos m\lambda + \Delta S_{nm}\sin m\lambda\right)\overline{P}_{nm}(\sin\phi), \qquad (4.8)$$

where $\gamma$ is the normal gravity. (see Chapter 2 for detailed description of the symbols)

### 4.3.2 The Contribution of topographic masses

For the harmonization of the gravity field outside the geoid, the topographic effect has to be removed from the measured gravity signal *g* (Vanicek and Janak 2000, Novak et al. 2001). This can be achieved by using different techniques for gravity reductions. In this chapter we shall deal with two of them: the second Helmert's condensation method and the Residual Terrain Model (RTM) method.

#### 4.3.2.1 Second Helmert's condensation method

One of the most widely used techniques for solving the geodetic boundary value problem is the Stokes-Helmert scheme (Vanicek and Martinec, 1994). The essence of this method is that topographical masses are replaced by a condensed mass layer on the geoid surface, resulting in the introduction of an abstract space, called Helmert's space (Vanicek and Martinec, 1994) in which the solution is sought. The basic idea behind this technique is that the disturbing potential $T^H(r,\Omega)$ in Helmert's space is harmonic everywhere above the geoid (Vanicek et al. 2001). The relationship between the real disturbing potential $T(r,\Omega)$ and Helmert's disturbing potential $T^H(r,\Omega)$ is:

$$T^H(r,\Omega) = T(r,\Omega) - \delta V^{TC}(r,\Omega), \tag{4.9}$$

where the residual topographical potential $\delta V^{TC}(r,\Omega)$ is defined as:

$$\delta V^{TC} = V^T - V^{CT}, \tag{4.10}$$

where, $V^T$ is the potential of topographical masses, $V^{CT}$ is the potential of condensed layer (see chap. 3.2.1).
Figure 4.2 shows in general the relationship between the measured point P and integration points P'. The principle of the definition of terrain correction yields in determination of the deviation of actual topography from Bouguer plate of point P, with the assumption that the masses between the geoid and the Earth's surface have a constant density (ρ=2.67gr/cm³) (Heiskanen and Moritz, 1967).

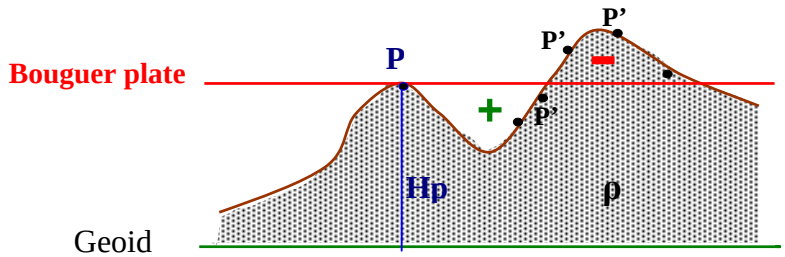


Figure 4.2 Terrain correction and Bouguer plate

According to Martinec (1998), the potential of topographical masses in spherical approximation is given by the equation:

$$V^{TC}(r,\phi,\lambda) = G\int_{\lambda'}\int_{\phi'}\int_{R}^{R+H(\phi',\lambda')} \frac{\rho(r',\phi',\lambda')}{L(r,\psi,r')} r'^2 dr' \cos\phi' d\phi' d\lambda', \qquad (4.11)$$

where $G$ is the gravitational constant (see Eq. 2.2)

$\rho$ - Density of the topography

$r$, $\Phi$, $\Lambda$ - Spherical coordinates of the computation point

$r'$, $\Phi'$, $\Lambda'$ - Spherical coordinates of the running integration point

$L(r,\psi,r') = \sqrt{r^2 + r'^2 - 2rr'\cos\psi}$ - Distance between the computation and running points

$\psi$ - Angular distance between the computation and running points

$R$= 6371 km - Mean radius of the Earth

The final equation used for the terrain correction (TC) to gravity in the second Helmert's condensation method has the form, considering the density of the topography as a constant ($\rho$=2.67 gr/cm³):

$$V^{T}(r,\phi,\lambda) = G\rho\iint\left[\frac{\partial\tilde{L}^{-1}(r,\psi,r')}{\partial r}\Bigg|_{r'=R}^{R+H(\phi',\lambda')} - \frac{\partial\tilde{L}^{-1}(r,\psi,r')}{\partial r}\Bigg|_{r'=R}^{R+H(\phi,\lambda)}\right]\cos\phi' d\phi' d\lambda'. \qquad (4.12)$$

The condensed TC (CTC) can be expressed by the following equation:

$$V^{CT}(r,\phi,\lambda) = GR^2\iint[\sigma(\phi',\lambda') - \sigma(\phi,\lambda)]\frac{\partial\tilde{L}^{-1}(r,\psi,R)}{\partial r}\Bigg|_{r=R+H(\phi,\lambda)}\cos\phi' d\phi' d\lambda', \qquad (4.13)$$

where; $\sigma(\varphi,\lambda) = \rho H\left(1 + \frac{H}{R} + \frac{H^2}{3R^2}\right)$ is the surface density of the condensation masses

evaluated at the measuring location. The symbol $\tilde{L}^{-1}(r,\psi,r')$ substitute the radial integral of the Newton kernel, $\int_{r'} \frac{r'^2}{L(r,\psi,r')} dr'$ and the radial derivative of the kernel is:

$$\frac{\partial \tilde{L}^{-1}(r,\psi,r')}{\partial r} = \left[(r'^2+3r^2)\cos\psi + (1-6\cos^2\psi)rr'\right]\tilde{L}^{-1}(r,\psi,r') + \\ + (3\cos^2\psi)\cdot \ln\left|r'-r\cos\psi + \tilde{L}(r,\psi,r')\right| \quad , \tag{4.14}$$

and

$$L^{-1}(r,\psi,r') = \frac{1}{2}(r'+3r\cos\psi)\tilde{L}(r,\psi,r') + \\ + \frac{r^2}{2}(3\cos^2\psi - 1)\cdot \ln\left|r'-r\cos\psi + \tilde{L}(r,\psi,r')\right| + C \quad , \tag{4.15}$$

where C is a constant, and

$$\frac{\partial L^{-1}(r,\psi,r')}{\partial r} = -\frac{r - r'\cos\psi}{(r^2+r'^2-2rr'\cos\psi)^{3/2}} \tag{4.16}$$

is the radial derivative of the Newton kernel $1/L(r,\psi,r')$, (for more details see Martinec, 1998). The Direct Topographic Effect (DTE) is the difference between the T and CTC;

$$\delta T^{TC}(DTE) = V^T - V^{CT}. \tag{4.17}$$

The topographic indirect effect of both the actual and condensed topography is expressed as follows:

$$\delta N^{IND}(\phi,\lambda) = \frac{G}{\gamma(\phi,\lambda)}\left[-2\pi\rho(\phi,\lambda)H^2\left(1+\frac{2H(\phi,\lambda)}{3R}\right)+\right. \\ + \iint\left(\rho(\phi',\lambda')\partial\tilde{L}^{-1}(R,\psi,r')\Big|_{r'=R}^{r'=R+H(\phi',\lambda')} - \rho(\phi,\lambda)\partial\tilde{L}^{-1}(R,\psi,r')\Big|_{r'=R}^{r'=R+H(\phi,\lambda)} - \tag{4.18} \\ \left. - R^2\frac{\sigma(\phi',\lambda')-\sigma(\phi,\lambda)}{L(R,\psi,R)}\right)\cos\phi' d\phi' d\lambda'\Big]$$

#### 4.3.2.2 Residual Terrain Model method

In the case of geoid determination using airborne gravity data, especially in mountainous areas, the use of rigorous terrain reduction, such as residual terrain model (RTM) reduction (Forsberg, 1984) would contribute to the stabilization of the downward continuation process, since the removal of terrain effects will limit the short wavelength variability of the gravity data significantly (Forsberg, 1984).
In the computation of the RTM effect, the mean elevation surface with a crustal density of 2.67 gr/cm³ up to the reference level $H_{REF}$ is used. The reference surface can be defined as a mean surface with the resolution that corresponds to a Global Geopotential Model (e.g.EGM96), a surface computed by the simple filtering of local terrain heights, or a sphere with corresponding elevation. All these possibilities will be examined and analyzed in this work. The topographic RTM density anomalies will make a "balanced set" of positive and negative density anomalies, representing areas where the topography is either above or below the reference topography (see Figure 4.3). The effect of the RTM density anomalies will therefore, in general, be cancelled out in zones at larger distances from a computation point (say, for example, at a distance of 2-3 times the resolution of the mean height surface). In a practical sense, this makes RTM reductions easy to work with (Forsberg, 1984).

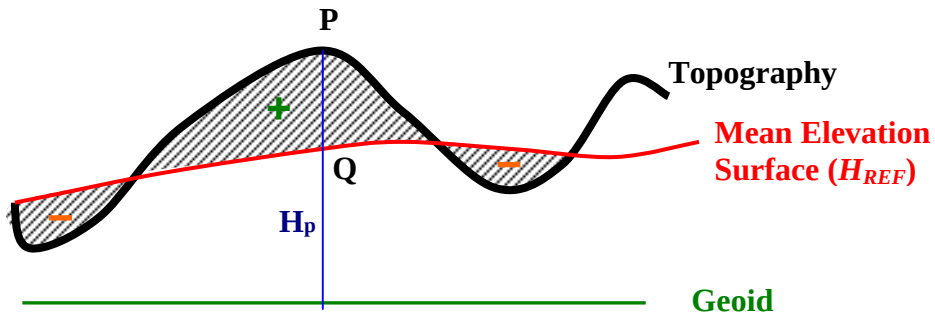


Figure 4.3 Mean elevation surface (MES) and Digital Terrain Model (DTM)

The RTM gravity terrain effect in planar approximation is given by an integral of the form (Forsberg, 1984):

$$\delta g_{RTM} = G\rho \iint_{A} \int_{H_{REF}}^{H} \frac{H - H_P}{[(x_Q - x_P)^2 + (y_Q - y_P)^2 + (z_Q - H_P)^2]^{3/2}} dx_Q dy_Q dz_Q \ , \qquad (4.19)$$

where,

$P(x,y,z)$ - Computational point (On Topography)

$Q(x,y,z)$ - Point on Mean Elevation Surface (integration point)

$G$ - Gravitational constant (as defined above)

$\rho(x,y,z)$ - Density of the differential element

$H$ - Height of integration point

$H_{REF}$ - Mean elevation surface heights

$H_P$ - Height of computational point

When the mean elevation surface is a sufficiently long-wavelength surface, the RTM reduction may be approximated by a Bouguer reduction to the reference level (Forsberg, 1984)

$$\delta g_{RTM} \approx 2\pi G\rho(H - H_{REF}) - TC \tag{4.20}$$

This approximation shows that the classical terrain correction (TC) is a key quantity for gravity reduction by RTM technique.

### 4.3.2.3 Analysis of a test area by using different terrain correction techniques

For the calculation of terrain effect, the GTOPO (U.S. Geological Survey, EROS Data Center) Digital Terrain Model was applied. This model has the resolution of 30"x30" and an accuracy of ~25m. The whole area has a rough topography whereby the minimal height is 1660m and the maximal height is 2641m (see Figure 4.4). For the computation of the various terrain correction techniques, the GRAVSOFT Package has been used.

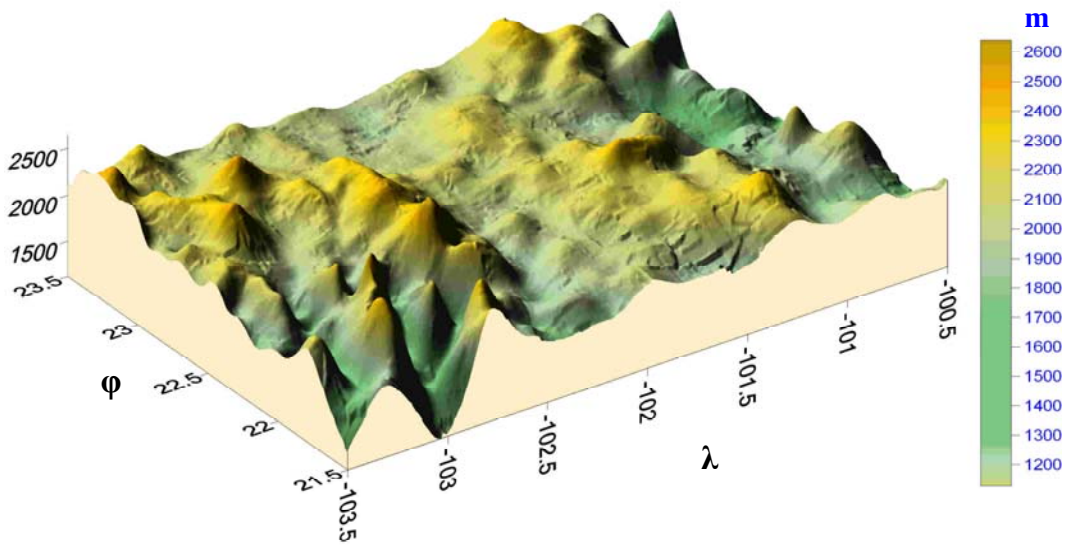


Figure 4.4 DTM with resolution of 1km x 1km in Zacatecas-Aguascalientes area

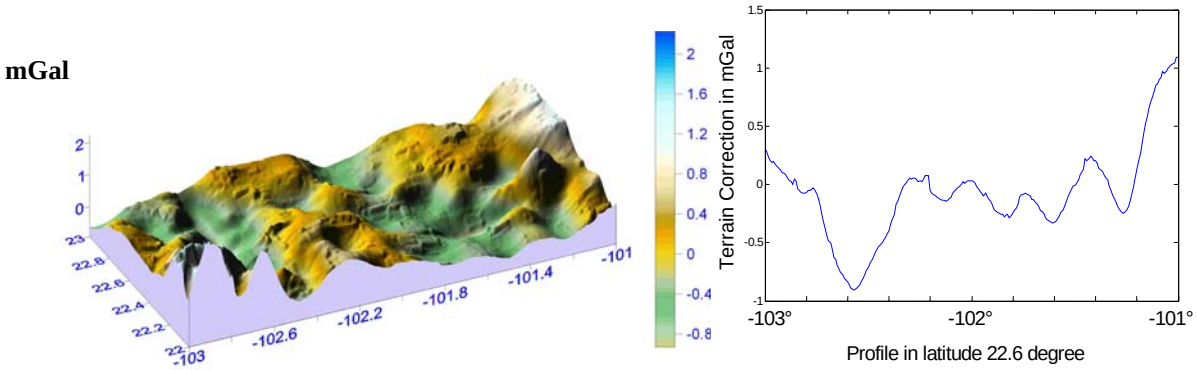


Figure 4.5 Terrain corrections in Zacatecas-Aguascalientes area computed by the well known Prism Integration method.

The terrain correction values are everywhere positive in general, The negative values presented in the Figure 4.5 are caused by planar approximation. In order to fulfill the Stokes condition for the boundary value problem (in the case of airborne gravimetry), gravity data (gravity potential, anomalies or disturbances) from the flight line must be continued downwards onto the geoid. The best way to achieve a stable downward continuation process (in mountain areas) is to use the RTM reduction technique (Forsberg, 1984). If this is used, it may reduce the impact of the short-wavelength components of the Earth's gravity field. Figure 4.6 shows the relationship between the DTM and the reference surface. The reference surface (*MES*) is computed by the filtering of local height data , taking into account the mean values of elevation (Table 4.1) and the resolution of the global spherical harmonic potential expansion (GRAVSOFT Package).

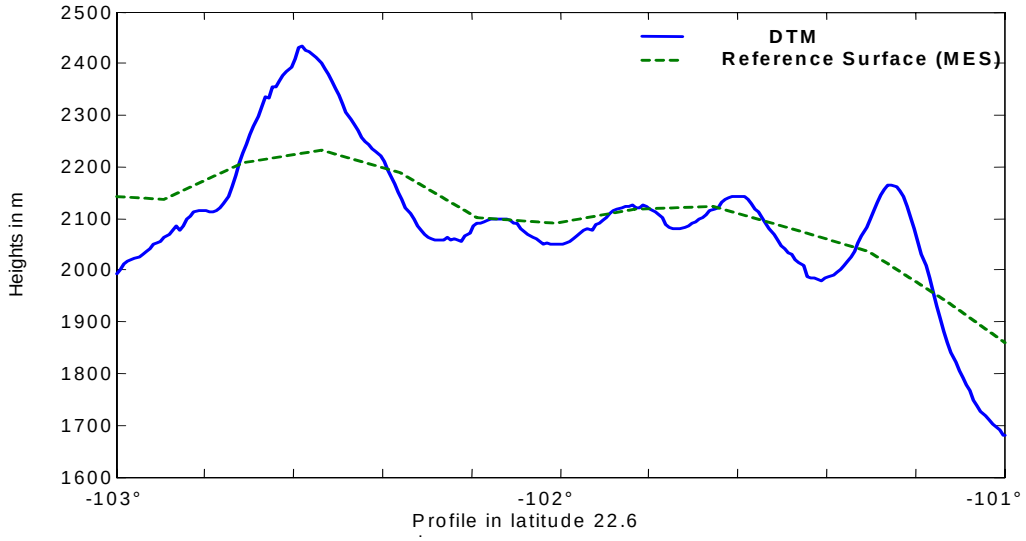


Figure 4.6 Relation between DTM and Mean Elevation Surface in profile $22^0.6$.

| | Min | Mean | Max | St.Dev | RMS |
|---|---|---|---|---|---|
| **MES (m)** | 1859 | 2096 | 2232 | 103.70 | 2100 |
| **DTM (m)** | 1679 | 2096 | 2433 | 143.23 | 2100 |

*Table 4.1 Statistics of the Mean Elevation Surface (MES) Digital Terrain Model (DTM) in the Zacatecas-Aguascalientes area*

Below, Figures 4.7 and 4.8 graphically present the results for the RTM effect computed by the integration method and the well known FFT method. In Figure 4.9, the difference between the two methods can clearly be seen. The shifts between lines, once in the edge of the area and again in the rough topography. Both effects are incoming from the edge and periodicity effect of FFT. We can in fact conclude that these differences are not very large, and therefore cannot have any great impact in geoid undulation. As matter of fact, the DTM in itself (with accuracy of ~25m) does not present the topography with high precision. If we observe the results incoming from the FFT method, and compare them to those from the prism integration method (Table 4.2), it is evident that its advantage lies in its quick calculation time. I is often assumed that the FFT can be a very useful method for most computations where a very dense Digital Terrain Model is available.

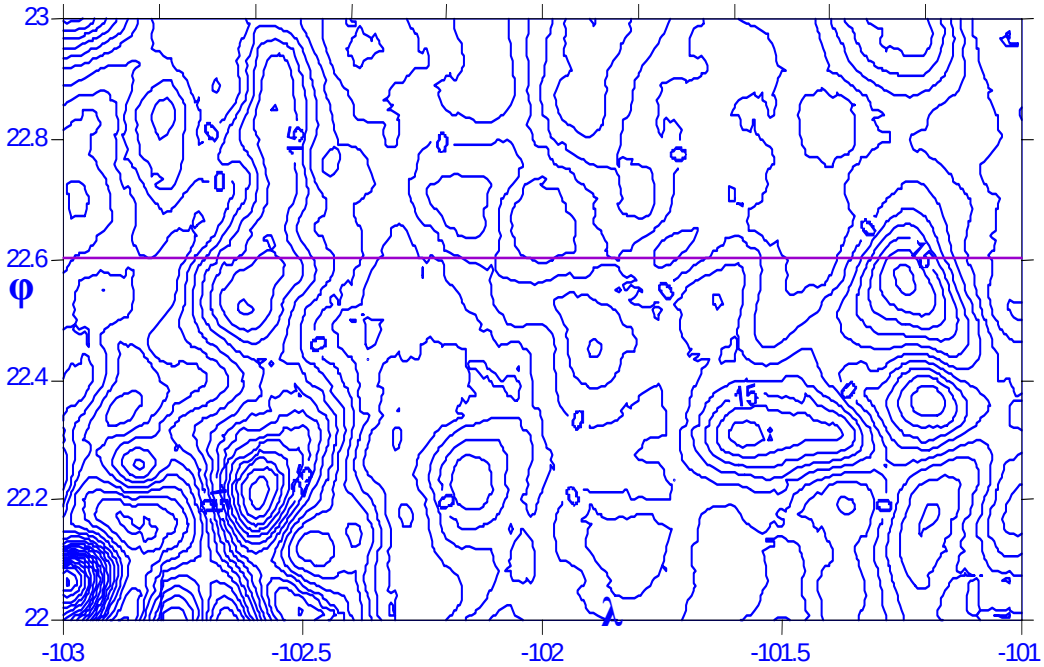


Figure 4.7 RTM effects computed by Prism integration method (Isoline interval=5mGal).

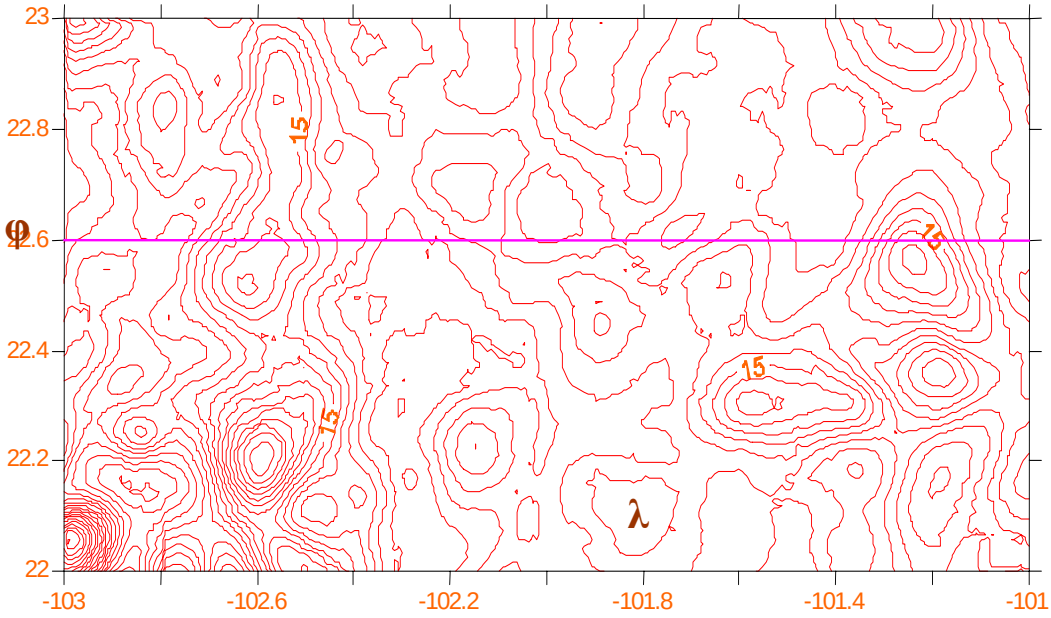


Figure 4.8 RTM effects computed by FFT method (Isoline interval=5mGal)

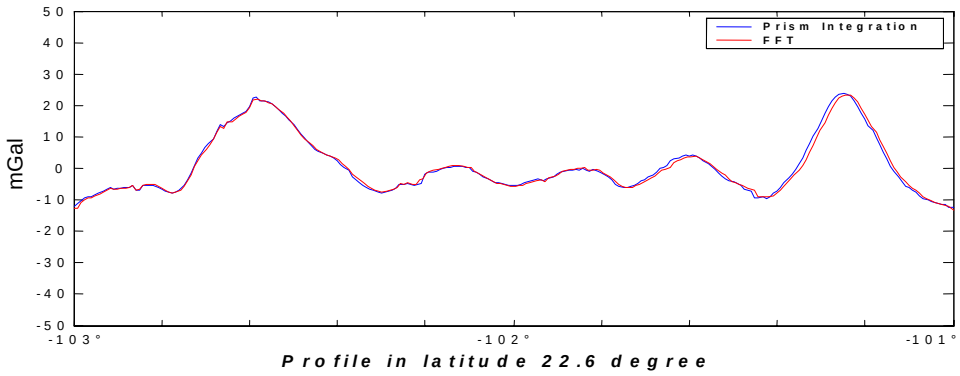


Figure 4.9 Differences between RTM effects computed by FFT method and Integration method

| | Min | Mean | Max | St.Dev | RMS |
|---|---|---|---|---|---|
| **Integration (*mGal*)** | *-12.51* | *0.50* | *23.66* | *9.04* | *9.04* |
| **FFT (*mGal*)** | *-13.87* | *0.36* | *23.24* | *8.94* | *8.93* |
| **Differences (*mGal*)** | *1.36* | *0.14* | *0.42* | *0.80* | *0.81* |
| **DTM (*m*)** | *1679* | *2096* | *2433* | *143.23* | *2100* |

*Table 4.2 Statistics of RTM effects computed by different methods*

In the computation of RTM reduction, it is the determination of the reference frame that plays the essential role. In this work, the reference frame is not only defined by the filtering of local data (with respect to spherical harmonic expansion). Other reference surfaces, such as spheres with different heights and surfaces with EGM96 geoid heights have also been treated and analyzed (Figure 4.10).

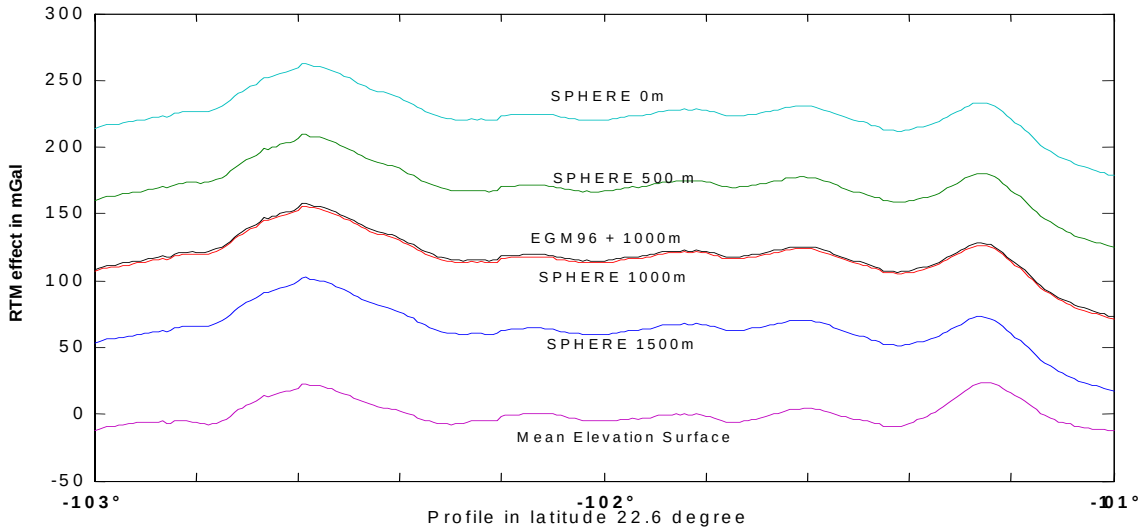


Figure 4.10 RTM effect on different reference surfaces

| | Min (mGal) | Mean (mGal) | Max (mGal) | St.Dev (mGal) | RMS (mGal) |
|---|---|---|---|---|---|
| **Sphere R+H (H=0m)** | *178.70* | *225.04* | *262.45* | *15.76* | *225.59* |
| **Sphere R+H (H=500m)** | *125.22* | *171.71* | *209.27* | *15.82* | *172.44* |
| **H=EGM96+1000m** | *73.01* | *119.75* | *157.48* | *15.90* | *120.80* |
| **Sphere R+H (H=1000m)** | *71.51* | *118.19* | *155.87* | *15.88* | *119.24* |
| **Sphere R+H (H=1500m)** | *17.56* | *64.50* | *102.27* | *15.93* | *66.43* |
| **MES** | *-12.33* | *0.50* | *23.86* | *9.07* | *9.09* |

*Table 4.3 Statistics of the RTM effects computed by different methods*

In analyzing the data statistics of the RTM effect on a sphere of specific elevation, we see that the standard deviation of the effect in different elevations are very close to each other (Table 4.3). In a sphere with 0 elevation as reference surface, we compute the effect of all topography above the geoid. That is to say, we compute at the same time, both terrain correction and thickness of the Bouguer plate. The presented data statistics are the RTM effects computed on the mean elevation surface and spheres of specific elevations. The maximal deviation of the RTM effects computed on different surfaces plus Bouguer-plate correction is not more than 2 mGal (Table 4.4). This deviation is caused by the large distances between computation and integration points. Presented in Figure 4.11 are the deviations between results computed on different reference surfaces and compared to mean elevation surface (MES).

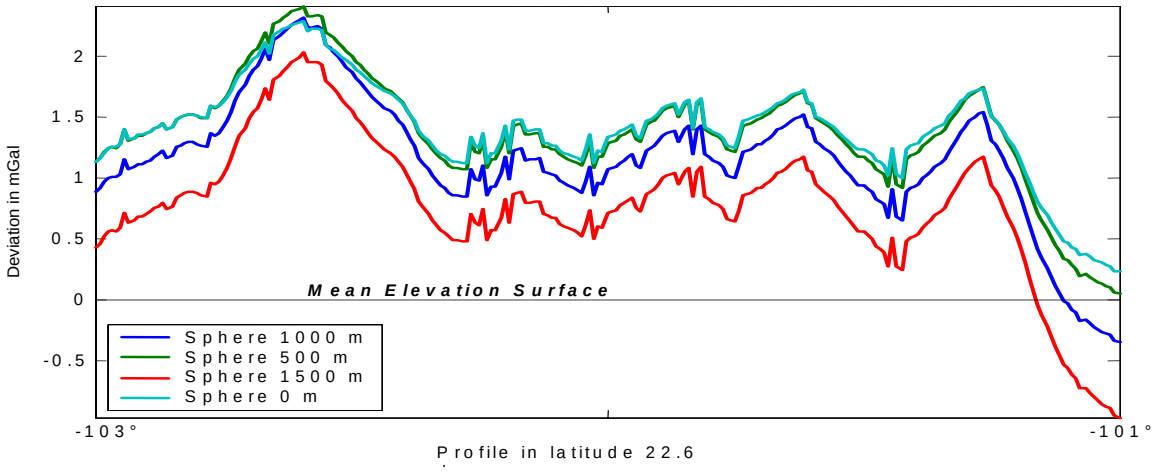


Figure 4.11 Differences of the RTM effect computed on the mean elevation surface and sphere with specific elevation (R+H)

| | **Min** (mGal) | **Mean** (mGal) | **Max** (mGal) | **St.Dev** (mGal) | **RMS** (mGal) |
|---|---|---|---|---|---|
| MES – Sph. 0m + $\Delta g_B$ | *0.23* | *1.40* | *2.28* | *0.41* | *1.46* |
| ***MES – Sph. 500m*** + $\Delta g_B$ | *0.05* | *1.38* | *2.41* | *0.47* | *1.46* |
| ***MES – Sph. 1000m*** + $\Delta g_B$ | *-0.35* | *1.16* | *2.32* | *0.52* | *1.27* |
| ***MES – Sph. 1500m*** + $\Delta g_B$ | *-0.97* | *0.78* | *2.03* | *0.57* | *0.97* |
| ***MES*** | *0* | *0* | *0* | *0* | *0* |

*Table 4.4 Statistics of the RTM effects computed in different surfaces ($\Delta g_B$-Bouguer correction)*

For a suitable downward continuation of airborne gravity data, it is essential and advantageous to use RTM reduction with Mean Elevation Surface. This is due to the fact that the impact of long-wave components of the gravity is small, together with the effect of large differences of DTM heights (Forsberg, 1984).

# 5 Downward continuation of airborne gravity data

## 5.1 Formulation of the problem

The aim of this study, as is mentioned above, is to carry out the best and stable solution for the downward continuation of airborne gravity data to the mean sea level. The data are obtained from the airborne gravimetric survey campaign of Switzerland (Klingele et al. 1996). The input data used for this task are stored in set of 55448 points with gravity disturbances as well as two grids with the gravity disturbances of the resolution of 3'x3' and 5'x5' respectively.
Let's start with a general approach to geodetic boundary value problems for geoid determination. The surface of the geoid can be determined by using Bruns' formula (Moritz, 1980);

$$N = \frac{T}{\gamma}, \tag{5.1}$$

where N is geoid undulation, $\gamma$ is normal gravity at ellipsoid and $T$ representing the disturbing potential on the geoid. The disturbing potential can be formulated as the difference between actual gravity potential $W$ and the normal gravity potential U of a reference ellipsoid

$$T(P) = W(P) - U(P). \tag{5.2}$$

To fulfill the Bruns formula for geoid undulation, we need to reduce the disturbing potential T, from point P in space to the reference point Q (geoid). This process is called *downward continuation*. The main purpose of the downward continuation of disturbing potential T from point P to point Q is to satisfy the following harmonicity condition (Moritz, 1980):

*A function T is harmonic in a space t bounded by S, if it satisfies Laplace's differential equation*

$$\Delta T = 0 \tag{5.3}$$

*at every point of t. This problem of finding the harmonic function from its boundary values on S is called Dirichlet's problem or geodetic boundary value problem.*

In general, it is difficult to find an analytical form of the solution for the boundary surface. For this reason, the best approximation of the boundary surface is a spherical approximation. The explicit solution of Dirichlet's problem for an exterior space is given by Poisson's integral (Heiskanen and Moritz, 1967):

$$V(r,\theta,\lambda) = \frac{R(r^2 - R^2)}{4\pi} \int_{\lambda'=0}^{2\pi} \int_{\theta'=0}^{\pi} \frac{V(R,\theta',\lambda')}{l^3} \sin\theta' d\theta' d\lambda', \tag{5.4}$$

where $l = \sqrt{r^2 + R^2 - 2Rr\cos\psi}$ ; $V$ is a harmonic function and l is the angular distance;

$\psi = \arccos\left[\cos\theta\cos\theta' + \sin\theta\sin\theta'\cos(\lambda - \lambda')\right]$

Gravity disturbances (or anomalies) in the space outside the sphere (upward continuation), can be expressed in terms of the Poisson integral (Nahavandchi and Sjöberg, 2001).

$$\delta g^H = \frac{R}{4\pi.r} \iint_{\sigma} \delta g \; K(r,\psi,R) d\sigma \tag{5.5}$$

Where $K(r,\psi,R)d\sigma$ is Poisson's kernel, defined as:

$$K(r,\psi,R) = \sum_{n=0}^{\infty} (2n+1)\left(\frac{R}{r}\right)^{n+1} P_n(\cos\psi) = R\frac{r^2 - R^2}{l^3}, \tag{5.6}$$

$l = (r^2 + R^2 - 2Rr\cos\Psi)^{\frac{1}{2}}$

where:

$\delta g^H$ - Gravity disturbances at the height H outside the sphere

$\delta g$ - Gravity disturbances at the sphere with radius R

$l$ - Angular distance

r - Geocentric radius of a point outside the sphere

$P_n(\cos\Psi)$ - Legendre polynomials

Equation (5.5) is the basic formula for continuation of gravity disturbances (or anomalies) at any point in the space (r), when the gravity disturbances are known on the surface of the sphere (R).

## 5.2 Downward continuation of disturbing potential by using the iterative solution of Poisson's integral

Formulation of the downward continuation problem by solving the Poisson integral in the iterative way can be achieved starting with the Poisson equation (5.4). The discrete Poisson integral for the point-to-point downward continuation of gravity disturbances can be written as (Martinec et al. 1996)

$$\delta g_i^t = \frac{R}{4\pi(R+H_i)} \sum_i K_{ij} \cdot \delta g_j^g + F_{\delta g} \,, \tag{5.7}$$

where subscripts *t* and *g* stands for on the Earth's surface (flight line) and the geoid, respectively; indices *i* and *j* indicate computation and integration points, respectively; $H_i$ is the height of a computation point; $K_{ij}$ are the kernel coefficients; $F_{\delta g}$ represents the contribution outside the chosen near-zone cap, called the far-zone contribution.

The discrete Poisson integral for the mean-to-mean downward continuation procedure can be expressed as (Vanicek et al. 1996);

$$\overline{\delta g_i^t} = \frac{R}{4\pi(R+H_i)} \sum \overline{\overline{K_{ij}}\,\overline{\delta g_j^g}} + \overline{F_{\delta g}} \,, \tag{5.8}$$

where the single over-bars indicates the mean values of the corresponding variables; the doubly over-bared $K_{ij}$ represent the doubly averaged Poisson's kernel coefficients.

The Seidel iterative method is used to solve the linear system of equation. Let *B* represent the coefficient matrix, and *b* the constant vector (e.g. gravity disturbances on the Earth's surface or flight line), and *x* be the unknown vector (gravity disturbances on the geoid), then discrete Poisson integral equation can written as follows (Martinec, 1998)

$$B \cdot x = b \ . \tag{5.9}$$

By substituting

$$B = I - A, \tag{5.10}$$

where *I* is the identity matrix, then becomes the Jacobi's iteration form (Martinec, 1998):

$$x = A \cdot x + b \,. \tag{5.11}$$

The iterative solution of the above equation can be formulated as follows (Gauss-Seidel iterative procedure):

$$x_1^1 = a_{1,1}x_1^0 + a_{12}x_2^0 + a_{13}x_3^0 + \ldots\ldots\ldots\ldots\ldots + a_{1,n}x_n^0 + b_1, \quad (5.12)$$

$$x_2^1 = a_{2,1}x_1^1 + a_{22}x_2^0 + a_{23}x_3^0 + \ldots\ldots\ldots\ldots\ldots + a_{2,n}x_n^0 + b_2, \quad (5.13)$$

$$x_3^1 = a_{3,1}x_1^1 + a_{32}x_2^1 + a_{33}x_3^0 + \ldots\ldots\ldots\ldots\ldots + a_{3,n}x_n^0 + b_3, \quad (5.14)$$

$$x_n^1 = a_{n,1}x_1^1 + a_{n2}x_2^1 + a_{n3}x_3^1 + \ldots\ldots\ldots\ldots\ldots + a_{n,n}x_n^0 + b_n. \quad (5.15)$$

Where $x^0 = b$. In the iteration process, the most recent x-values are used in improving the subsequent x-values. The second subsequent iterations follow the same approach until the Tchebyshev norm of the difference between two consecutive x-values is smaller than a specified threshold value.

### 5.2.1 Integration

Similar to equation (5.4), the Poisson integral can be expressed as follows (Martinec, 1998):

Denoting the residual disturbing potential for a point *P* in the space with $T^l(r,\Omega) = T\ (r,\Omega) - T^{GM} - T^{TC}$, we may write (for details see Martinec 1998):

$$T^l(r,\Omega) = \frac{1}{4\pi}\int_{\Omega_0} T^l(R,\Omega')\cdot K^l(r,\psi,R)\cdot d\Omega' \quad , \quad (5.16)$$

with the kernel $K^l(r,\psi,R) = K(r,\psi,R) - \sum_{j=0}^{l-1}(2j+1)\left(\frac{R}{r}\right)^{j+1} P_j(\cos\psi)$

$K^l(r,\psi,R)$ - Spheroidal Poisson kernel

$T(r,\Omega)$ - Disturbing potential at the point P (flight line)

$T^l(R,\Omega')$ - Residual disturbing potential at the spheroidal surface

$T^{GM}$ - Contribution of Earth's Geopotential Model (e.g. EGM96)

$T^{TC}$ - Contribution of the Topographical masses

$K(r,\psi,R) = R\frac{r^2 - R^2}{l^3}$ - Spherical Poisson kernel

$\psi$ - Angular distance between geocentric direction $\Omega$ and $\Omega'$

$l$ - Spatial distance between points $(r,\Omega)$ and $(R,\Omega')$

In regional gravity field determination, the integration domain $\Omega_0$ can be divided into near-zone and far-zone sub-domains. The near-zone sub-domain can be created by a spherical cap of a small angular radius ($\psi_0$) surrounding the computation point while the rest of the full solid angle forms the far-zone sub-domain (for details see Martinec and Matyska, 1997). Therefore, Poisson's integral (Eq. 5.4) may be written as the sum of three terms;

$$T^l(r,\Omega) = T_0^l(r,\Omega) + T_{\psi_0}^l(r,\Omega) + T_{\pi-\psi_0}^l(r,\Omega), \tag{5.17}$$

where the first term on the right hand side expresses the contribution to Poisson's integral from the integration point being on the same direction as the computation point. The second term expresses the contribution of integration points lying within the near-zone spherical cap of radius $\psi_0$ (except the point $\Omega' = \Omega$), and the third term expresses the contribution of the far-zone integration points.

### 5.2.2 Discretization

Formulation of the downward continuation problem by using the equation (5.16) can be realized if the function $T^l(r,\Omega)$ satisfies Fredholm's integral equation of the 1st kind (Martinec, 1998):

$$\frac{1}{4\pi}\int_{\Omega_0} T^l(R,\Omega')\cdot K^l(R + H(\Omega),\psi,R)d\Omega' = f(\Omega). \tag{5.18}$$

The discretization of the Fredholm's equation of the 1st kind can be realized forming the regular angular grid of the observations of boundary functional $f(\Omega)$ with grid step $\Delta\Omega = (\Delta\vartheta,\Delta\lambda)$, where $\Delta\vartheta$ and $\Delta\lambda$ are grid steps in latitude and longitude respectively, thus denoting the observation results in a finite set of discrete values $f_i = f(\Omega_i)$, where $i = 1,.....,N$. After that, the functional $T^l(R,\Omega)$, may be parametrized by discrete values $T^l(R_i,\Omega_i)$, evaluated over the same angular grid as observations $f_i$. The practical solution of the equation 5.18 can be realized by transforming them into a system of linear algebric equations. Therefore we may decompose the Poisson integral into three components. The

smallest one, far-zone contribution $T^{l}_{\pi-\psi_0}(r,\Omega)$, is assumed to be computed in advance, before solving a discrete problem. This can be done using global geopotential models as a input variable (For more details see Martinec, 1998).

The discrete form of the equation 5.18 reads (Martinec, 1998):

$$\sum_{j=1}^{N} A_{ij} T^{l}(R,\Omega_j) = f(\Omega_i) - T^{l}_{\pi-\psi_0}(r_i,\Omega_i), \tag{5.19}$$

where $i = 1,.....,N$. The diagonal elements of square $N \times N$ matrix $A_{ij}$ are:

$$A_{ii} = d^{l}(r_i,\psi_0,R) - \frac{1}{4\pi}\sum_{j=1}^{N} \omega_j K^{l}(r_i,\psi_{ij},R), \tag{5.20}$$

where, $\omega_j$ denotes weights and $d^{l}(r,\psi_0,R)$ is given by (Martinec, 1998):

$$d^{l}(r,\psi_0,R) = \frac{1}{2}\left[\frac{r+R}{r}\left(1-\frac{r-R}{l(\psi_0)}\right) - \frac{R}{r}(1-\cos\psi_0) + \sum_{j=1}^{l-1}(2j+1)\left(\frac{R}{r}\right)^{j+1} R_{j0}(\cos\psi_0)\right]. \tag{5.21}$$

The off-diagonal elements $A_{ij}$, for $i \neq j$, reads:

$$A_{ij} = \begin{cases} \dfrac{1}{4}\omega_j K^{l}(r_i,\psi_{ij},R) & if \quad \psi_{ij} \le \psi_0 \\ 0 & otherwise \end{cases}, \tag{5.22}$$

where, $r_i = R + H(\Omega_i)$

## 5.3 Least-squares collocation – Theoretical backgrounds

Least-squares collocation is a method for determining the anomalous gravitational field by a combination of geodetic measurements of different kinds (Moritz, 1980). Consider the anomalous potential *T* at point *P* as a signal to be estimated. The measurements forming vector *l* are arbitrary quantities of the anomalous gravitational field. That is to say, vector *l* is defined by using either gravity anomalies or deflections of the vertical.
These quantities may be represented as a linear functional of the potential *T*, in spherical approximation (Moritz, 1980); see Eq. (2.36)

$$\Delta g = -\frac{\partial T}{\partial r} - \frac{2}{r}T \ , \tag{5.23}$$

The simple linear model for a least-squares fit can be expressed as follows (Moritz, 1980):

$$l_i = L_i \cdot T \ , \tag{5.24}$$

or

$$L = B \cdot T \ , \tag{5.25}$$

where the vector B comprises the partial derivatives $L_i$ :

$$B = \begin{bmatrix} L_1 \\ L_2 \\ \vdots \\ L_q \end{bmatrix} , \tag{5.26}$$

where $L_i$ is a linear operator. Thus the problem is to find *T* if *q* linear functionals $L_i \cdot T$ are given by measurement.
Application of related formulas of the least-squares prediction to the present problem yields (For more details see Moritz, 1980):

$$\hat{T}(P) = \begin{bmatrix} C_{P1} & C_{P2} & \cdots & C_{Pq} \end{bmatrix} \cdot \begin{bmatrix} C_{11} & C_{12} & \cdots & C_{1q} \\ C_{21} & C_{22} & \cdots & C_{2q} \\ \vdots & \vdots & & \vdots \\ C_{q1} & C_{q2} & & C_{qq} \end{bmatrix}^{-1} \begin{bmatrix} l_1 \\ l_2 \\ \vdots \\ l_q \end{bmatrix} . \tag{5.27}$$

The elements $C_{P1,}C_{P2,\ldots\ldots}C_{Pq}$ are covariances obtained from the covariance function $C(d_{pq})$, otherwise, the elements $C_{11,}C_{12,\ldots\ldots}C_{qq}$ are auto-covariance matrices of the vector *l*.

### 5.3.1 Linearization

We shall start from mathematical representation of geodetic measurements as nonlinear functionals. Every geodetic measurement depends on (Moritz, 1980):

a) one or several points in space,
b) the Earth's gravitational field.

The above-mentioned formulations may be written by the following expression:

$$l = F(X, W), \tag{5.28}$$

where, $l$ denotes the measurement under consideration, $W$ stands for the gravity potential and the vector $X$ comprises of the coordinates of the points to which the measurements refer. Every observation $l$ gives an equation of type (5.28). Thus we can obtain a system of funtional equations that are to be solved for the unknown parameters X and the potential function W.

$$\begin{aligned} l_1 &= F_1(X, W) \\ l_2 &= F_2(X, W) \\ &\vdots \\ l_q &= F_q(X, W) \end{aligned}, \tag{5.29}$$

The usual procedure for the linearization of these non-linear equations is the Taylor's method or theorem. The Taylor's theorem is based on the introduction of an approximate value $X_0$ for the vector $X$ and an approximation $U$ to the gravity potential $W$. The function $U$ denotes the normal potential of an equipotential ellipsoid.

After the introduction of the approximate values, we obtain the following expressions:

$$X = X_0 + \delta X, \tag{5.30}$$

$$W = U + T. \tag{5.31}$$

The differences $\delta X = X - X_0$ and T=W-U are considered to be small. Adding these terms to the equation (5.28) we get:

$$l = F(X_0 + \delta X, U + T), \tag{5.32}$$

and the Taylor expansion gives us:

$$l = F(X_0, U) + a^T \delta X + LT, \tag{5.33}$$

$a$ is the column vector of ordinary partial derivatives

$$a_k = \frac{\partial F}{\partial X_k}(X_0, U), \tag{5.34}$$

$a^T$ is the corresponding row vector, so that $a^T \delta X$ is a scalar product. By means of the substitution $\delta l = F(X,W) - F(X_0,U)$, the nonlinear system (5.29) thus becomes the linear system:

$$\begin{aligned} \delta l_1 &= a_1^T \delta X + L_1 T \\ \delta l_2 &= a_2^T \delta X + L_2 T \\ &\vdots \\ \delta l_q &= a_q^T \delta X + L_q T \end{aligned} \quad . \tag{5.35}$$

### 5.3.2 Varitional Principles

According to the equation (5.35), we may replace $\delta l_i$ by $l_i$ and $\delta X$ by $X$, obtaining:

$$\begin{aligned} l_1 &= a_1^T X + L_1 T \\ l_2 &= a_2^T X + L_2 T \\ &\vdots \\ l_q &= a_q^T X + L_q T \end{aligned} \quad , \tag{5.36}$$

Denoting the elements of $l$, $A$ and $B$ with:

$$l = \begin{bmatrix} l_1 \\ l_2 \\ \vdots \\ l_q \end{bmatrix}, \qquad A = \begin{bmatrix} a_1^T \\ a_2^T \\ \vdots \\ a_q^T \end{bmatrix} \quad \text{and} \quad B = \begin{bmatrix} L_1 \\ L_2 \\ \vdots \\ L_q \end{bmatrix}, \tag{5.36a}$$

with these notations, the system (5.36) becomes:

$$l = A \cdot X + B \cdot T \tag{5.37}$$

The above equations hold exactly (within limits of the linearization) if there are no measuring errors. If measuring errors are present, then equation (5.37) gets the form:

$$l = A \cdot X + B \cdot T + n \tag{5.38}$$

where $n$ is the effect of the measuring errors on the observation vector $l$.

## 5.4 Determination of the regional gravity field by means of the least-squares collocation

According to Moritz (1980), a problem is regarded as properly posed if the solution satisfies the following three requirements:

- Existence,
- Uniqueness,
- Stability.

This means that only one solution must exist for arbitrary data and that this solution must depend continuously on the data. If one or more of these requirements are violated, then the solution is deemed improperly posed or an ill-posed problem. This task, the determination of the regional gravity field from regionally bounded measurements at altitude *h*, is a typical ill-posed problem. The potential is a irregular function, which can not be completely described by any finite set of parameters. Otherwise, we have only a finite number of measurements. Hence, there is no unique solution and the second condition is violated.
After the linearization, vector **l** ($q\times1$) of measured geodetic functionals may be described by the following model (Moritz, 1980):

$$AX + BT + n = l \tag{5.39}$$

where $T$ is the disturbing potential; **n** ($q\times1$) is the vector of errors in the measurements **l; X** ($p\times1$) is the vector of $p$ parameters, which describes a systematic part of observations; **A** ($q\times p$) is the matrix of coefficients; **B** is the discrete linear operator formed by $q$ linear functionals $L_i$:

$$B = \begin{pmatrix} L_1 \\ L_2 \\ \vdots \\ L_q \end{pmatrix}, \qquad \text{see Eq. (5.26)} \tag{5.40}$$

It is supposed that $p < q$.

The solution for the disturbing potential $T$ should be obtained in accordance with the general variational principle (Moritz, 1980):

$$\alpha(T,T) + n^T C_{nn}^{-1} n = \min \ , \tag{5.41}$$

where $\alpha > 0$ is the regularization parameter, $\mathbf{C}_{nn}$ is the covariance matrix of the measurement errors, $(T,T)$ is the squared norm of disturbing potential $T$ in Hilbert space with the reproducing kernel $K = K(P,Q)$ (see, Moritz, 1980; Marchenko, 1998). The requirement (5.41) should be provided with observation equations (5.39). This is equivalent to finding of absolute minimum of the functional

$$\Phi_\alpha = \alpha(T,T) + n^T C_{nn}^{-1} n + 2k^T (AX + BT + n - l) \ . \tag{5.42}$$

Minimization (5.42) yields the following estimations

$$X_\alpha = \left[A^T (C_{tt} + \alpha C_{nn})^{-1} A^T (C_{tt} + \alpha C_{nn})^{-1} l\right] \ , \tag{5.43}$$

$$T_\alpha = (BK)^T (C_{tt} + \alpha C_{nn})^{-1} (l - AX_\alpha) \ , \tag{5.44}$$

where $\mathbf{C}_{tt}$ is $(q \times q)$ matrix

$$C_{tt} = B(BK)^T \tag{5.45}$$

with the elements

$$c_{ij} = L_i^P L_j^Q K(P,Q) \tag{5.46}$$

The expression (5.44) allows the determining of the disturbing potential $T$ as a function, which is an element of Hilbert space with reproducing kernel.

### 5.4.1 Determination of gravity functionals in a finite set of points

By introducing the discrete linear operator **S** formed by $m$ linear functionals $S_i$:

$$S = \begin{pmatrix} S_1 \\ S_2 \\ \vdots \\ S_m \end{pmatrix} \ , \text{(see Eq. 5.26)} \tag{5.47}$$

we can apply it to both sides of the expression (5.44):

$$ST_\alpha = S(BK)^T (C_{tt} + \alpha C_{nn})^{-1} (l - AX_\alpha) \tag{5.48}$$

and get the linear estimation

$$s_\alpha = C_{st} (C_{tt} + \alpha C_{nn})^{-1} (l - AX_\alpha) \tag{5.49}$$

of the gravity functionals

$$s = S \cdot T \ . \tag{5.50}$$

In (5.48) $C_{st}$ is ($m$×$q$) matrix

$$C_{st} = S(B \cdot K)^T \tag{5.51}$$

with the elements

$$c_{ki} = S_k^P L_i^Q K(P,Q) \, . \tag{5.52}$$

Now we can see that (5.43) and (5.49) are nothing else but the solutions of the system (Moritz, 1980):

$$A \cdot X + U \cdot s + n = l \tag{5.53}$$

in accordance with the principle

$$\alpha \cdot s^T \cdot C_{ss}^{-1} \cdot s + n^T \cdot C_{nn}^{-1} \cdot n = \min \, . \tag{5.54}$$

In (5.53) **U** is ($q$×$m$) matrix, formed by 2 blocks

$$U = \begin{bmatrix} I & 0 \end{bmatrix} \tag{5.55}$$

where **I** is ($q$×$q$) unit matrix, and **0** is ($q$×($m$-$q$)) zero matrix. It is evident that in such a consideration, first $q$ functionals in the discrete operator in (5.47) coincide with the functionals in the discrete operator in (5.40):

$$S = \begin{pmatrix} S_1 = L_1 \\ S_2 = L_2 \\ \vdots \\ S_q = L_q \\ S_{q+1} \\ \vdots \\ S_m \end{pmatrix} \tag{5.56}$$

and the following connection is valid:

$$B = U \cdot S \, . \tag{5.57}$$

In other words, vector **s** may be represented in the form

$$s = \begin{pmatrix} t \\ h \end{pmatrix} \tag{5.58}$$

Where

$$t = B \cdot T = U \cdot s \tag{5.59}$$

$$h = H \cdot T \tag{5.60}$$

and the discrete linear operator $H$ contains $m–q$ linear functionals $S_{q+1}, S_{q+2}, \ldots\ldots S_m$ :

$$H = \begin{pmatrix} S_{q+1} \\ S_{q+2} \\ \vdots \\ S_m \end{pmatrix} \tag{5.61}$$

In view of this consideration, we can write

$$C_{ss} = \begin{bmatrix} C_{tt} & C_{th} \\ C_{ht} & C_{hh} \end{bmatrix} \tag{5.62}$$

$$C_{st} = \begin{bmatrix} C_{tt} \\ C_{ht} \end{bmatrix} \tag{5.63}$$

As a result of the last expression we can split (5.49) into 2 parts:

$$t_\alpha = C_{tt}(C_{tt} + \alpha C_{nn})^{-1}(l - AX_\alpha) \tag{5.64}$$

$$H_\alpha = C_{ht}(C_{tt} + \alpha C_{nn})^{-1}(l - AX_\alpha) \tag{5.65}$$

Together with (5.43), expression (5.64) provides smoothing of gravity functionals at the data points, whereas expression (5.65) provides predictions (interpolation) of the functionals between data points. In the considered discrete formulation, all matrixes $C_{ss}, C_{tt}, C_{hh}, C_{ht} = C_{th}^T$ are treated as the covariance matrixes, and the reproducing kernel $K(P,Q)$ is treated as the covariance function of disturbing potential $T$ (Moritz, 1980). In this view, the expressions (5.45), (5.46) and (5.51), (5.52) provide covariance propagation rule that allows compute covariance functions between various functionals of disturbing potential. Estimations of the accuracy of (5.43), (5.49) may be obtained by the standard way, as it was done by Moritz (1980) for the least-squares collocation. However, due to existence $\alpha \neq 1$ we get more complicated expressions for corresponding covariance matrixes of errors:

$$E_{xx}^{\alpha} = N_{\alpha}^{-1} - (\alpha - 1) G_{\alpha}^{T} C_{nn} G_{\alpha} \tag{5.66}$$

$$E_{ss}^{\alpha} = C_{ss} - C_{st} L_{\alpha} C_{ts} - (\alpha - 1) C_{st} L_{\alpha} C_{ts} \tag{5.67}$$

where

$$N_{\alpha} = A^{T} \overline{C}_{\alpha}^{-1} A \tag{5.68}$$

$$G_{\alpha} = N_{\alpha}^{-1} A^{T} \overline{C}_{\alpha}^{-1} \tag{5.69}$$

$$L_{\alpha} = \overline{C}_{\alpha}^{-1} (I - A G_{\alpha}) = L_{\alpha}^{T} \tag{5.70}$$

$$\overline{C}_{\alpha} = C_{tt} + \alpha C_{nn} . \tag{5.71}$$

With the notations (5.68) – (5.70), the estimations (5.43), (5.64), (5.65) may be written in the form

$$X_{\alpha} = G_{\alpha} l \tag{5.72}$$

$$t_{\alpha} = C_{tt} L_{\alpha} l \tag{5.73}$$

$$h_{\alpha} = C_{ht} L_{\alpha} l \tag{5.74}$$

It is obvious that for $\alpha = 1$ these expressions are nothing else but solutions obtained in the frames of classical least-squares collocation method. In practice, where the systematic part is absent ( $X \equiv 0$ ), the model (5.53) becomes

$$t + n = U \cdot s + n = l \tag{5.75}$$

and the estimations (5.73), (5.74), and (5.67) transform into

$$t_{\alpha} = C_{tt} \overline{C}_{\alpha}^{-1} l \tag{5.76}$$

$$h_{\alpha} = C_{ht} \overline{C}_{\alpha}^{-1} l \tag{5.77}$$

$$E_{ss}^{\alpha} = C_{ss} - C_{st} \overline{C}_{\alpha}^{-1} C_{ts} - (\alpha - 1) C_{st} \overline{C}_{\alpha}^{-1} C_{nn} \overline{C}_{\alpha}^{-1} C_{ts} . \tag{5.78}$$

### 5.4.2 Determination of the regularization parameter

The traditional approach to the determination of the regularization parameter is based on the misclosure principle (Tikhonov and Arsenin, 1986; Neyman, 1979; Morozov, 1987). This principle allows for the determining of $\alpha$ in an agreement with a priori estimations of measured data errors. According to Morozov (1987) there are two additional principles for the determination of the regularization parameter. These are the quasi-solution principle, which allows $\alpha$ to be determined in agreement with a priori estimation of solution norm, and the so-called principle of the smoothing functional, based on the fitting of $\alpha$ to a priori known estimations of the functional (5.54).
In general, all mentioned principles use a priori information about corresponding norms. Obviously, in the case considered in the previous section we have such information by means of corresponding covariance matrixes. Therefore, a technique for the determination of the regularization parameter may be based on the application of these matrixes. Such an approach developed by Abrikosov (1999b), where, the formulas for computation $\alpha$ were derived on the basis of the estimation (5.76) correspondingly to the three above-mentioned principles.

#### 5.4.2.1 Misclosure principle

We should keep in mind that in model (5.75) the noise vector **n** is characterized by the a priori covariance matrix $C_{nn}$ whereas the estimation of the misclosure

$$n_\alpha = \alpha C_{nn} \overline{C}_\alpha^{-1} l \tag{5.79}$$

is characterized by the a posteriori covariance matrix

$$\hat{C}_{nn} = \alpha^2 C_{nn} \overline{C}_\alpha^{-1} (C_{tt} + C_{nn}) \overline{C}_\alpha^{-1} C_{nn} \ , \tag{5.80}$$

which may be derived in an elementary way by applying the famous covariance propagation rule (Moritz, 1980) to the estimation (5.79). Thus, the next condition was considered

$$\left\| C_{nn} - \hat{C}_{nn} \right\| = \left\| \Delta C_{nn}(\alpha) \right\| = \min \tag{5.81}$$

Here the norm is the Euclidean matrix norm (Horn and Johnson, 1986):

$$\left\| A \right\|^2 = trace(A^T A) = trace(A A^T) \tag{5.82}$$

and **A** is a real matrix of general kind. After some obvious transformations, the residual matrix $\Delta C_{nn}(\alpha)$ was represented in the form

$$\Delta C_{nn}(\alpha) = C_{tt}\overline{C}_{\alpha}^{-1} D_n(\alpha)\overline{C}_{\alpha}^{-1} C_{nn} \tag{5.83}$$

where

$$D_n(\alpha) = -\alpha^2 C_{nn} + 2\alpha C_{nn} + C_{tt} \tag{5.84}$$

As a result, the condition (5.81) was transformed to

$$\left\| D_n(\alpha) \right\| = \min \tag{5.85}$$

and the following values of the regularization parameter were derived:

$$\alpha = 1 + \sqrt{1 + \frac{trace(C_{tt}C_{nn})}{trace(C_{nn}C_{nn})}} \tag{5.86}$$

#### 5.4.2.2 Quasi-solution principle

Another principle, which can be used for the determination of the regularization parameter, is the so-called quasi-solution principle (Abrikosov, 1999b), which is connected with a priori information about the size of the domain that contains the solution. In our case, such information is provided by the a-priori covariance matrix of the signal vector **t** together with the a-posteriori covariance matrix of the estimation (5.76):

$$\hat{C}_{tt} = C_{tt}\overline{C}_{\alpha}^{-1}(C_{tt} + C_{nn})\overline{C}_{\alpha}^{-1} C_{tt} \tag{5.87}$$

On this ground, the condition appears

$$\left\| C_{tt} - \hat{C}_{tt} \right\| = \left\| \Delta C_{tt}(\alpha) \right\| = \min \tag{5.88}$$

where the residual matrix $\Delta C_{tt}(\alpha)$ was represented in the form

$$\Delta C_{tt}(\alpha) = C_{nn}\overline{C}_{\alpha}^{-1} D_t(\alpha)\overline{C}_{\alpha}^{-1} C_{tt} \tag{5.89}$$

$$D_t(\alpha) = -\alpha^2 C_{nn} + 2\alpha C_{tt} + C_{tt} \tag{5.90}$$

Thus, the condition (5.88) was transformed to

$$\left\| D_t(\alpha) \right\| = \min \tag{5.91}$$

and the following recursive formula was derived

$$\alpha = \frac{trace(C_{tt}C_{tt}) + \alpha \cdot trace(C_{tt}C_{nn})}{\alpha^2 \cdot trace(C_{nn}C_{nn}) + 3 \cdot \alpha \cdot trace(C_{tt}C_{nn}) + 2 \cdot trace(C_{tt}C_{tt})} \tag{5.92}$$

with the starting value $\alpha = 0$. It was shown that the value of the regularization parameter belongs to the interval

$$0 < \alpha < \frac{1}{2}. \tag{5.93}$$

### 5.4.2.3 Smoothing functional principle

The third principle, which was considered for the determination of the regularization parameter, is the so-called smoothing functional principle (Abrikosov, 1999b), which is provided by the joint application of the misclosure and quasi-solution principles. In our case it is equivalent to the condition

$$\left\| D_n(\alpha) \right\|^2 = \left\| D_t(\alpha) \right\|^2 = \min. \tag{5.94}$$

For this minimum the recursive formula was derived

$$\alpha = \frac{f_1(\alpha)}{2 \cdot f_2(\alpha)} \ , \tag{5.95}$$

which starts from the value $\alpha$=0. In (5.95):

$$\begin{aligned} f_1(\alpha) = 4 \cdot \alpha^3 \cdot trace(C_{nn}C_{nn}) + 3 \cdot \alpha^2 \left( trace(C_{tt}C_{nn}) - trace(C_{nn}C_{nn}) \right) \\ + trace(C_{tt}C_{tt}) - trace(C_{tt}C_{nn}) \end{aligned} \tag{5.96}$$

$$\begin{aligned} f_2(\alpha) = 3 \cdot \alpha^2 \cdot trace(C_{nn}C_{nn}) + 3 \cdot \alpha \left( trace(C_{tt}C_{nn}) - trace(C_{nn}C_{nn}) \right) \\ + trace(C_{tt}C_{tt}) - trace(C_{tt}C_{nn}) + trace(C_{nn}C_{nn}) \end{aligned} \tag{5.97}$$

### 5.4.3 Construction of covariance functions

The determination of the covariance function of the disturbing potential $T$ plays a fundamental role for a successful application of the least-square collocation technique.
Let $\widetilde{T}$ be an approximate element of $T$ in a Hilbert space $H_2^q(\Sigma)$, with the reproducing kernel computed from a finite set of measurements or geodetic functionals. The solution of the inverse problem can then be done in the model approach as well as in the operational approach to physical geodesy, both requiring a suitable parametrization of the potential $\widetilde{T}$ (Lelgemann and Marchenko, 2001). The operational approach is connected closely to the least-squares collocation method (or variational method) and requires a preliminary (a priori) study of the Earth's gravity field. The inclusion of this a priori information in the form of the covariance function of $T$ provides the solution of the inverse problem and at the same time optimal linear estimation (Marchenko, 1998).

### 5.4.4 Bjerhammar sphere and Kelvin transformation

The kernel function can be represented in the form of an infinite series in the following way (Krarup, 1969):

$$K^q(P,Q) = \sum_{m=1}^{\infty} k_m^q \cdot \sigma^{m+1} P(\cos\psi_{PQ}) \quad , \tag{5.98}$$

where:

$\sigma = \dfrac{R_B^2}{r_P r_Q}$ - Relationship between radius of the Bjerhammar sphere ($R_B$) and radius-vectors ($r_P$, $r_Q$) of the external point $P$ and $Q$.

$\psi_{PQ}$ - Spherical distance between radius vectors $r_P$ and $r_Q$.

$P_m(\cos\psi_{PQ})$ - Legendre's polynomial of degree $m$

$k_m^q \geq 0$ - Non-negative coefficients

The additional relationship is an asymptotic equality (Marchenko, 1998):

$$k_m^q \sim \frac{c_q}{m^{2(q-1)}}, \qquad c_q = const. \tag{5.99}$$

Where $q$ corresponds to the index $q$ of the Sobolev space $H_2^q(\Sigma)$ of the harmonic functions in the domain $\Sigma$ outside the Bjerhammar sphere. The index can be also used for a certain

classification of the kernel functions of $H_2^q(\Sigma)$, since the asymptotic equality (5.99) defines practically the behavior of $K^q(P,Q)$ in the case that $R_B$ is fixed. In the case that the coefficients $k_m^q$ are equal to the empirical degree variances of the disturbing potential *T*, then such kernel function of $H_2^q(\Sigma)$ coincides with the covariance function of *T* (Marchenko, 1998). The Kelvin transformation, with respect to the Bjerhammar sphere, can be expressed by the following relations (Marchenko, 1998):

$$R_B^2 = l_{\tilde{Q}} \cdot r_Q, \tag{5.100}$$

it follows

$$\sigma = \frac{l_{\tilde{Q}}}{r_P}\ , \tag{5.101}$$

that can be derived by means of the Kelvin transformation of the point $Q$ into the point $\tilde{Q}$ with respect to the Bjerhammar sphere (see Figure 5.1). After substitution of the equation (5.101) into (5.98), it reads (Marchenko, 1998):

$$K^q(P, l_{\tilde{Q}}) = \sum_{m=1}^{\infty} k_m^q \left(\frac{l_{\tilde{Q}}}{r_P}\right)^{m+1} P_m(\cos\psi_{PQ})\ , \tag{5.102}$$

where $l_{\tilde{Q}}$ is the distance between the origin *0* and the internal point $\tilde{Q}$.

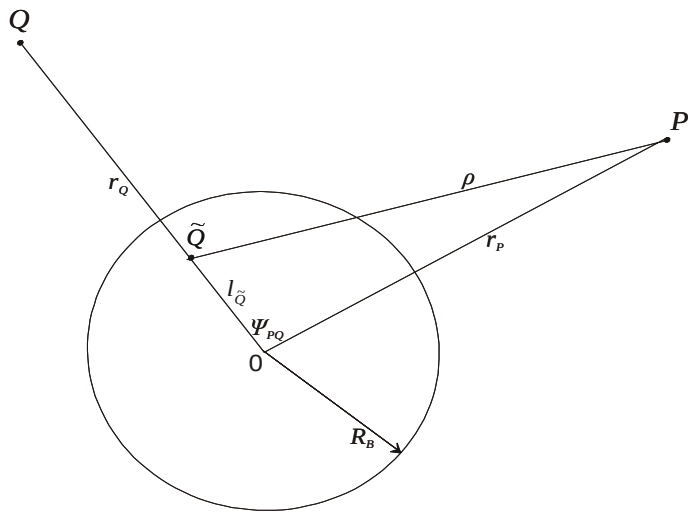


Figure 5.1 Kelvin transformation with respect to Bjerhammar sphere

### 5.4.5 Reproducing kernels of point potentials

According to Marchenko (1987), the kernel functions can be derived by using the potentials of radial multipoles as point harmonic functions and by applying the Kelvin transformation respectively. The corresponding kernel reads:

$$\tilde{v}_n(P,Q) = \sum_{m=n}^{\infty} \binom{m}{n} \cdot \sigma^{m+1} P_m(\cos\psi_{PQ}) \,. \tag{5.103}$$

The analytical covariance function (ACF) of the disturbing potential *T* can be written in the following form (Marchenko, 1998):

$$K(P,Q) = K_n(P,Q) = \left(\frac{GM}{R}\right)^2 \cdot \alpha_n \cdot \sigma^{n+1} \cdot v_n \tag{5.104}$$

where *GM* is the Earth's gravitational constant; *R* is the Earth's mean radius; $\alpha_n$ is an arbitrary dimensionless factor, which should be found from empirical data (see below);

$$\sigma = \frac{R_B^2}{r_P r_Q}, \tag{5.105}$$

$R_B$ is the Bjerhammar sphere radius; $v_n$ is the dimensionless potential of the radial multipole of degree *n*:

$$v_n = \frac{1}{n!}\frac{\partial^n}{\partial\sigma}\left(\frac{1}{L}\right), \tag{5.106}$$

where, $L = \sqrt{1+\sigma^2 - 2\sigma\cdot\cos\psi_{PQ}}$ .

These potentials may be computed by means of the recursive formulas

$$\left.\begin{aligned} v_0 &= \frac{1}{L}, \\ v_1 &= \frac{\cos\psi_{PQ} - \sigma}{L^3}, \\ nL^2 v_n &= (2n-1)(\cos\psi_{PQ} - \sigma)v_{n-1} - (n-1)v_{n-2} \end{aligned}\right\} \tag{5.107}$$

### 5.4.6 Covariance functions of disturbing potential

By applying the corresponding linear operators to the function (5.104), we get analytical covariance functions for various linear functionals of disturbing potential *T*:

$$\mathrm{cov}_n(T_P, T_Q) = K_n(P,Q) = \left(\frac{GM}{R}\right)^2 \cdot \alpha_n \cdot \sigma^{n+1} \cdot v_n \quad , \tag{5.108}$$

$$\mathrm{cov}_n(N_P, N_Q) = \frac{1}{\gamma_P \gamma_{\tilde{Q}}} K_n(P,Q) = \left(\frac{GM}{R}\right)^2 \cdot \frac{\alpha_n}{\gamma_P \gamma_{\tilde{Q}}} \cdot \sigma^{n+1} \cdot v_n \ , \tag{5.109}$$

$$\begin{aligned} \mathrm{cov}_n(\Delta g_P, \Delta g_Q) &= \left(-\frac{\partial}{\partial r} - \frac{2}{r}\right)_P \left(-\frac{\partial}{\partial r} - \frac{2}{r}\right)_Q K(P,Q) \\ &= \left(\frac{GM}{R}\right)^2 \cdot \frac{\alpha_n}{r_P r_Q} \cdot \sigma^{n+1} \cdot w_n \end{aligned} \quad , \tag{5.110}$$

$$\mathrm{cov}_n(T_P, N_Q) = \frac{1}{\gamma_{\tilde{Q}}} K_n(P,Q) = \left(\frac{GM}{R}\right)^2 \cdot \frac{\alpha_n}{\gamma_{\tilde{Q}}} \cdot \sigma^{n+1} \cdot v_n , \tag{5.111}$$

$$\begin{aligned} \mathrm{cov}_n(T_P, \Delta g_Q) &= \left(-\frac{\partial}{\partial r} - \frac{2}{r}\right)_Q K(P,Q) \\ &= \left(\frac{GM}{R}\right)^2 \cdot \frac{\alpha_n}{r_Q} \cdot \sigma^{n+1} \cdot g_n \end{aligned} \quad , \tag{5.112}$$

$$\begin{aligned} \mathrm{cov}_n(N_P, \Delta g_Q) &= \frac{1}{\gamma_P}\left(-\frac{\partial}{\partial r} - \frac{2}{r}\right)_Q K(P,Q) \\ &= \left(\frac{GM}{R}\right)^2 \cdot \frac{\alpha_n}{\gamma_P r_Q} \cdot \sigma^{n+1} \cdot g_n \end{aligned} \quad , \tag{5.113}$$

where;

$$g_n = (n+1)\sigma \cdot v_{n+1} + (n-1)v_n \ , \tag{5.114}$$

$$w_n = (n+1)\sigma \cdot g_{n+1} + (n-1)g_n\,, \tag{5.115}$$

and the following relationships are valid for the functions $v_n, g_n, w_n$:

$$\frac{\partial v_n}{\partial \sigma} = (n+1)v_{n+1}\,, \tag{5.116}$$

$$\frac{\partial g_n}{\partial \sigma} = (n+1)g_{n+1}\,, \tag{5.117}$$

$$\frac{\partial w_n}{\partial \sigma} = (n+1)w_{n+1}\,. \tag{5.118}$$

### 5.4.7 Determination of the parameters of covariance functions

Unknown parameters in covariance function equation (5.108) until (5.113) are the degree *n*, the radius $R_B$ of the Bjerhammar sphere and the coefficient $\alpha_n$. Their values can be determined by introducing three essential parameters of ACF (Moritz, 1980) and preliminary computation of empirical essential parameters. The formulae (5.108) – (5.110), (5.114), (5.115) lead to the following expressions of these parameters;

Firstly, the *variances* $C(*,*) = C_n(*,*)$ are expressed by

$$C_n(T_P, T_P) = \left(\frac{GM}{R}\right)^2 \cdot \alpha_n \cdot \left(\frac{\sigma}{1-\sigma}\right)^{n+1}, \tag{5.119}$$

$$C_n(N_P, N_P) = \left(\frac{GM}{R}\right)^2 \cdot \frac{\alpha_n}{\gamma_P^2} \cdot \left(\frac{\sigma}{1-\sigma}\right)^{n+1}, \tag{5.120}$$

$$C_n(\Delta g_P, \Delta g_P) = \left(\frac{GM}{R}\right)^2 \cdot \frac{\alpha_n}{r_P^2} \cdot \left(\frac{\sigma}{1-\sigma}\right)^{n+1} \left[4 - \frac{n+1}{1-\sigma}\left(3 - \frac{n+2\sigma}{1-\sigma}\right)\right]. \tag{5.121}$$

Secondly, the *correlation length* $\xi$ is such spherical distance $\psi_{PQ}$, which satisfies the well-known condition

$$\mathrm{cov}(*_P, *_Q)_{\psi_{PQ}=\xi} = \frac{1}{2} \cdot C(*,*) \ . \tag{5.122}$$

This relationship practically represents the non-linear equation with respect to the radius of the Bjerhammar sphere ($R_B$). It is obvious that equation (5.122) does not contain the parameter $\alpha_n$ and for this reason it admits the determination of $R_B$ independently on $\alpha_n$.

Thirdly, the *curvatures (for* $\psi_{PQ}$ *=0) or variances of the horizontal gradient* $G(*,*)$ are expressed by:

$$G_n(T_P, T_P) = \left(\frac{GM}{R}\right)^2 \cdot \alpha_n \cdot \frac{(n+1)\cdot(n+2\sigma)}{2(1-\sigma)^2} \cdot \left(\frac{\sigma}{1-\sigma}\right)^{n+1} , \tag{5.123}$$

$$G_n(N_P, N_P) = \left(\frac{GM}{R}\right)^2 \cdot \frac{\alpha_n}{\gamma_P^2} \cdot \frac{(n+1)\cdot(n+2\sigma)}{2(1-\sigma)^2} \cdot \left(\frac{\sigma}{1-\sigma}\right)^{n+1} , \tag{5.124}$$

$$\begin{aligned} G_n(\Delta g_P, \Delta g_P) = \left(\frac{GM}{R}\right)^2 \cdot \frac{\alpha_n}{r_P^2} \cdot \left(\frac{\sigma}{1-\sigma}\right)^{n+1} \frac{n+1}{2(1-\sigma)^2} * \\ * \left\{ 16n + 18\sigma - \frac{n+3}{1-\sigma} \cdot \left[ 11n + 18\sigma - \frac{(n+4)(n+2\sigma)}{1-\sigma} \right] \right\} \end{aligned} \tag{5.125}$$

The computation of analytical covariance function (ACF) parameters (with a fixed degree *n*) may consist of the following steps. Determination of the radius of the Bjerhammar sphere ($R_B$) for the fixed degree *n* by comparing the correlation length $\xi$ of the empirical covariance function (ECF) with the analytical covariance function (equation 5.122).

Determination of $\alpha_n$ for the same fixed degree *n* by comparing the variance $C(*,*)$ of ECF with ACF (and the variance of the horizontal gradient $G(*,*)$ if we have an empirical estimation of this value). Next, those parameters may be improved by means of least squares fitting to the ECF discrete values by analogy with the improvement of the parameters of the radial multipoles (Section 5.5). In this case we should solve two systems independently: the first one is the linearized system regarding correction $\delta\sigma$ to an approximate value of the parameter $\sigma$:

$$(n+1)\left[\frac{f_{n+1}(\psi_{PQ})}{f_n(\psi=0)} - \frac{f_{n+1}(\psi=0)}{f_n(\psi=0)} \cdot \frac{f_n(\psi_{PQ})}{f_n(\psi=0)}\right]\delta\sigma = \bar{f}(\psi_{PQ}) - \frac{f_n(\psi_{PQ})}{f_n(\psi=0)} , \tag{5.126}$$

where $f_n$ denotes one of functions $v_n$ or $w_n$; $\bar{f}(\psi_{PQ})$ is the normalized value of the corresponding ECF $f(\psi_{PQ})$ referred to the spherical distance $\psi_{PQ}$:

$$\bar{f}(\psi_{PQ}) = \frac{f(\psi_{PQ})}{f(0)} \ . \tag{5.127}$$

The second system is one of the linear systems

$$\left(\frac{GM}{R}\right)^2 \cdot \alpha_n \cdot \sigma^{n+1} \cdot v_n(\psi_{PQ}) = f(\psi_{PQ}) , \tag{5.128}$$

$$\left(\frac{GM}{R}\right)^2 \cdot \frac{\alpha_n}{\gamma_P \gamma_{\tilde{Q}}} \cdot \sigma^{n+1} \cdot v_n(\psi_{PQ}) = f(\psi_{PQ}) \ , \tag{5.129}$$

$$\left(\frac{GM}{R}\right)^2 \cdot \frac{\alpha_n}{r_P r_{\tilde{Q}}} \cdot \sigma^{n+1} \cdot w_n(\psi_{PQ}) = f(\psi_{PQ}) . \tag{5.130}$$

which should be solved regarding the unknown coefficient $\alpha_n$. Thus, step-by-step we can establish an optimal degree *n* of ACF as such degree for which a desired accuracy of the approximation of ECF by ACF is achieved.

### 5.4.8 Construction of an empirical covariance function

The empirical covariance function for a gravity data set $l_k$ may be constructed in a similar way as an empirical isotropic function in SMA algorithm (Section 5.5).
Let us split the maximal spherical distance $\psi$ between data points onto segments of size $\Delta\psi$:

$$\left[(j-1)\Delta\psi,\ j\Delta\Psi\right] , \qquad j=1,2,\ldots\ldots \tag{5.131}$$

The size $\Delta\psi$ of the segments may be obtained from the following consideration. Let us have *M* data points at a region bounded by spherical latitudes $\varphi_S$, $\varphi_N$ and longitudes $\lambda_W$, $\lambda_E$. The area of the region is equal on unit sphere to

$$S_R = 2(\lambda_E - \lambda_W)\cos\frac{\varphi_N + \varphi_S}{2}\sin\frac{\varphi_N - \varphi_S}{2} , \tag{5.132}$$

and the density of data distribution is

$$\delta_R = \frac{M}{S_R}. \tag{5.133}$$

Now we assume that any data point is located within a spherical cap of angular size $\frac{\Delta\psi}{2}$. Obviously, the area of a such cap is equal on unit sphere to

$$S_C = 2\pi\left(1-\cos\frac{\Delta\psi}{2}\right), \tag{5.134}$$

and the density of data distribution is

$$\delta_C = \frac{1}{S_C}\ . \tag{5.135}$$

Thus, the requirement

$$\delta_C = \delta_R\ , \tag{5.136}$$

may be considered for the computation of $\Delta\psi$. As a result, we get

$$\Delta\psi = 2\arccos\left(1-\frac{\lambda_E-\lambda_W}{\pi M}\cos\frac{\varphi_N+\varphi_S}{2}\sin\frac{\varphi_N-\varphi_S}{2}\right). \tag{5.137}$$

Note, that this formula may be used also for the construction of empirical isotropic functions in SMA method (Section 5.5). By the averaging of the products $l_i l_k$ over the azimuth within each segment separately we can find the discrete values

$$\begin{cases} f(0) = \dfrac{1}{M}\displaystyle\sum_{i=1}^{M} l_i^2 \\ f(\psi_j) = \dfrac{1}{m_j} \displaystyle\sum_{(j-1)\Delta\psi \le \psi_{ik} \le j\Delta\psi} l_i l_k, \quad (j=1,2,....) \end{cases}, \tag{5.138}$$

where the arguments $\psi_j$ are averaged spherical distances between the pairs of data points within each segment

$$\psi_{ij} = \frac{1}{m_j}\sum_{(j-1)\Delta\psi \le \psi_{ik} \le j\Delta\psi}, \quad (j=1,2,\ldots\ldots) \tag{5.139}$$

and $m_j$ is the number of pairs of data within each segment

$$m_j = \sum_{(j-1)\Delta\psi \le \psi_{ik} \le j\Delta\psi} , (j=1,2,\ldots\ldots) \tag{5.140}$$

For further approximation of ECF by ACF we should assume that all values (5.132) are referring to the geocentric distance

$$r_0 = \sqrt{\frac{1}{M}\sum_{k=1}^{M} r_k^2} . \tag{5.141}$$

## 5.5 Downward continuation of disturbing potential by combination of the Sequential multipole analysis and LSC in Bjerhammar-Krarup Model

The Runge-Krarup theorem is formulated as:
*The function $\Gamma$ is harmonic outside the Earth's surface p and regular at infinity as well as the sphere $\sigma_B$ (Bjerhammar sphere or regularization sphere) located inside the Earth. There are a sequence of functions $\Gamma_n$, harmonic outside $\sigma_B$ and regular at infinity, converging uniformly to the function $\Gamma$ on and outside an auxiliary surface p'(with finite curvature), which may be arbitrarily close to and surrounding completely the Earth's surface p.* (Krarup 1969, Moritz 1980, Freeden et al. 1997).

### 5.5.1 Approximation of disturbing potential by Sequential Multipole Analysis (SMA)

In this study we should use the gravity disturbances as input for the approximation of the disturbing potential *T* in the frame of the sequential multipole analysis (SMA) technique and the least-square collocation with regularization.

#### 5.5.1.1 Representation of the gravity disturbances by potentials of radial multipoles

According to Marchenko (1998), the representation of the disturbing potential *T* by potentials of non-central radial multipoles can be derived in following way:
*Each multipole represents a special point object located at point i inside the Bjerhammar sphere. The potential of a non-central radial multipole is characterized by the degree $n_i$ and by the geocentric spherical coordinates $d_i, \varphi_i, \lambda_i$ that are geocentric distances, latitude and longitude, respectively.*

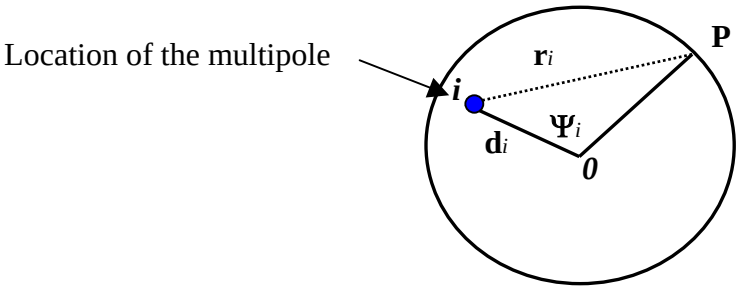


Figure 5.2 Non-central radial multipoles

Figure 5.2 shows a disturbing potential *T*, which can be represented at any external point P with the geocentric spherical coordinates *r*, $\varphi$, $\lambda$, by a convergent series of non-orthogonal harmonic functions

$$T(P) = T(r,\varphi,\lambda) = \frac{GM}{r}\sum_{i=1}^{\infty}\mu_i^n\left(\frac{a}{r}\right)^n v_n^i(r,\varphi,\lambda)\,, \tag{5.142}$$

where $\mu_i^n$, are the dimensionless coefficients of the expansion (5.142) or the dimensionless multipole moments; $v_n^i(r,\varphi,\lambda)$ is the dimensionless potential of the multipole at point *P*; each potential $v_n^i$ has an appropriate degree $n = n_i$ on the whole. The harmonic function $v_n^i$ of the degree *n* can be defined by the following expression

$$v_n^i = \frac{1}{n!}\frac{\partial^n}{\partial s_i^n}\left(\frac{1}{q_i}\right), \tag{5.143}$$

where $s_i$ is the relative geocentric distance between the origin and the multipole

$$s_i = \frac{d_i}{r}, \tag{5.144}$$

$q_i$ is the relative distance between the multipole and point *P*:

$$q_i = \frac{r_i}{r} = \sqrt{1 + s_i^2 - 2s_i\cdot\cos\psi_i}\,, \tag{5.145}$$

and $\psi_i$ is the geocentric spherical distance between the multipole and point *P*:

$$\cos\psi_i = \sin\varphi\sin\varphi_i + \cos\varphi\cos\varphi_i\cos(\lambda-\lambda_i)\,. \tag{5.146}$$

The functions $v_n^i$ can be computed by means of the recursion formula (Marchenko, 1998):

$$\left.\begin{aligned} v_0^i &= \frac{1}{q_i},\\ v_1^i &= \frac{\cos\psi_i - s_i}{q_i^3},\\ nq_i^2 v_n^i &= (2n-1)(\cos\psi_i - s_i)v_{n-1}^i - (n-1)v_{n-2}^i \end{aligned}\right\} \tag{5.147}$$

based on the well-known recursion formula for Legendre polynomials (Heiskanen and Moritz, 1967). Now to derive the gravity disturbance via the potentials (5.143) of radial multipoles with respect to *r* we get a final result in the following way

$$\delta g(P) = \delta g(r,\varphi,\lambda) = -\frac{\partial T}{\partial r} = \sum_{i=1}^{\infty} \sigma_i^n \delta\tilde{g}_n^i(r,\varphi,\lambda)\,, \tag{5.148}$$

or (interchange of summation and differentiation) we find

$$\begin{aligned}\delta g = -\frac{\partial T}{\partial r} &= \frac{\partial}{\partial r}\left( GM \cdot a^n \sum_{i=1}^{\infty} \mu_i^n \left(\frac{1}{r}\right)^{n+1} v_n^i(r,\varphi,\lambda) \right) \\ &= GM \cdot a^n \sum_{i=1}^{\infty} \mu_i^n \frac{\partial}{\partial r}\left( \left(\frac{1}{r}\right)^{n+1} v_n^i(r,\varphi,\lambda) \right).\end{aligned} \tag{5.149}$$

Then, as can be easily verified the coefficients of the expansion (5.148) are

$$\sigma_i^n = \mu_i^n\,, \tag{5.150}$$

and the functions $\delta\tilde{g}_n^i(r,\varphi,\lambda)$ are nothing else but the result of the differentiation in (5.149):

$$\delta\tilde{g}_n^i(r,\varphi,\lambda) = -\frac{GM}{r^2}\left(\frac{a}{r}\right)^n \left( r\frac{\partial v_n^i}{\partial r} - (n+1)v_n^i(r,\varphi,\lambda) \right) = -\frac{GM}{r^2}\left(\frac{a}{r}\right)^n \delta g_n^i(r,\varphi,\lambda)\,. \tag{5.151}$$

The relationship (5.151) can be simplified if the following basic equation (Abrikosov and Marchenko, 2001)

$$\frac{\partial v_n^i}{\partial s_i} = (n+1)v_n^i \quad \text{and for the derivative} \quad \frac{\partial v_n^i}{\partial r} = -\frac{s_i}{r}\frac{\partial v_n^i}{\partial s_i} \tag{5.152}$$

in the right hand side of (5.151) will be applied. Therefore,

$$\frac{\partial v_n^i}{\partial r} = -\frac{s_i}{r}(n+1)v_{n+1}^i \tag{5.153}$$

and our expressions (5.151) and (5.148) finally have the following form

$$\begin{aligned}\delta\tilde{g}_n^i(r,\varphi,\lambda) &= -\frac{GM}{r^2}(n+1)\left(\frac{a}{r}\right)^n\left(v_n^i(r,\varphi,\lambda)+s_i v_{n+1}^i(r,\varphi,\lambda)\right)\\ &= \frac{GM}{r^2}\left(\frac{a}{r}\right)^n \delta g_n^i(r,\varphi,\lambda)\end{aligned} \tag{5.154}$$

$$\delta g(P) = \delta g(r,\varphi,\lambda) = -\frac{GM}{r^2}\sum_{i=1}^{\infty}\mu_i^n(n+1)\left(\frac{a}{r}\right)^n\left(v_n^i(r,\varphi,\lambda)+s_i v_{n+1}^i(r,\varphi,\lambda)\right), \tag{5.155}$$

where the dimensionless function $\delta\tilde{g}_n^i(r,\varphi,\lambda)$ has the following form

$$\delta g_n^i(r,\varphi,\lambda) = -(n+1)\left(v_n^i(r,\varphi,\lambda)+s_i v_{n+1}^i(r,\varphi,\lambda)\right). \tag{5.156}$$

### 5.5.2 Approximation of disturbing potential by potentials of radial multipoles (inverse problem)

According to Marchenko (1998), the set $\{v_0^i/r^{n+1}\}$ of the potentials of radial multipoles of zero degree (without zero degree solid spherical harmonics) and the set $\{\tilde{v}_1^i/r^{n+1}\}$ of the potentials of eccentric dipoles are the non-orthogonal base systems in the Hilbert space $H_2^q(\Sigma)$. On the whole, every set of the potentials $\{\tilde{v}_n^i/r^{n+1}\}$, if n>1, is the linear independent and complete base system on any subset of $H_2^q(\Sigma)$ without all linear combinations of solid spherical harmonics from zero up to n-1 degree. This assertion holds the possibility of the approximation of disturbing potential by potentials of non-central radial multipoles. It is important to note that all multipoles should be placed on an auxiliary surface inside the Bjerhammar sphere (see Figure 5.3).

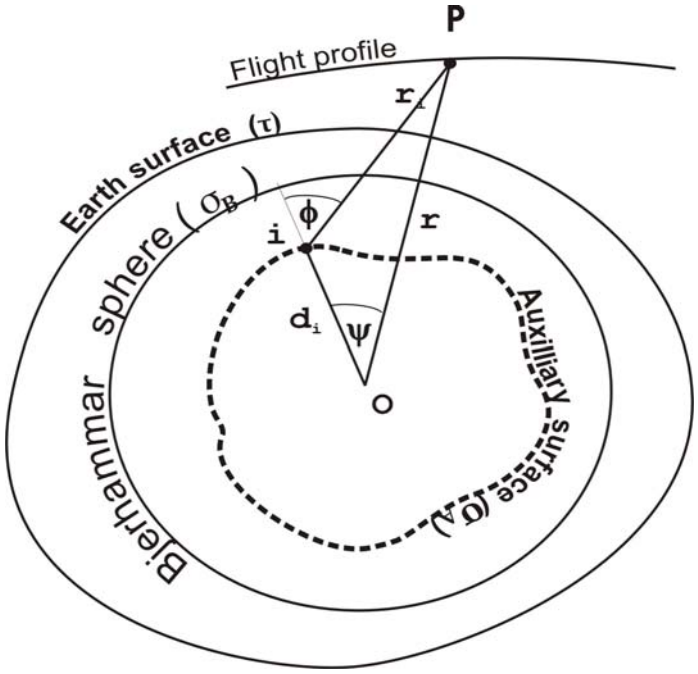


Figure 5.3 The Earth's surface $\tau$, the Bjerhammar sphere $\sigma_B$, the auxiliary surface $\sigma_A$ and the corresponding domains $(G, \Sigma, G_A)$

### 5.5.2.1 Functionals of disturbing potential expressed by radial multipoles

From (2.30) and (5.142), we get the next representation for the geoid undulations

$$N(P) = \frac{GM}{\gamma_Q \cdot r} \sum_{i=1}^{\infty} \mu_i^n \left( \frac{a}{r} \right)^n v_n^i(P) \ . \tag{5.157}$$

The expression for the gravity anomalies follows from (2.31), (5.142), and (2.45):

$$\Delta g(P) = \frac{GM}{r^2} \sum_{i=1}^{\infty} \mu_i^n \left( \frac{a}{r} \right)^n g_n^i(P) \ , \tag{5.158}$$

where the functions $g_n^i = g_n^i(P)$ can be obtained as

$$g_n^i(P) = (n+1) s_i v_{n+1}^i(P) + (n-1) v_n^i(P) \ . \tag{5.159}$$

The derivative of this function (5.159) may be expressed as

$$\frac{\partial g_n^i}{\partial s_i} = (n+1) g_{n+1}^i \, , \tag{5.160}$$

Practical application of the expressions (5.158) and (5.159) requires a solution of the special inverse problem:

*Given may be any set of the geodetic measurements (treated as linear functionals of the anomalous potential T). It is necessary to find some appropriate (and approximate) values of moments, locations, and degrees of a suitable finite set of radial multipoles for the further approximation of T only in the frame of a linear problem* (Marchenko, 1998).

### 5.5.2.2 Determination of optimal parameters of a multipole

Let the gravity data $\{\ell_k\}$ of the same type be given at some discrete set of points $\{P_k\}$. Let also the greatest absolute value of the data be located at the point $A = P_i$:

$$\ell_i = \max_k \left|\ell_k\right| . \tag{5.161}$$

Thus, we can postulate this external point as the epicenter of a multipole $v_n^i$ and put (Marchenko, 1998):

$$\left.\begin{aligned} \varphi_i &= \varphi_A \\ \lambda_i &= \lambda_A \end{aligned}\right\} \tag{5.162}$$

At this epicenter there is (Marchenko, 1998) global maximum of both functions, $v_n^i$ and $g_n^i$:

$$v_n^i(\psi_i = 0) = \left(\frac{1}{1-s_i}\right)^{n+1} , \tag{5.163}$$

$$g_n^i(\psi_i = 0) = \frac{n+2s_i-1}{(1-s_i)^{n+2}} . \tag{5.164}$$

The geocentric distance $d_i$, the degree $n$ and the moment $\mu_i^n$ of one multipole (located at point $i$) may be determined on the basis of the so-called *empirical isotropic (i.e. independent of the azimuth) function* (EIF). (Marchenko, 1998) introduced EIF as any discrete function $f(\psi_i)$ of the spherical distance $\psi_i$, which is computed by means of an *averaging of the initial data over the azimuth.*

### 5.5.3 Construction of empirical isotropic function

Let us split spherical distance $\psi_i$ between multipole and data points onto segments of size $\Delta\psi$:

$$[(j-1)\Delta\psi,\, j\Delta\psi], \quad j=1,2,... \tag{5.165}$$

By the averaging of the gravity data $\{\ell_k\}$ over the azimuth within each segment separately we can find the discrete values

$$\left.\begin{aligned} f(0) &= \ell_i, \\ f(\psi_{ij}) &= \frac{1}{m_j} \sum_{(j-1)\Delta\psi<\psi_{ik}\le j\Delta\psi} \ell_k, \quad (j=1,2,...) \end{aligned}\right\} \tag{5.166}$$

where the arguments $\psi_{ij}$ are averaged spherical distances between the multipole and data points within each segment

$$\psi_{ij} = \frac{1}{m_j} \sum_{(j-1)\Delta\psi<\psi_{ik}\le j\Delta\psi} \psi_{ik}, \quad (j=1,2,...), \tag{5.167}$$

and $m_j$ is the number of data within each segment

$$m_j = \sum_{(j-1)\Delta\psi<\psi_{ik}\le j\Delta\psi} 1, \quad (j=1,2,...). \tag{5.168}$$

In general, different values of the function (5.166) should be referred to different geocentric distances

$$r_j = \frac{1}{m_j} \sum_{(j-1)\Delta\psi<\psi_{ik}\le j\Delta\psi} r_k, \quad (j=1,2,...). \tag{5.169}$$

However, for the next approximation of EIF by either $v_n^i$ or $g_n^i$, we can assume that all values (5.166) are referring to one geocentric distance

$$r_0 = \frac{1}{M}\sum_{k=1}^{M} r_k \,. \tag{5.170}$$

### 5.5.4 Determination of the preliminary value of a multipole's moment

Because all considered functions, $f(\psi_i)$, $v_n^i$, $g_n^i$, have their global extreme at point *A*, (especially, $f(0) \neq 0$ by definition) we can determine the preliminary value of the moment $\mu_i^n$ as

$$\mu_i^n = \frac{r_0}{GM}\left(\frac{r_0}{a}\right)^n \frac{f(0)}{v_n^i(\psi_i = 0)} \ , \tag{5.171}$$

if the data $\{\ell_k\}$ are represented by values of disturbing potential, or

$$\mu_i^n = \frac{r_0^2}{GM}\left(\frac{r_0}{a}\right)^n \frac{f(0)}{g_n^i(\psi_i = 0)} \ , \tag{5.172}$$

if the data $\{\ell_k\}$ are represented by values of gravity anomalies.
It is important to note here that the application of geoid (quasi-geoid) heights as initial data may lead to some inconveniences, caused by the necessity to compute normal gravity at projections of data points onto ellipsoid (telluroid) during the approximation process. However, taking into account the above discussed removal of the global gravity model impact (see Section 4.3.1), we can perform a preliminary transformation of such data by multiplying those by normal gravity. After such a transformation we can consider that the data set $\{\ell_k\}$ consists of corresponding values of disturbing potential *T*.

### 5.5.5 Determination of the geocentric distance of the multipole

Now, with the preliminarily known value of the moment $\mu_i^n$, we can describe EIF as an analytic isotropic function (AIF) given by one of functions, $v_n^i$:

$$\frac{GM}{r_0}\mu_i^n\left(\frac{a}{r_0}\right)^n v_n^i\left(\psi_{ij}\right) = f(\psi_{ij}) \ , \tag{5.173}$$

or $g_n^i$:

$$\frac{GM}{r_0^2}\mu_i^n\left(\frac{a}{r_0}\right)^n g_n^i\left(\psi_{ij}\right) = f(\psi_{ij}) \ . \tag{5.174}$$

By substituting (5.171) and (5.172) into (5.173) and (5.174), respectively, we get;

$$\frac{f_n^i\left(\psi_{ij}\right)}{f_n^i\left(\psi_i=0\right)}=\overline{f}\left(\psi_{ij}\right)\ , \tag{5.175}$$

where $f_n^i$ corresponds to one of the functions $v_n^i$ or $g_n^i$, and $\overline{f}(\psi_{ij})$ is the normalized value of EIF:

$$\overline{f}(\psi_{ij})=\frac{f(\psi_{ij})}{f(0)}. \tag{5.176}$$

Because (5.175) does not depend on a multipole's moment $\mu_i^n$, we are not in need of a preliminary determination of this value. In practice, we can construct directly the normalized EIF $\overline{f}(\psi_{ij})$ and then consider (5.175) as non-linear equation regarding the relative geocentric distance of the multipole

$$s_i=\frac{d_i}{r_0}. \tag{5.177}$$

After the linearization of (5.175) we get;

$$(n+1)\left[\frac{f_{n+1}^i(\psi_{ij})}{f_n^i(\psi_i=0)}-\frac{f_{n+1}^i(\psi_i=0)}{f_n^i(\psi_i=0)}\frac{f_n^i(\psi_{ij})}{f_n^i(\psi_i=0)}\right]\delta s_i=\overline{f}(\psi_{ij})-\frac{f_n^i(\psi_{ij})}{f_n^i(\psi_i=0)}. \tag{5.178}$$

Therefore, if any approximate value of $s_i$ is given, it may be improved by iterations. On each iteration, a system (for $j$=1,2,…) of linear equations (5.178) should be solved for correction $\delta s_i$ by the least squares method.

### 5.5.6 Determination of the preliminary relative distance of the multipole

By analogy with essential parameters of a covariance function (Moritz, 1980), those parameters may be introduced (Marchenko, 1998) for considered isotropic functions as well. One of such parameters is the magnitude at the epicenter (5.163) or (5.164). It was already used for the preliminary determination of the multipole's moment in (5.171) or (5.172). Another parameter is the so-called decreasing length (Marchenko, 1998) that is such value $\xi$ of the spherical distance $\psi_i$, which fulfills the equation

$$f_n^i(\psi_i=\xi)=\frac{1}{2}\cdot f_n^i(\psi_i=0)\ . \tag{5.179}$$

By using this definition, we can determine decreasing length numerically from normalized EIF (for example by means of inverse linear interpolation) and perform the equation:

$$\xi = \xi_{emp} . \tag{5.180}$$

With this fixed value, we can consider the non-linear equation

$$2\frac{f_n^i(\psi_i = \xi_{emp})}{f_n^i(\psi_i = 0)} - 1 = 0 \tag{5.181}$$

regarding relative distance $s_i$. This equation may be solved in closed form for the function $v_0^i$ (Marchenko, 1998):

$$s_0 = \frac{4}{3} - \frac{1}{3}\left(\cos\xi_{emp} + \sqrt{\cos^2\xi_{emp} - 8\cos\xi_{emp} + 7}\right). \tag{5.182}$$

For functions $v_n^i$ ($n$>0) and $g_n^i$ ($n$≥0) the equation should be solved numerically by iterations. It can be shown (Marchenko, 1998) that for a fixed value of decreasing length, the relative distance of a multipole decreases as its degree n increases. Thus, the distance of a multipole of zero degree (point mass) is greater than the distance of a multipole of first degree (dipole). This last distance is greater than the distance of a multipole of second degree (quadrupole). A graphical presentation is given in Figure 5.4, which, shows some normalized functions $v_n^i(\psi_i)/v_n^i(\psi_i = 0)$.

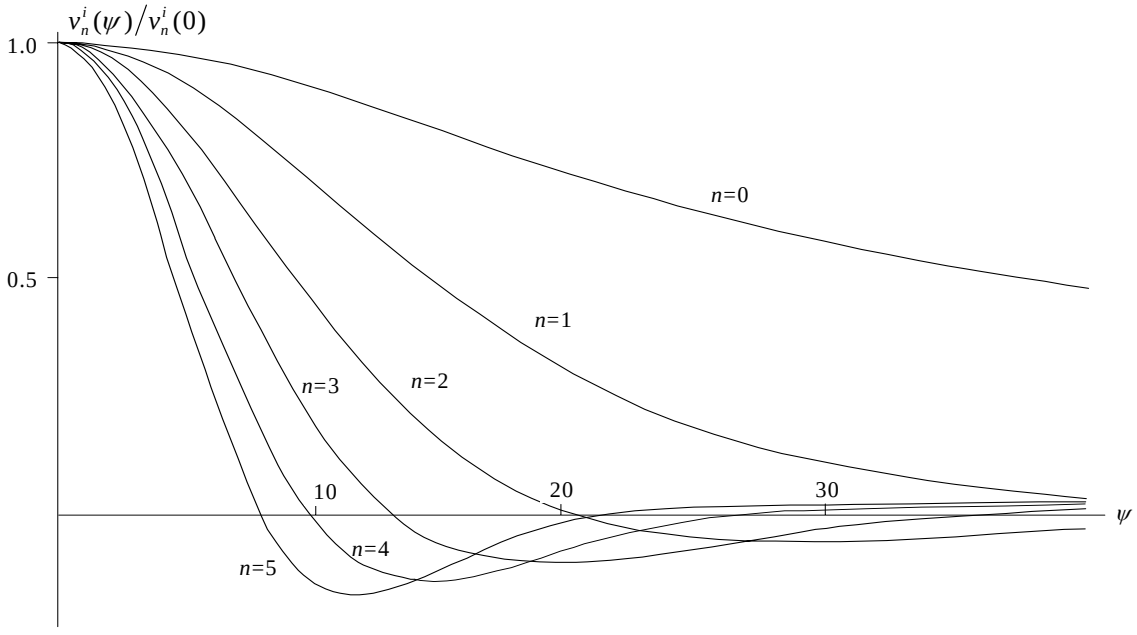


Figure 5.4 The normalized values of potentials of radial multipoles for $s_i = 0.7$ (Marchenko, 1998)

Thus, we can use the relative distance (5.182) of a zero-degree radial multipole as the starting value for a solution of the equation (5.181). As a result, we get the value

$$s_i \le s_0 < 1 \ , \tag{5.183}$$

which may be improved finally by the least-squares adjustment of normalized empirical isotropic functions (Section 5.5.3).

### 5.5.7 Determination of the multipole's moment by least-squares adjustment

Now, with the known values *n* and $d_i = r_0 s_i$, we can determine the multipole's moment $\mu_i^n$ by means of the local least-squares approximation of the analyzing gravity field by one potential $v_n^i$. In this case the expressions (5.142), (5.157) and (5.158) lead at any data point *P* to the following linear equations regarding the unknown $\mu_i^n$:

$$\left[ \frac{GM}{r_P} \left( \frac{a}{r_P} \right)^n v_n^i(P) \right] \cdot \mu_i^n = T(P) \, , \tag{5.184}$$

$$\left[ \frac{GM}{r_P} \left( \frac{a}{r_P} \right)^n v_n^i(P) \right] \cdot \mu_i^n = \gamma_{Q(P)} N(P) \, , \tag{5.185}$$

$$\left[ \frac{GM}{r_P^2} \left( \frac{a}{r_P} \right)^n g_n^i(P) \right] \cdot \mu_i^n = \Delta g(P) \, . \tag{5.186}$$

Considering such equations for all data points $\{P\}$, we can compute corresponding least-squares solution for $\mu_i^n$.

#### 5.5.7.1 Final readjustment of multipole moments

The last step of constructing a gravity model based on potentials of radial multipoles consists of final total least-squares readjustment of the whole set $\{\mu_i^n\}$ in the frame of a linear problem. Obviously, *heterogeneous data may be used for such a readjustment*. In general, we have the system of linear equations

$$\mathbf{AX = l}, \quad \mathbf{l = L - AM} \, , \tag{5.187}$$

where **L** is the vector of gravity functionals (initial data); **A** is the matrix of coefficients with elements as corresponding base functions (see (5.142), (5.157), (5.158)) depending on types of data; M is the vector of known multipole moments $\{\mu_i^n\}$ determined by SMA; X is the vector of unknown corrections $\{\delta\mu_i^n\}$ to the multipole moments.

In addition, we should suppose that values of some gravity functionals must be restored exactly at some points. Such a requirement may appear if we use, for example, precise absolute gravity data (Marchenko et al. 1995) or results of GPS/leveling together with measured values of gravity functionals. It leads to the linear system of additional conditions

$$\mathbf{BX} = \mathbf{w}, \quad \mathbf{w} = \mathbf{W} - \mathbf{BM}, \tag{5.188}$$

in which matrix B and vector L have a similar meaning as matrix A and vector L in (5.187). Finally, we should take into account the possible numerical instability of the system (5.187) that may be caused, for example, by the very close location of some multipoles in the case of processing of very dense data set by sequential multipole analysis. Therefore, we should use one of the known methods of stable estimation for the solution of the system (5.187).

It is well-known that the most general approach to derive a stable solution of a system of linear equations is Tikhonov's regularization (Tikhonov and Arsenin, 1986), which is based on the minimization of so-called smoothing functionals that includes the Euclidean norm of residuals in the linear system and the norm of solution corresponding to a certain space. If the Euclidean norm of solution is applied, we come to the so-called quasi solution, which is the most famous and simplest practical case of regularization. Thus, we should solve (5.187) with conditions (5.188) by minimizing the smoothing functional

$$\Phi_\alpha = \alpha\mathbf{X}^{\mathrm{T}}\mathbf{X} + (\mathbf{AX}-\mathbf{l})^{\mathrm{T}}\mathbf{C}_{nn}^{-1}(\mathbf{AX}-\mathbf{l}) + 2\mathbf{k}^{\mathrm{T}}(\mathbf{BX}-\mathbf{w}), \tag{5.189}$$

where $\mathbf{C}_{nn}$ is the covariance matrix of errors in measured data, k is the vector of unknown multipliers (correlates), $\alpha$ is the so-called regularization parameter, which must be non negative

$$\alpha \geq 0. \tag{5.190}$$

It is obvious that we come to the classical least-squares solution (with additional conditions) in the case where $\alpha = 0$. Minimization (5.184) leads to the following system of normal equations

$$\left.\begin{aligned} \mathbf{N}_\alpha\mathbf{X} + \mathbf{B}^{\mathrm{T}}\mathbf{k} &= \mathbf{U}, \\ \mathbf{BX} &= \mathbf{w}, \end{aligned}\right\} \tag{5.191}$$

where

$$\mathbf{N}_\alpha = \mathbf{A}^{\mathrm{T}}\mathbf{C}_{nn}^{-1}\mathbf{A} + \alpha\mathbf{I}, \tag{5.192}$$

$$\mathbf{U} = \mathbf{A}^{\mathrm{T}}\mathbf{C}_{nn}^{-1}\mathbf{l}\,. \tag{5.193}$$

The solution of the system (5.191) is

$$\mathbf{X} = \mathbf{N}_{\alpha}^{-1}(\mathbf{U} - \mathbf{B}^{\mathrm{T}}\mathbf{k})\,, \tag{5.194}$$

$$\mathbf{k} = (\mathbf{B}\mathbf{N}_{\alpha}^{-1}\mathbf{B}^{\mathrm{T}})^{-1}(\mathbf{B}\mathbf{N}_{\alpha}^{-1}\mathbf{U} - \mathbf{w})\,. \tag{5.195}$$

As we can see, this solution depends on an adopted value of the regularization parameter. In accordance with the general approach (Tikhonov and Arsenin, 1986), such a value as $\alpha_{opt}$ must be made to agree with the accuracy of the measured data and corresponding operator, which is represented here by the normal matrix

$$\mathbf{N}_0 = \mathbf{A}^{\mathrm{T}}\mathbf{C}_{nn}^{-1}\mathbf{A}\,. \tag{5.196}$$

Standard determination of $\alpha_{opt}$ requires an iterative process, which starts from the initial value $\alpha = 0$ and may lead to essential difficulties in a case of an ill-conditioned matrix $\mathbf{N}_0$.

According to Abrikosov (1999a), the regularization algorithm was developed on the basis of such an approach of the normal operator, which is closed to a system of linear equations with scalar or unit matrix. The following condition

$$\left\|(\bar{\mathbf{N}}_0 + \bar{\alpha}\mathbf{I})^{-1}\right\| = \left\|\bar{\mathbf{N}}_0 + \bar{\alpha}\mathbf{I}\right\| \tag{5.197}$$

was used for the determination of the regularization parameter. Here,

$$\bar{\mathbf{N}}_0 = \frac{n}{\|\mathbf{N}_0\|}\mathbf{N}_0\,, \tag{5.198}$$

$$\bar{\alpha} = \frac{n}{\|\mathbf{N}_0\|}\alpha\,, \tag{5.199}$$

*n* is the order of the normal matrix (5.196), and the simplest matrix norm was applied

$$\|\mathbf{N}_0\| = \operatorname{trace}\mathbf{N}_0\,. \tag{5.200}$$

The condition (5.197) led to the recursive formula

$$\bar{\alpha}_{m+1} = \frac{\bar{\alpha}_m}{n(1+\bar{\alpha}_m)} \left\| \left( \bar{\mathbf{N}} + \bar{\alpha}_m \mathbf{I} \right)^{-1} \right\|, \tag{5.201}$$

which starts from the value

$$\bar{\alpha}_1 = -\frac{n+1}{3} - \frac{2\sqrt{n^2-n+4}}{3} \sin\left( \frac{1}{3} \arcsin \frac{2n^3-3n^2-21n+38}{2\sqrt{(n^2-n+4)^3}} - \frac{\pi}{3} \right) \tag{5.202}$$

and should be finished by such value, for which the inequality

$$\left| \frac{\left\| \left( \bar{\mathbf{N}}_0 + \bar{\alpha}_m \mathbf{I} \right)^{-1} \right\|}{n(1+\bar{\alpha}_m)} - 1 \right| < \varepsilon \tag{5.203}$$

is valid with a given precision $\varepsilon$>0. It is important that for any fixed $n$>1, the value (5.202) is the upper limit of the normalized regularization parameter:

$$\bar{\alpha} \le \bar{\alpha}_1, \tag{5.204}$$

and, in addition

$$\lim_{n\to\infty} \bar{\alpha}_1 = \bar{\alpha}_0 = \frac{\sqrt{5}}{2} - \frac{1}{2}. \tag{5.205}$$

According to Marchenko (1998), Figure 5.5 shows the behavior of $\bar{\alpha}_1$.

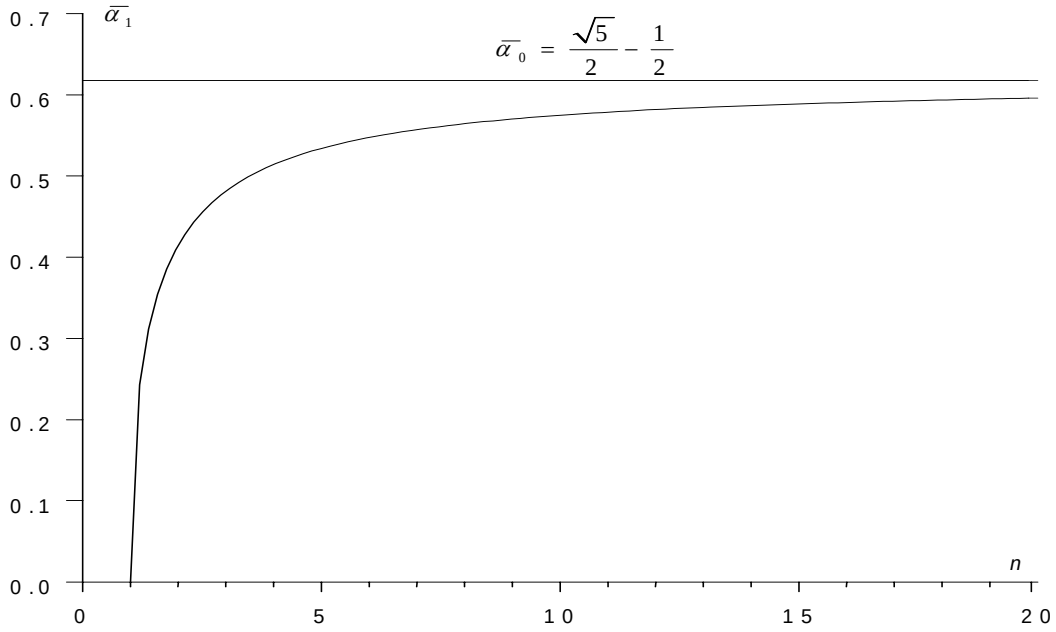


Figure 5.5 Upper limit of the parameter $\bar{\alpha}$ for various *n*

In view of the general theory, the described approach of Tikhonov and Arsenin (1986) yields the regularization parameter, which is due to the accuracy of the initial operator and therefore, provides a stable inversion.

# 6 Numerical tests and analysis

In the Stokes approach of the geodetic boundary value problem, the solution is sought on the boundary (geoid), while the observations (gravity data) are available on the topography or the flight altitude. To obtain the boundary values, the observation has to be reduced from the flight altitude or topography onto the geoid (Heiskanen and Moritz, 1967). This reduction is called *downward continuation*.

## 6.1 Introduction

In recent years the airborne gravity measurements are used for the determination of precise local or regional geoid, (Forsberg and Brozena 1997, Kearsley et al. 1998, Wei and Schwarz 1998). Thus, the accuracy of 5-10cm airborne gravity derived geoid can be used as precise vertical reference of orthometric height. This provides an efficient way to determine orthometric height without traditional leveling. The application of airborne gravimetry shows its efficiency, basically due to advantages in the determination of gravity by the combination of kinematical GPS, INS (Inertial Navigation System) and gravity meters with stabilized platforms. In general, airborne surveys are treated as very good tool to cover large scale and mountain areas, which is difficult and very expensive to cover with traditional land surveys. By the way, these areas requires a large survey altitude. For this reason it is important to conclude that the height of the flight altitude, as well as topographical and filtering effect plays a major role in the downward continuation process.

## 6.2 Formulation of the problem

The main topic of this study case is to carry out the best and stable solution for the downward continuation of airborne gravity data (Geopotential) in the Switzerland. This is also an interesting area to analyze the stability of the downward continuation process. First, the flight altitude (5000m) seems not to be usual for until yet performed airborne gravimetric campaigns. Second, the topography of the Switzerland plays also an important role in the continuation of the data from the flight altitude to the sea level. The topography consists of mountains (Alps) with maximal height of approximate 4000m above sea level, as well as many lakes and flat areas. In the last decade there are many research studies, which investigate the stability of the downward continuation of airborne gravity data. The studies were concentrated mainly on direct inversion of free air anomalies or disturbances through Poisson's integral, as well as application of many topographical reduction methods. In this study the focus should be given to the downward continuation of disturbing potential by using combination of the collocation and regularization in Bjerhammar-Krarup model (method) using Sequential Multipole Analysis for the determination of the disturbing potential from measured gravity disturbances at constant altitude of 5000m above mean sea level. By the way, the determined disturbing potential using Sequential Multipole Analysis is our input in the downward continuation process. For the accuracy estimation, these results are compared with Inverse Poisson method. The basic idea in this study is to determine the gravity field

(disturbing potential) at the flight altitude using Sequential Multipole Analysis (Chapter 5.5). After this, follows the continuation of disturbing potential by the combination of the regularization and least-squares collocation method to mean sea level always using Runge-Krarup theory (Chapter 5.5). For the stabilization of the downward continuation process, using combination of the regularization and least squares collocation, numerous of land data has been used (land gravity data and GPS/leveling points). This land data are principally used for the construction of the covariance function between disturbing potential at the flight and the reference altitude. The results below show that combination of the regularization and is an efficient and stable solution. I have to mention that for the stability of the downward continuation of airborne gravity data by using Sequential Multipole Analysis is the adequate tool for the determination of disturbing potential at the flight altitude. According to Runge-Krarup Theory, we can determine the gravity field in the flight altitude which is harmonic outside the Earth (Moritz, 1980). Results show that the determination of disturbing potential by using Sequential Multiple Analysis gave relative smooth signal ($T_{5000}$), which is essential factor for the stability of the downward continuation.

## 6.3 Airborne gravimetric survey of Switzerland

The Swiss airborne campaign was performed with a Twin Otter two engines aircraft, on board with a LaCoste Romberg gravimeter and three GPS receivers, one for navigation purposes and the other two for positioning and for the monitoring of the aircraft accelerations. The ground GPS network consists of four GPS reference station. Flights were performed during November and December 1992 at an approximate barometric altitude of 5100m above sea level (Klingele et al. 1996). The survey includes area over all Switzerland with 24 profiles (see Figure 6.1) and the distance between lines of 12 km and gravimetric sampling rate of 1 sec.
The survey is characterized by following parameters (Klingele et al. 1996):

- Distance between lines…….12 km
- Flight altitude……5200 m
- Flight azimuth……..76°
- Aircraft speed……..240 km/h
- GPS sampling rate……0.5 sec
- Gravimetric sampling rate……...1 sec
- Cross-coupling rate……10 sec

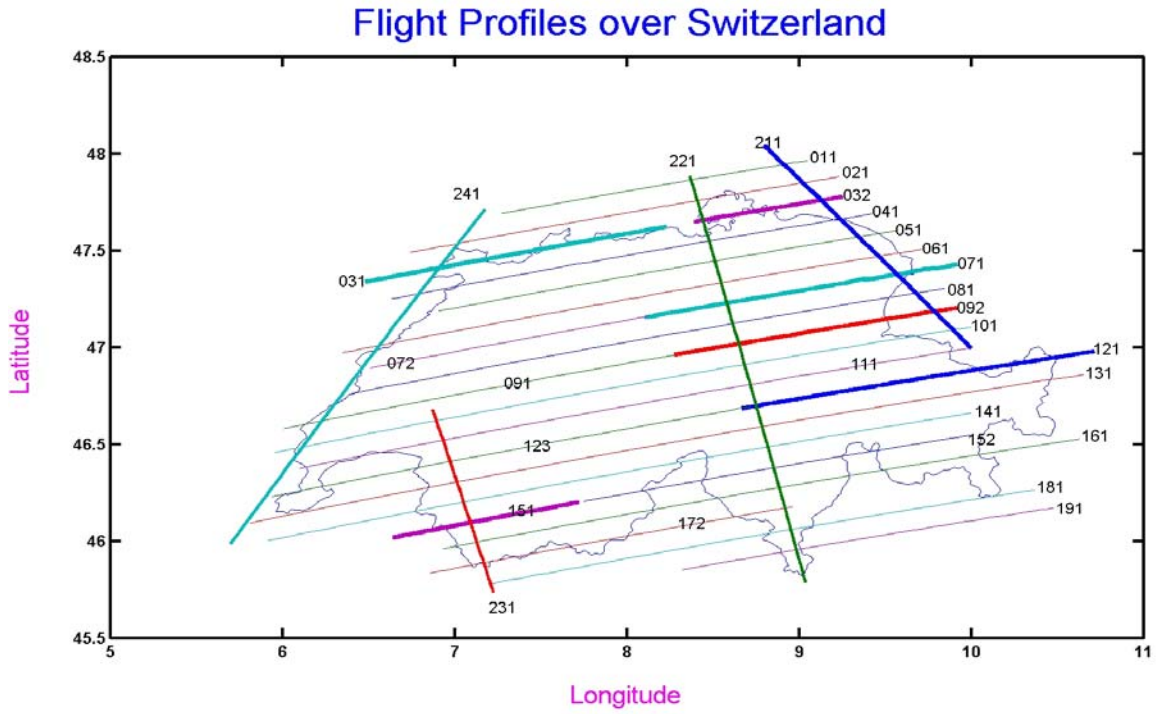


Figure 6.1 Measured profiles from the Swiss Airborne Gravity Survey (SAGS)

### 6.3.1 Campaign results

As final results of the Swiss campaign, there are 24 profiles with measured gravity ($g$) in the approximate altitude of 5000m. For the further computation, all measured points are recalculated to the constant height of 5000m above mean sea level. Because of the small deviation of the observed points from the constant flight altitude, the reduction is done by free air gradient, which is in this case sufficiently accurate.

One of the major problem of airborne data handling (Except separation of the gravity from the aircraft acceleration) is the contamination of profiles by filtering edge effects. These effects are so large that the only solution is to cut them out from profiles. In some cases, the "cutting process" contains more than 50% (see Figure 6.2) of the observed points, which has to be removed from the measured profiles. The resulting values at the constant altitude can be used for the construction of the grid of gravity disturbances that can be analyzed to study the measured signal and its power, which is very important for field gridding and filtering (Childers et al. 1999). Figure 6.2 shows the filtering effect in the edges of profiles. As is usual in the airborne gravimetry, flying cross section profiles enables to reduce this effect.

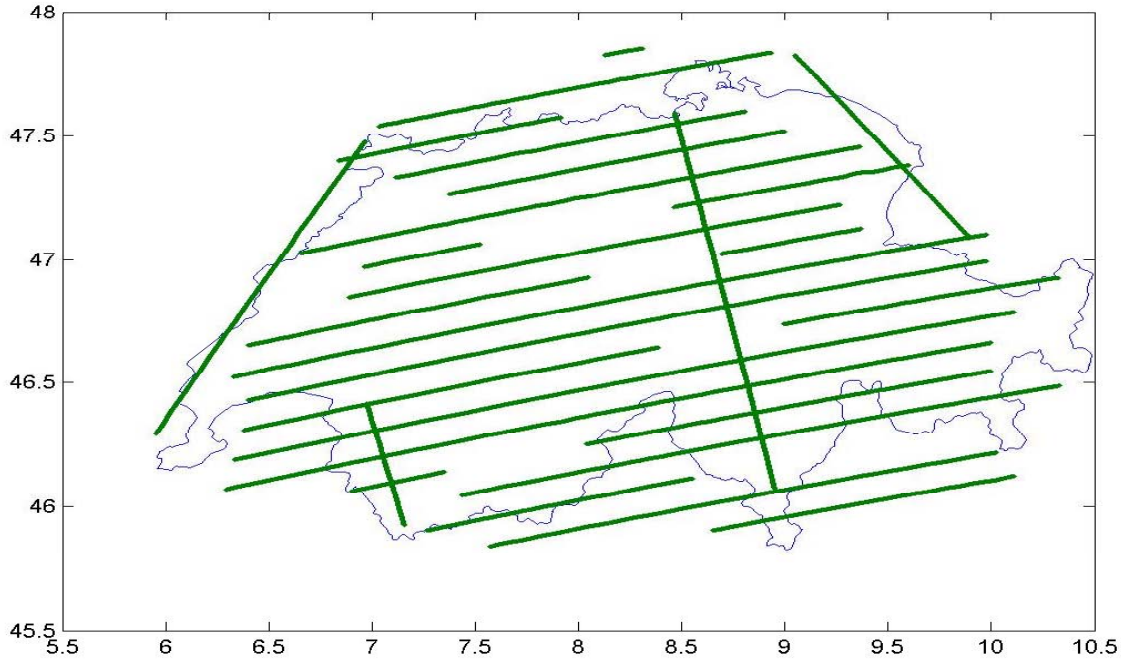


Figure 6.2 Profiles after removing the edge effects

### 6.3.2 Description of the test area used for the analysis of the downward continuation

After processing the flight profiles separately, the resulting set of points with 55448 gravity disturbances at constant altitude of 5000m is obtained. These points should be used as input data set for downward continuation process and for construction of a 5'x5' grid of mean gravity disturbances. The problem of the gaps, which comes as result of the filtering edge effect, has been solved by imposing upward continued land gravity data. The land gravity data from BGI (Bureau Gravimetrique International, Langellier, 2003) , SGC data (Swiss Geophysical Commission, Klingele, 2003) and Swisstopo (Urs Marti, 2003) data were also used for the upward continuation (see Figure 6.3), as well as for the expansion of the regular grid to 5°x3°. The coverage of the grid lies from the latitude 45° to 48° and from the longitude 5° to 10°. The area of interest for the downward continuation lies from 46° - 47°.5 and 7° - 9°, (see Figure 6.4). The incorporation of the extended area has the aim to reduce the grid edge effects, as well as the effect of neighborhood topography during the downward continuation process. For the stabilization of the downward continuation as well as for the comparison of results, 19 GPS/leveling points were used (see Figure 6.4).

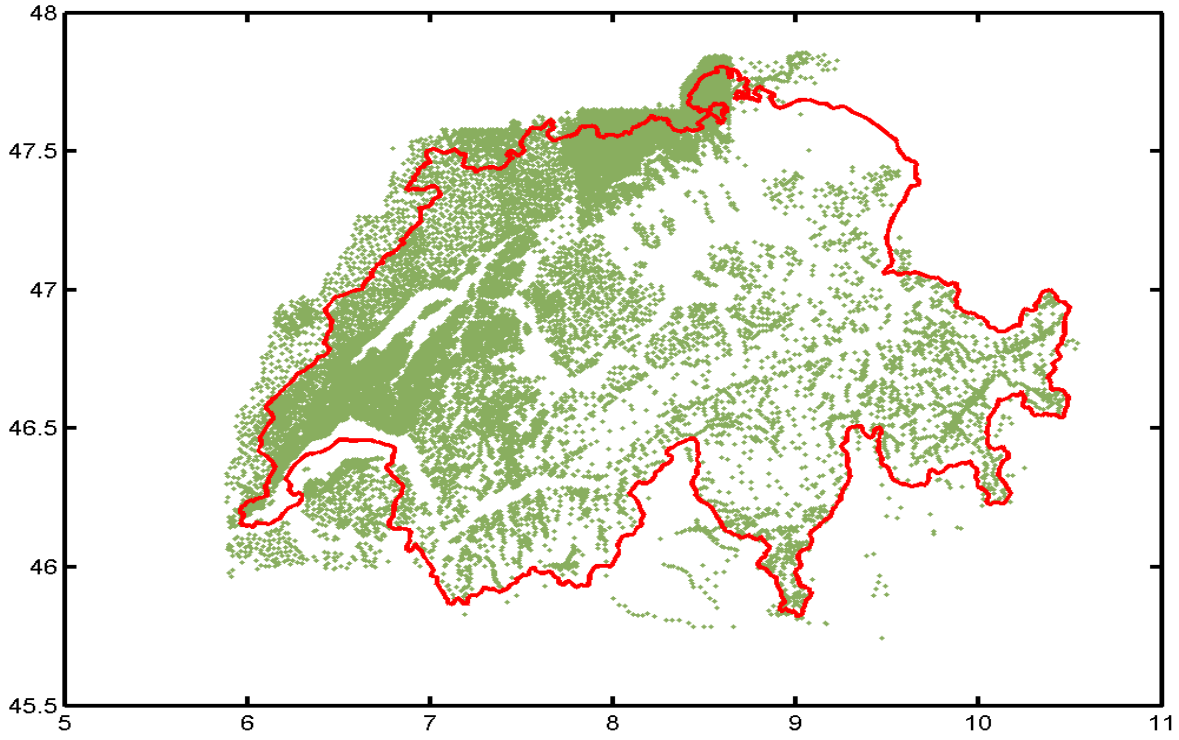


Figure 6.3 Land gravity data over Switzerland, particularly used to fill gaps between profiles

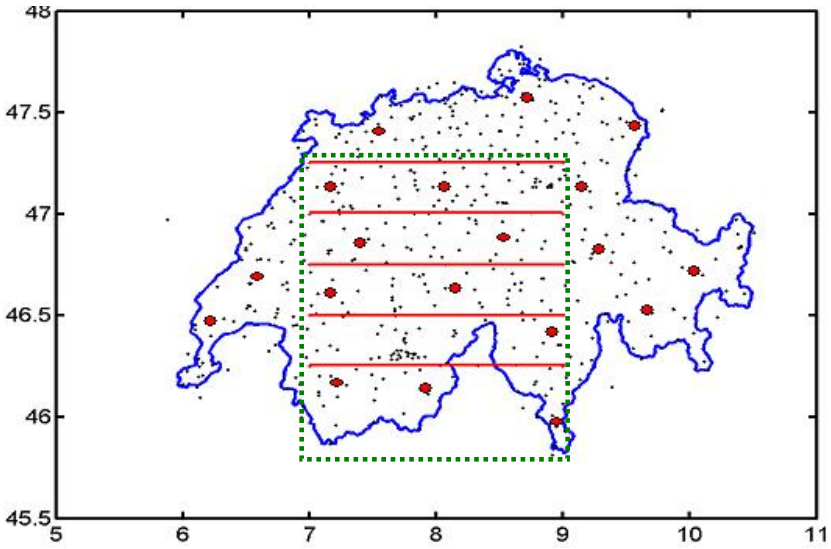


Figure 6.4 Selected 19 GPS/leveling points included in calculation.

The red points in Figure 6.4 are 19 GPS/leveling used for the stabilization of the downward continuation process. The dotted line shows a selected area, which has been chosen for the analysis of the downward continuation of airborne data to mean sea level (geoid). The actual

geoid of Switzerland CHGeo98 (Marti, 1999) has been used for the comparison of downward continuation results (see Figure 6.5).

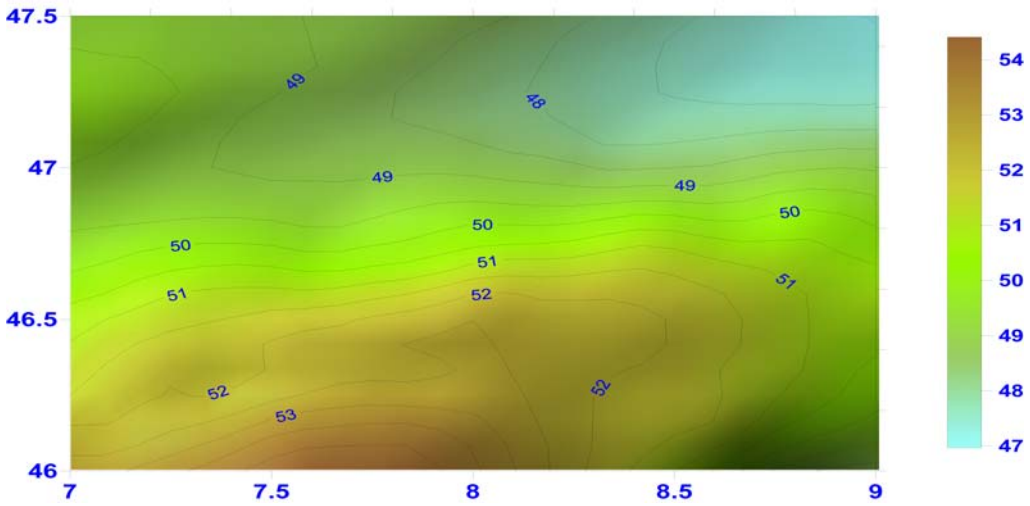


Figure 6.5 CHGeo98 geoid of Switzerland (Marti, 1999)

| | Min | Mean | Max | St.Dev |
|---|---|---|---|---|
| **$N_{(CHGeo98)}$ (m)** | *46.97* | *49.86* | *52.73* | *1.56* |

*Table 6.1 Statistics of the CHGeo98 geoid undulations in meters*

## 6.4 Topographical effects and terrain correction

In the remove-restore technique of geoid determination, the shifting of all topographic masses below the geoid can compensate for some deficiencies in the application of the Stokes method. In practice, this is achieved using the digital terrain model (DTM) to reduce the topographic masses on the geoid in order to preserve harmonicity. The corresponding indirect effect of this reduction is then computed. The terrain information can also provide very short-wavelength geoid undulations that are not always sampled by gravity observations alone. In our case we used a DTM from the GTOPO with a resolution of 30''x 30'' (see Figure 6.6) for computation of terrain corrections, as well as the indirect effect on geoid undulation.

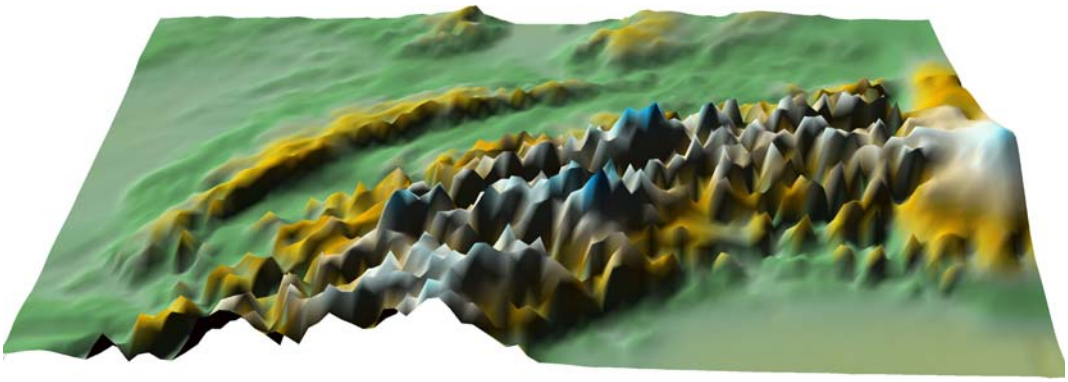

Figure 6.6 Digital Terrain Model of Switzerland (GTOPO)

The computation of terrain correction is carried out by the prism method with an integration radius of 167km and a constant density of 2.67gr/cm³. Otherwise, the GRAVSOFT Package has been used for the reconstruction of mean elevation grid and computation of RTM effects $\delta g^{RTM}$ (e.g. indirect effect. $\delta N^{IND}$). In the Table 6.2 and 6.3 are presented results of the terrain correction using both techniques and should be used for later computation, respectively downward continuation.

| | **Min** | **Mean** | **Max** | **St.Dev** |
|---|---|---|---|---|
| **DTM (m)** | *8.20* | *908.95* | *4068.00* | *731.89* |
| **TC (mGal)** | *1.37* | *93.16* | *386.06* | *74.63* |
| **CTC (mGal)** | *1.37* | *92.47* | *385.23* | *73.79* |
| **TC-CTC (mGal)** | *0.00* | *0.69* | *18.16* | *1.38* |
| **Indirect effect (m)** | *-0.91* | *-0.11* | *0.00* | *0.15* |

*Table 6.2 Statistics of the terrain effects computed by Helmert's second compensation method using a DTM derived from GTOPO data with resolution 30'' x 30''*

| | **Min** | **Mean** | **Max** | **St.Dev** |
|---|---|---|---|---|
| **DTM (m)** | *8.20* | *908.95* | *4068.00* | *731.89* |
| **RTM (mGal)** | *-62.71* | *-0.02* | *89.20* | *14.63* |
| **Indirect effect (m)** | *-0.56* | *0.02* | *1.01* | *0.22* |

*Table 6.3 Statistics of the terrain effects computed by the Residual Terrain Model (RTM) method using a DTM derived from GTOPO data with resolution 30'' x 30''.*

## 6.5 Downward continuation procedure

In this section, the downward continuation procedure is part of the traditional remove-restore technique for the geoid determination. The method consists of the following steps (Figure 6.7):

1. Computation of the residual gravity disturbances $\delta g^{RES}$ by removing the global gravity model $\delta g^{GM}$ and topographical effects $\delta g^{TC}$ from the initial gravity disturbances δg:

$$\delta g^{RES} = \delta \mathbf{g} - \delta g^{GM} - \delta g^{TC} .$$

2. Approximation of $\delta g^{RES}$ by the sequential multipole analysis technique (SMA) and computation of the residual disturbing potential $\delta T$ at the altitude of 5000 m.

$$\delta T = \delta g^{RES}(SMA) .$$

***3. Downward continuation of residual disturbing potential $\delta T$ (5000 m) to residual disturbing potential at mean sea level $\delta T_0$ (0 m).***

4. Computation of residual geoid heights $\delta N^{RES}$ from disturbing potential at mean sea level (geoid) $\delta T_0$

5. Computation of the geoid heights *N* by restoring the global gravity model $\delta N^{GM}$ and the indirect effect $\delta N^{IND}$ to the residual geoid heights $\delta N^{RES}$:

$$N = \delta N^{RES} + \delta N^{GM} + \delta N^{IND}$$

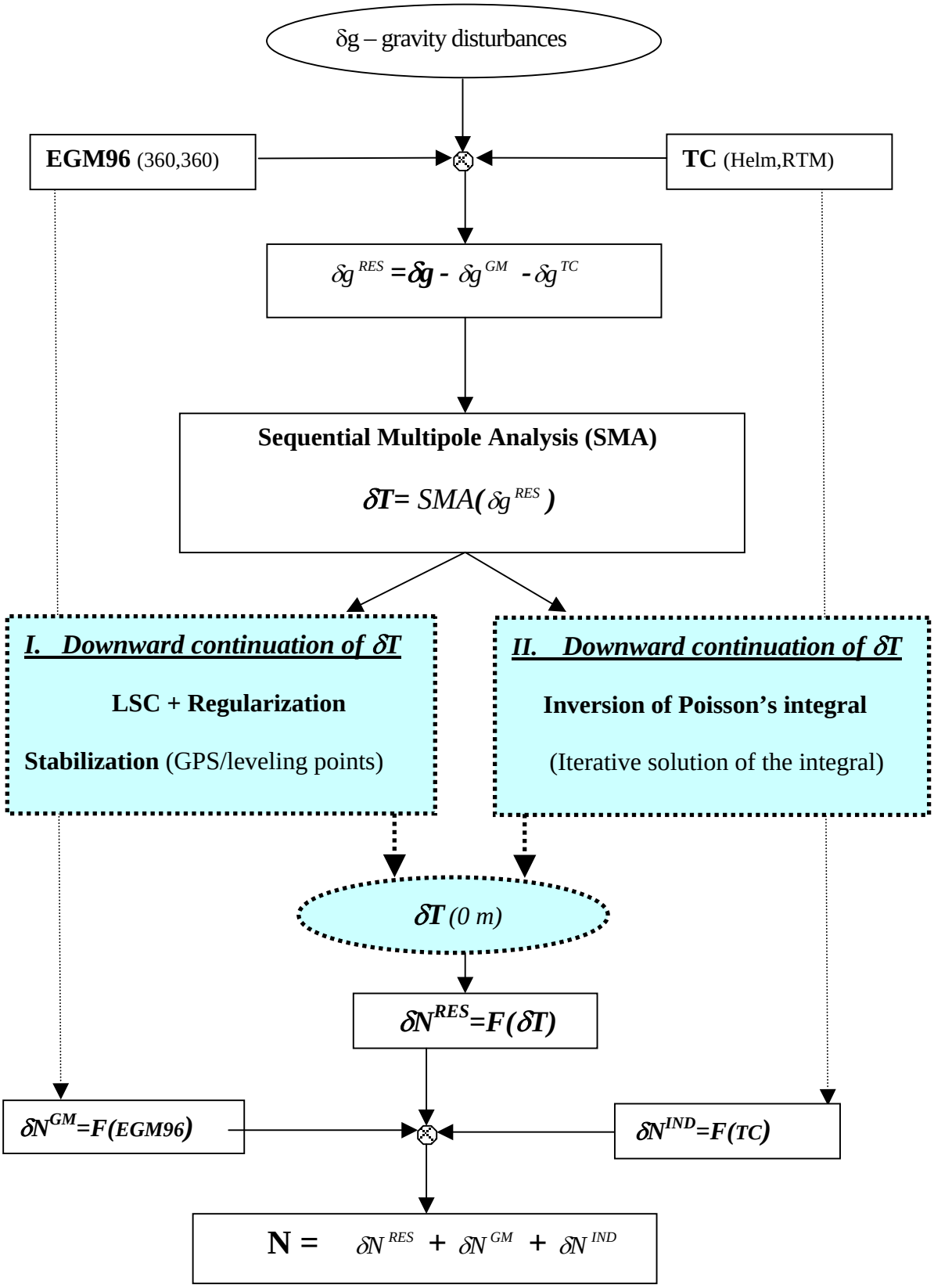


Figure 6.7 Downward continuation procedure

## 6.6 Downward continuation of disturbing potential by combination of the SMA and LSQ in Bjerhammar-Krarup Model

The computation is carried out by the AGF software version 4.2e developed at GeoForschunsZentrum Potsdam (Abrikosov and Marchenko, 2001). The software strategy is based on the Bjerhammar-Krarup theory for gravity field determination and has two independent optional techniques for the approximation of gravity field. First, the approximation of disturbing potential by the potentials of radial multipoles, second one is the least-squares collocation with regularization. The optional possibility is to combine both methods(Abrikosov and Marchenko, 2001) . During the processing of the flight profiles, the measured gravity values are recalculated to a constant flight height *H=5000m*. The height of measured flight lines lies between $H_{\min} \approx 4800m$ and $H_{\max} \approx 5200m$ . The input data used in the computation are gravity disturbances (55448 points with a constant height *H=5000m*) in the area with latitudes $45^\circ \le \varphi \le 48^\circ$ and longitudes $5^\circ \le \lambda \le 10^\circ$. To build this area which is not completely covered by airborne survey campaign are used land gravity data continued upward to the constant flight line (see chap. 6.3). The aim of the extended area is to reduce the impact effects which income in the edges of the area. This is especially important for the Iterative solution of Poisson's integral. This solution is tested by many scientists (e.g. Martinec, 1998) and it is recommended to extend the research area by 2° in the latitude direction and 1° in the longitude direction to reduce the edge effects and truncation error. Opposite to the discrete Poisson method, the main method of this thesis, which is the combination of Sequential Multipole Analysis with least-squares collocation, doesn't requires the grid data for calculation. The grid data are needed only for the output results and for the internal software calculations. Below is described the computation strategy of AGF4.2e software (see Figure 6.8).

Start:

- Definition of Reference Coordinate System (eg. GRS80, WGS84)
- Compute terrain corrections (optional)
- Remove global geopotential model (EGM96)
- Construct regional model by SMA
- Improve regional model (regularization is optional)
- Construct empirical covariance function
- Construct analytical covariance function
- Predict by collocation
- Restore global geopotentional model
- Compile final results

end

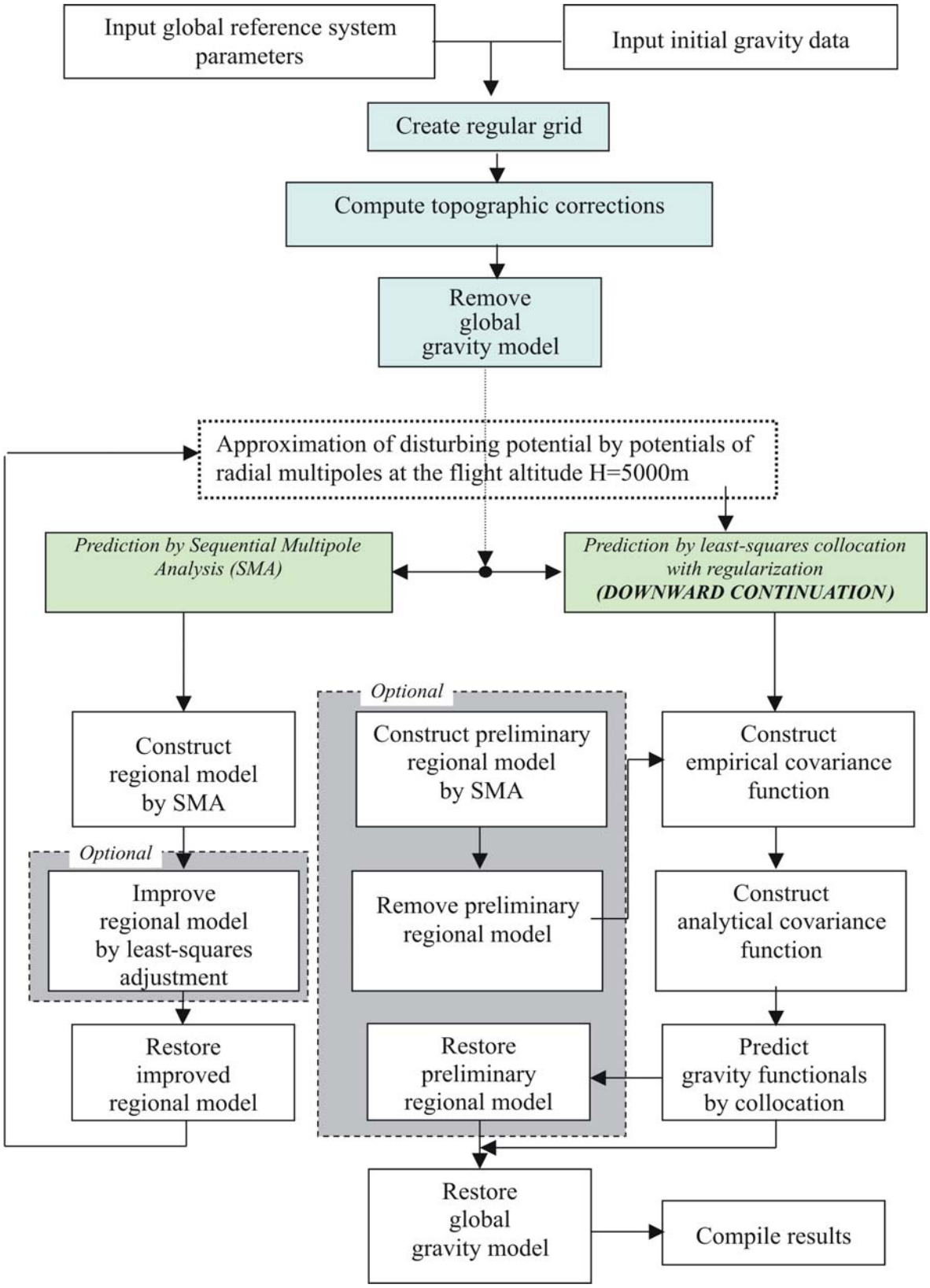


Figure 6.8 Computation structure of AGF software

### 6.6.1 Downward continuation results using RTM reduction technique

The Figures below show results after downward continuation process by using the RTM terrain correction method (Figure 6.10) as well as the relationship between analytical and empirical covariance function (see formulas in chap. 5.4) in Swiss area (Figure 6.9).

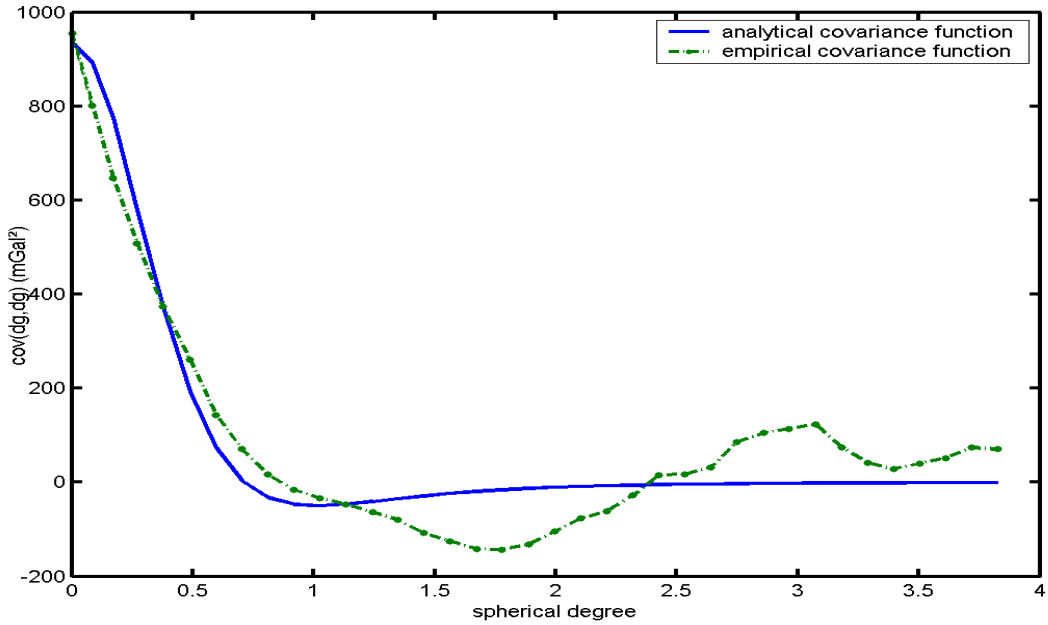


Figure 6.9 Empirical and analytical covariance functions of gravity disturbances in Switzerland

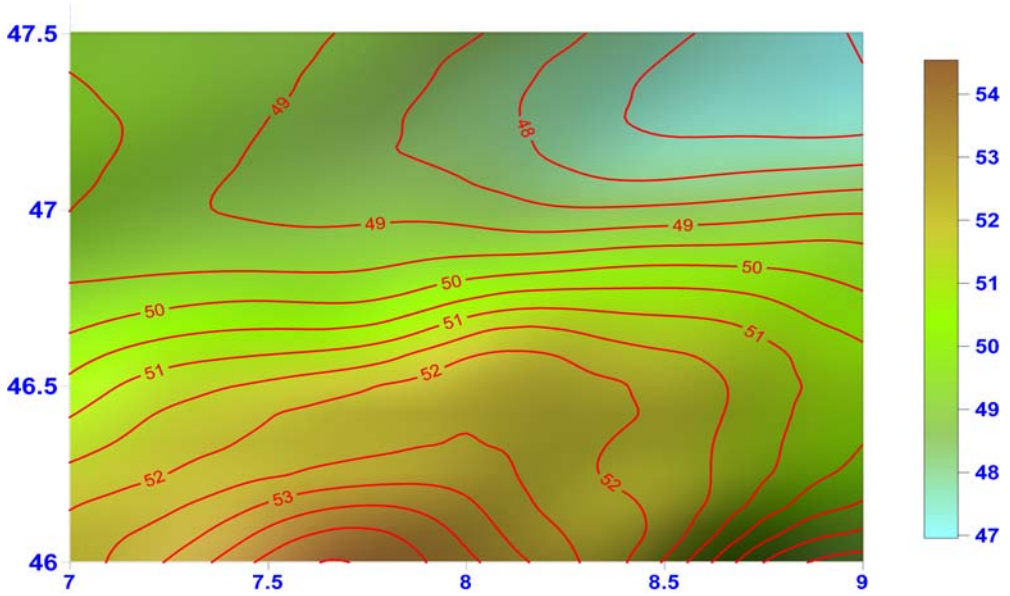


Figure 6.10 Geoid undulations computed by using airborne gravity data and RTM effects (m)

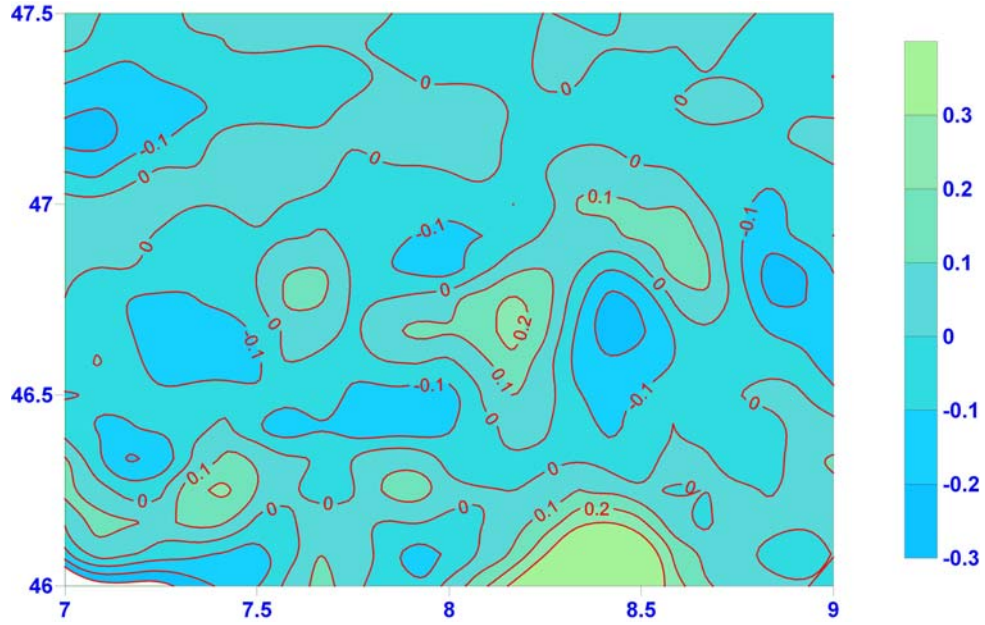


Figure 6.11 Differences between airborne and CHGeo98 geoid (m)

The Figure 6.10 shows the geoid undulations, which are calculated after downward continuation of Geopotential from the flight altitude downwards to the mean sea level. The geoid undulation values at mean sea level are computed by Bruns' formula ($N=T/\gamma$) and compensated by geopotential model contribution and indirect effect.
In the Figure 6.11 are presented the differences between the geoid undulations computed from airborne gravity data and the geoid undulations of Switzerland (CHGeo98, Swisstopo, Urs Marti, 1999). The relative large values of the indirect effect when the RTM reduction method has been used (see Figure 6.12) are caused by the terrain corrections which are calculated on the mean elevation surface.

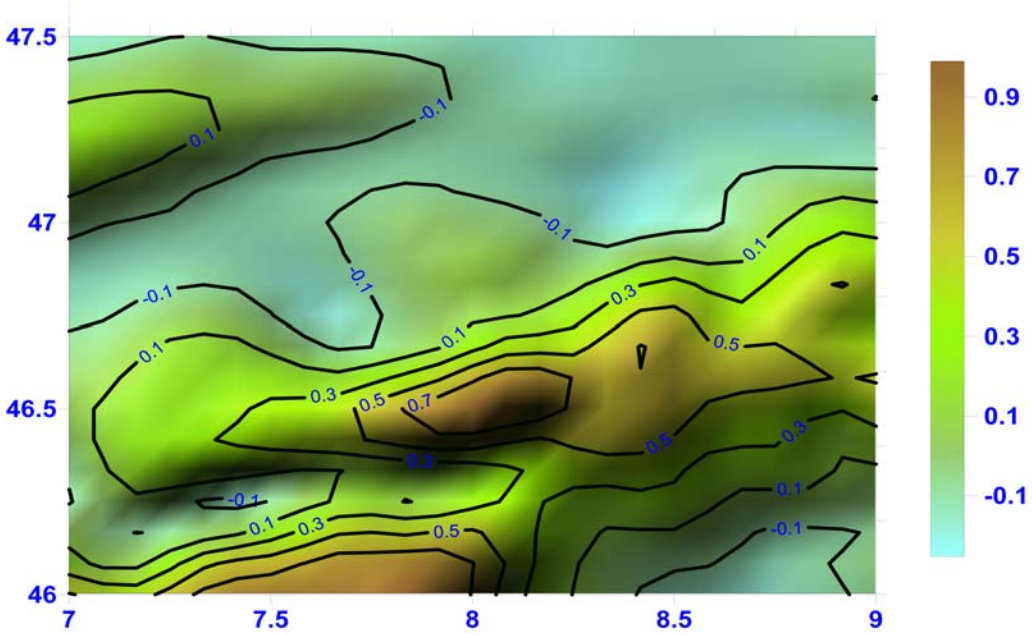


Figure 6.12 RTM indirect effect of on geoid (m)

| | Min (m) | Mean (m) | Max (m) | St.Dev (m) |
|---|---|---|---|---|
| $\delta N$ (indirect) | *-0.25* | *0.12* | *0.89* | *0.29* |
| $N_{(airborne)}$ | *46.96* | *49.84* | *52.82* | *1.55* |
| $N_{(CHGeo98)}$ | *46.97* | *49.86* | *52.73* | *1.56* |
| $dN_{(CHGeo98\text{-}airborne)}$ | *-0.32* | *0.02* | *0.28* | *0.08* |

Regularization principle: *miclosure*

Bjerhammar sphere: *R= 6365809.468*

Top bounding sphere: *R= 6373449.007*

*Table 6.4 Statistics of the downward continuation in the area 46°.25 – 47°.5 and 7°.0 – 9°.0*

Statistics in the Table 6.4 and above presented Figures show that the differences between the actual geoid of the Switzerland and the geoid computed from airborne gravity data lies at the scale ~±25cm (standard deviation is 0.08m), which is an optimistic amount, taking to account the topography of Switzerland with the heights more than 4000 meters. In all computations, the miclosure principle of regularization is used, which has been tested by AGF software and delivered the best results in comparison with quasi-solution and smoothing functional principle.

### 6.6.2 Downward continuation results using Helmert's condensation method

The computation procedure is the same as in the section 6.6.1. The results are shown below.

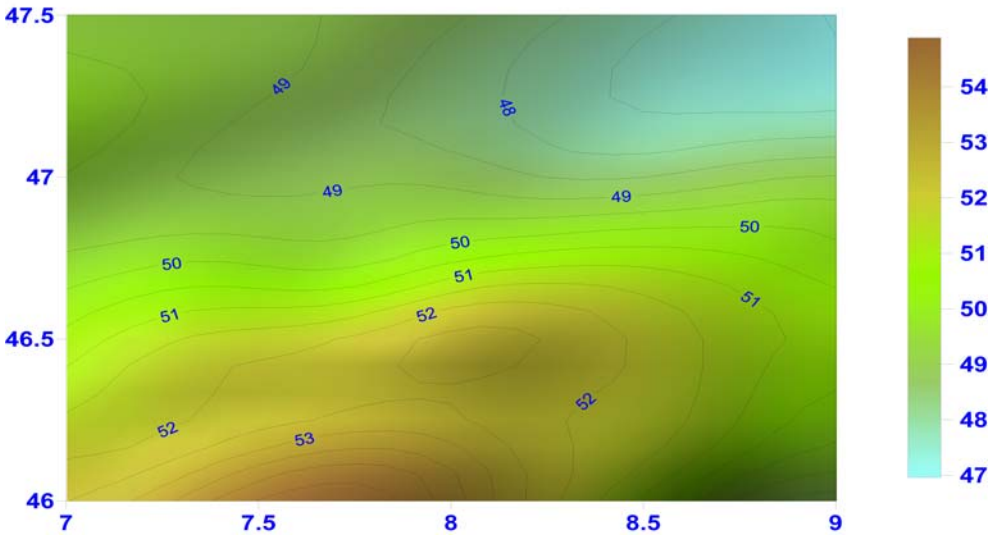


Figure 6.13 Geoid undulations computed by using airborne gravity data and Helmert's reduction (m)

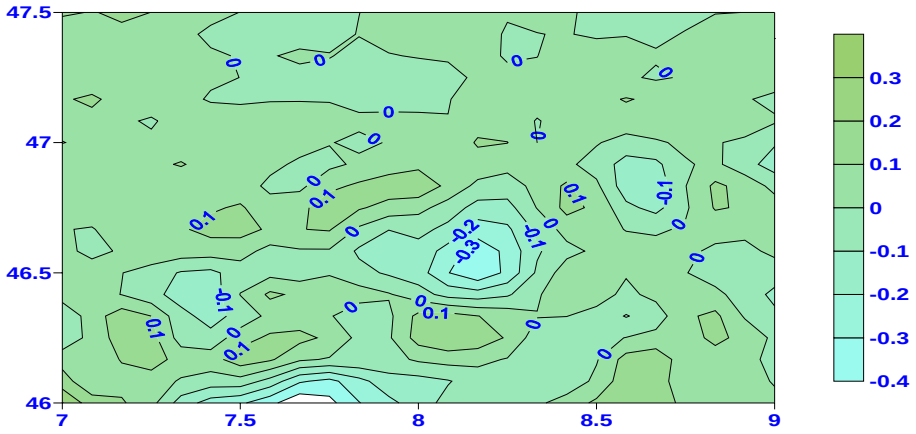


Figure 6.14 Differences between airborne and CHGeo98 geoid (m)

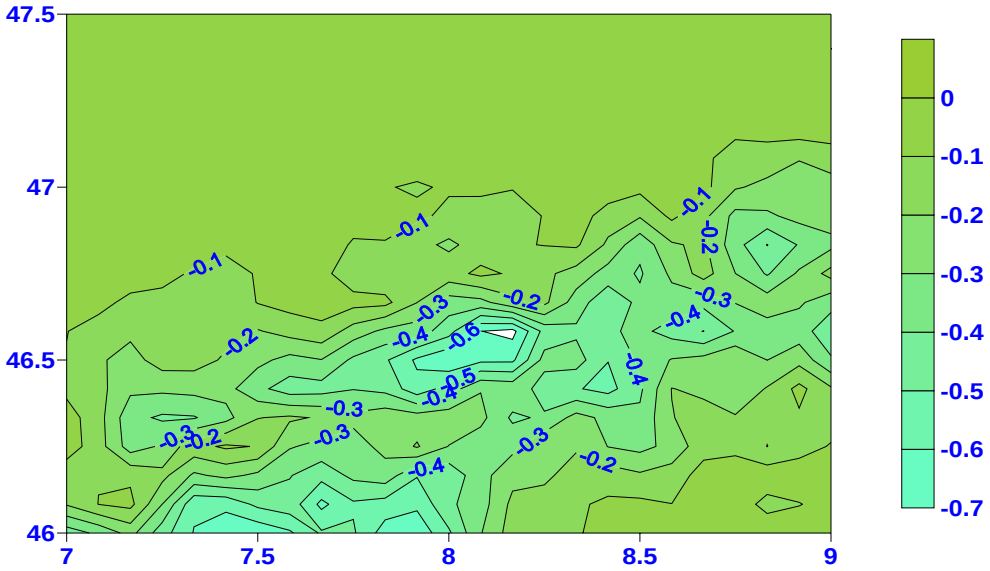


Figure 6.15 Indirect effect (2nd Helmert's condensation method) on geoid (m)

| | **Min** (m) | **Mean** (m) | **Max** (m) | **St.Dev** (m) |
|---|---|---|---|---|
| $\delta N_{(indirect)}$ | *-0.73* | *-0.17* | *0.00* | *0.17* |
| $N_{(airborne)}$ | *46.96* | *49.85* | *52.82* | *1.57* |
| $N_{(CHGeo98)}$ | *46.97* | *49.86* | *52.73* | *1.56* |
| $\delta N_{(CHGeo98\text{-}airborne)}$ | *-0.38* | *0.01* | *0.22* | *0.08* |

Regularization principle:
*miclosure*

Bjerhammar sphere:
*R= 6365809.468*

Top bounding sphere:
*R= 6373449.007*

*Table 6.5 Statistics of the downward continuation in the selected area 46°.25 – 47°.5*

### 6.6.3 Estimation of geoid accuracy after downward continuation process with different reduction techniques

In this section, the accuracy of the downward continuation will be presented in different profiles (see Figure 6.16). The aim is to show the variation of the accuracy, which depends mostly on the topography. In the area where the topography is very rough, the accuracy is smaller as in the flat areas. The accuracy increases in the north region, where the topography is smoother, as in the south region. Observing the accuracy of the both methods, which amounts to a standard deviation of more than 0.08m in the geoid undulations, its preferably to analyze the accuracy of downward continuation results in the whole area separately and carry out a conclusion about their variations. The Figures below display the accuracy of the downward continuation in different areas and for the different method of calculation.

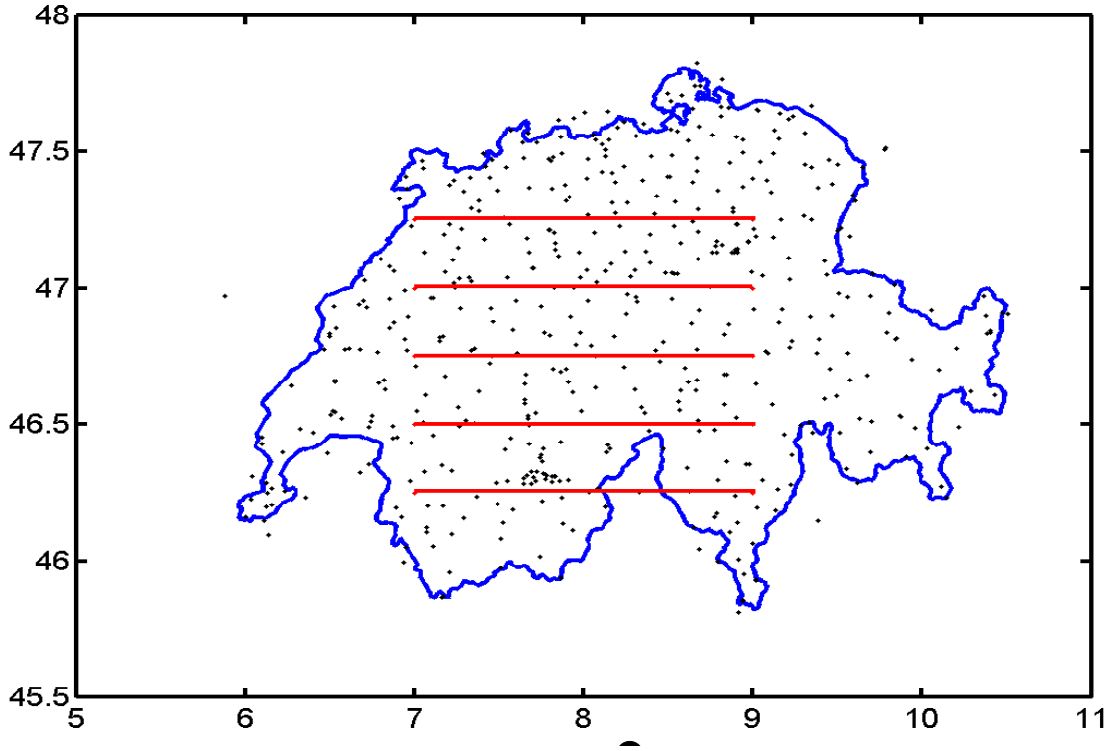


Figure 6.16 Selected profiles for the accuracy estimation

### 6.6.4 Comparison of geoid undulations using airborne gravity data (LSC+SMA) with actual geoid of Switzerland CHGeo98.

| **CHGeo98 –airborne** *Profile 46°.25* | **Min** (m) | **Mean** (m) | **Max** (m) | **St.Dev** (m) |
|---|---|---|---|---|
| | | | | |
| ***RTM*** | *-0.31* | *-0.05* | *0.07* | *0.09* |
| ***Helmert*** | *-0.16* | *0.05* | *0.21* | *0.10* |

| **CHGeo98 -airborne** *Profile 46°.50* | **Min** (m) | **Mean** (m) | **Max** (m) | **St.Dev** (m) |
|---|---|---|---|---|
| | | | | |
| ***RTM*** | *-0.10* | *0.05* | *0.18* | *0.08* |
| ***Helmert*** | *-0.38* | *-0.08* | *0.10* | *0.12* |

| **CHGeo98 –airborne** *Profile 46°.75* | **Min** (m) | **Mean** (m) | **Max** (m) | **St.Dev** (m) |
|---|---|---|---|---|
| | | | | |
| ***RTM*** | *-0.24* | *0.02* | *0.26* | *0.14* |
| **Helmert** | *-019* | *0.04* | *0.17* | *0.10* |

| **CHGeo98 –airborne** *Profile 47°.00* | **Min** (m) | **Mean** (m) | **Max** (m) | **St.Dev** (m) |
|---|---|---|---|---|
| | | | | |
| ***RTM*** | *-0.15* | *0.00* | *0.14* | *0.07* |
| ***Helmert*** | *-0.04* | *0.02* | *0.17* | *0.05* |

| **CHGeo98 –airborne** *Profile 47°.25* | **Min (m)** | **Mean (m)** | **Max (m)** | **St.Dev (m)** |
|---|---|---|---|---|
| | | | | |
| ***RTM*** | *-0.09* | *0.03* | *0.20* | *0.08* |
| ***Helmert*** | *-0.08* | *0.01* | *0.12* | *0.05* |

*Table 6.6 Statistics of geoid undulations after downward continuation process*

## 6.7 Downward continuation of disturbing potential by combination of the SMA and iterative solution of the Poisson Integral

The downward continuation of disturbing potential by inverting Poisson's integral in an iterative way, began after determination of disturbing potential in the constant flight line by Sequential Multipole Analysis method. The input data are mean values of disturbing potential discretized in a 5'x5' grid. The area of interest consists of 2160 points that are lying in latitudes $45^\circ \le \varphi \le 48^\circ$ and longitudes $5^\circ \le \lambda \le 10^\circ$. The Jacobi iteration has been used to solve the large system of equations. The purpose of the Poisson integral method used in this thesis is to compare results with above proposed main method (LSC+SMA).
The source code used for the continuation of the data is based on the spherical Abel-Poisson kernel function and spherical approximation of the geoid surface (Novak et al. 2003). Tables 6.7 and 6.8 show the results after downward continuation of disturbing potential by inversion of Poisson's integral in an iterative way.

| | **Min** (m) | **Mean** (m) | **Max** (m) | **St.Dev** (m) |
|---|---|---|---|---|
| $\delta N_{(indirect)}$ | *-0.25* | *0.12* | *0.89* | *0.29* |
| $N_{(airborne)}$ | *47.04* | *50.40* | *53.50* | *1.72* |
| $N_{(CHGeo98)}$ | *46.97* | *49.86* | *52.73* | *1.56* |
| $\delta N_{(CHGeo98\text{-}airborne)}$ | *-0.66* | *0.05* | *0.92* | *0.32* |

*Table 6.7 Statistics of geoid undulations after downward continuation process using RTM reduction technique*

| | **Min** (m) | **Mean** (m) | **Max** (m) | **St.Dev** (m) |
|---|---|---|---|---|
| $\delta N_{(indirect)}$ | *-0.73* | *-0.17* | *0.00* | *0.17* |
| $N_{(airborne)}$ | *47.19* | *49.85* | *52.58* | *1.45* |
| $N_{(CHGeo98)}$ | *46.97* | *49.86* | *52.73* | *1.56* |
| $\delta N_{(CHGeo98\text{-}airborne)}$ | *-0.39* | *0.13* | *0.85* | *0.20* |

*Table 6.8 Statistics of geoid undulations after downward continuation process using Helmert's second condensation method*

### 6.7.1 Comparison of geoid undulations using iterative solution of Poisson's integral with actual geoid of Switzerland CHGeo98.

| **CHGeo98 –airborne** *Profile 46°.25* | **Min (m)** | **Mean (m)** | **Max (m)** | **St.Dev (m)** |
|---|---|---|---|---|
| | | | | |
| ***RTM*** | *-0.32* | *-0.11* | *0.15* | *0.14* |
| ***Helmert*** | *-0.11* | *0.35* | *0.85* | *0.27* |

| **CHGeo98 –airborne** *Profile 46°.50* | **Min (m)** | **Mean (m)** | **Max (m)** | **St.Dev (m)** |
|---|---|---|---|---|
| | | | | |
| ***RTM*** | *-0.06* | *0.34* | *0.90* | *0.28* |
| ***Helmert*** | *-0.34* | *0.02* | *0.46* | *0.21* |

| **CHGeo98 –airborne** *Profile 46°.75* | **Min (m)** | **Mean (m)** | **Max (m)** | **St.Dev (m)** |
|---|---|---|---|---|
| | | | | |
| ***RTM*** | *-0.63* | *-0.19* | *0.25* | *0.27* |
| **Helmert** | *-0.22* | *0.16* | *0.56* | *0.19* |

| **CHGeo98 –airborne** *Profile 47°.00* | **Min (m)** | **Mean (m)** | **Max (m)** | **St.Dev (m)** |
|---|---|---|---|---|
| | | | | |
| ***RTM*** | *-0.43* | *0.07* | *0.34* | *0.15* |
| ***Helmert*** | *-0.03* | *0.12* | *0.38* | *0.09* |

| **CHGeo98 –airborne** *Profile 47°.25* | **Min (m)** | **Mean (m)** | **Max (m)** | **St.Dev (m)** |
|---|---|---|---|---|
| | | | | |
| ***RTM*** | *-0.12* | *0.07* | *0.34* | *0.14* |
| ***Helmert*** | *-0.14* | *0.02* | *0.17* | *0.09* |

*Table 6.9 Statistics of the geoid undulations after downward continuation process in the selected area 46°.25 – 47°.5*

## 6.8 Comparison of both methods with the geoid of Switzerland CHGeo98

One of the objectives of this thesis is to investigate the application of airborne gravity data to gravity field and geoid analysis. Figures below show that there is no unique method which can fulfill predefined requirements for a stable downward continuation process for geoid determination. It is evident that the accuracy of the downward continuation depend on many factors, such as: Topography, flight altitude, measurement accuracy, data processing etc. For this reason, I tried to analyze the accuracy of the downward continuation in different areas separately and compare it with the geoid of Switzerland. There are five latitudes with geoid undulations selected for the comparison of results carried out by different methods.

### 6.8.1 Results of geoid undulations after downward continuation process in latitude φ=46°.25 ($7^\circ \le \lambda \le 9^\circ$)

The first selected profile ( $\varphi=46°.25$ ) lies in south region of Switzerland which contains a very rough topography with heights 1000m –3000m (see Annexes 9.1). The best results (St.Dev= 9cm) are acquired by least-squares collocation method with RTM reduction technique. The Poisson integral with Helmert's reduction technique gave the poorly and unstable results (St.Dev=27cm).

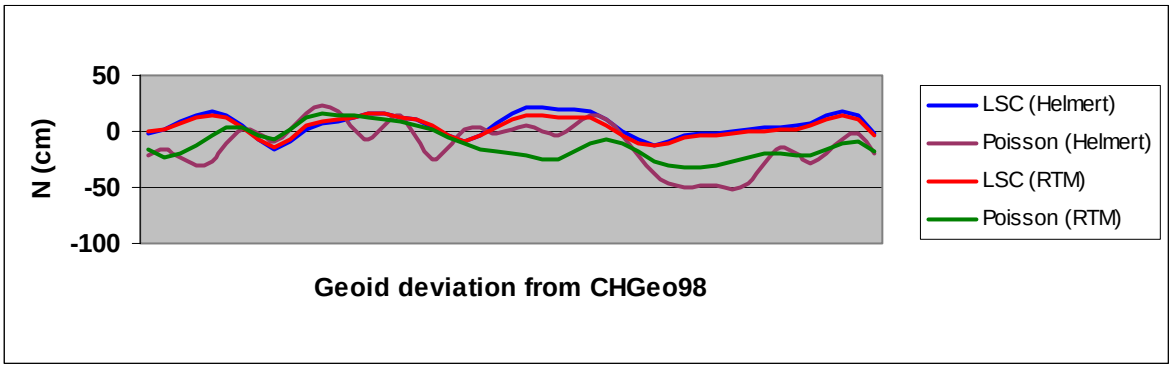


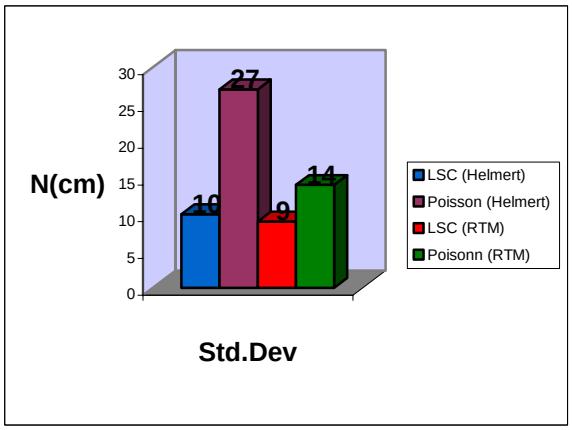


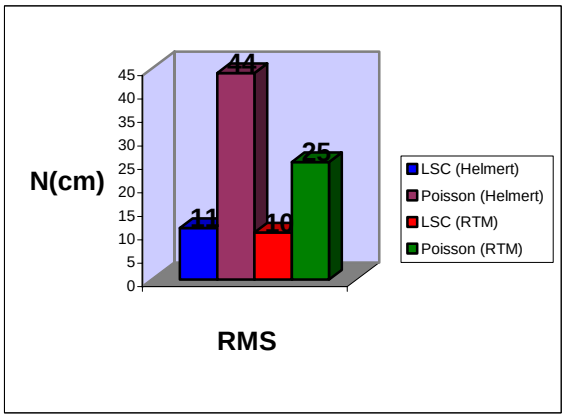

### 6.8.2 Results of geoid undulations after DC process in latitude φ=46°.50 ($7^\circ \le \lambda \le 9^\circ$)

In the profile at latitude $\varphi=46°.50$ that lies in the middle of Swiss Alps with the topographical heights > 4000m (see Ann. 9.2), it is obvious that the Poisson integral method has very sharp signals. The standard deviations equal to 28cm and 62cm acquired by Poisson's integral method are not credibility values, because the signals computed with different reduction techniques has un-proportional trend, versus the least-squares collocation contains a smooth and credible signal. The large deviation of geoid undulations computed by airborne gravity data from the CHGeo98 geoid are present in the middle of the profile. This is caused by the gaps in the measured profiles and very large topographical heights.

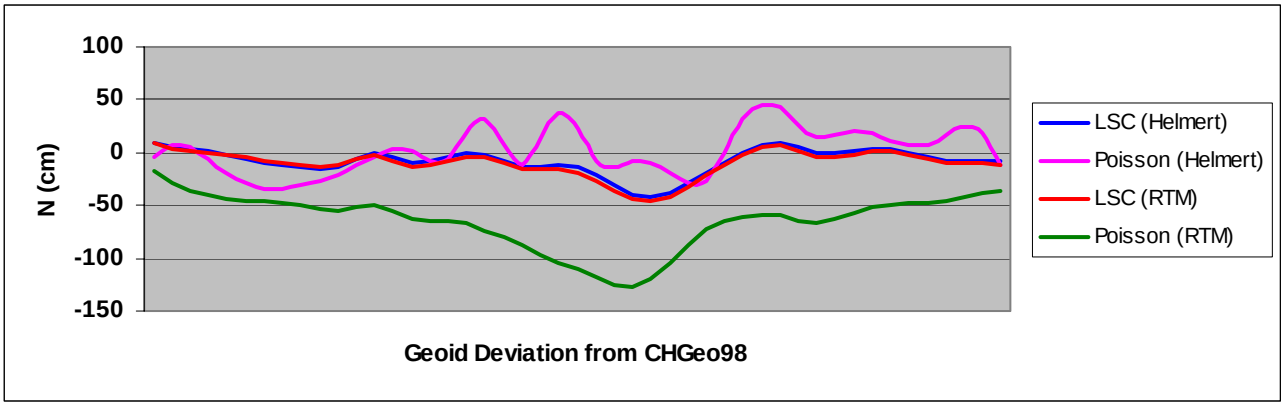


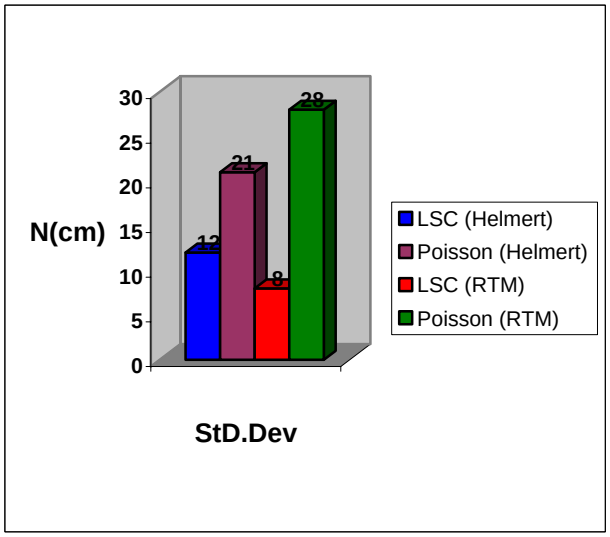


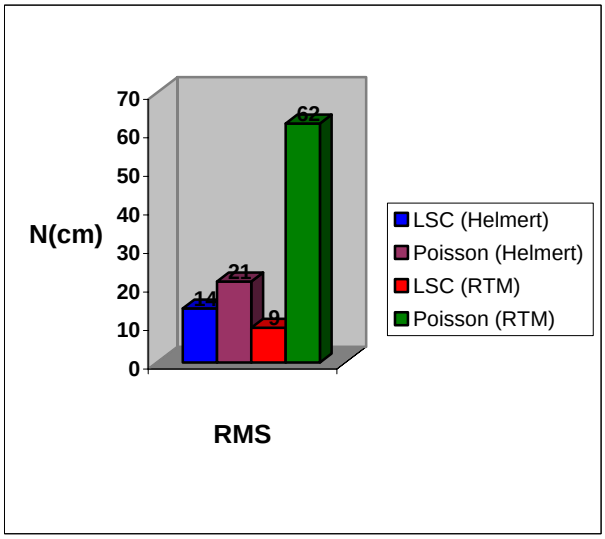

### 6.8.3 Results of geoid undulations after DC process in latitude φ=46°.75 ($7^\circ \le \lambda \le 9^\circ$)

The signals with geoid undulations below have proportional trend; here is also present an evident change in the accuracy. The best accuracy is acquired by least-squares collocation with Helmert's terrain correction technique. This is an evidence which proves that there is no unique terrain correction technique for the whole area.

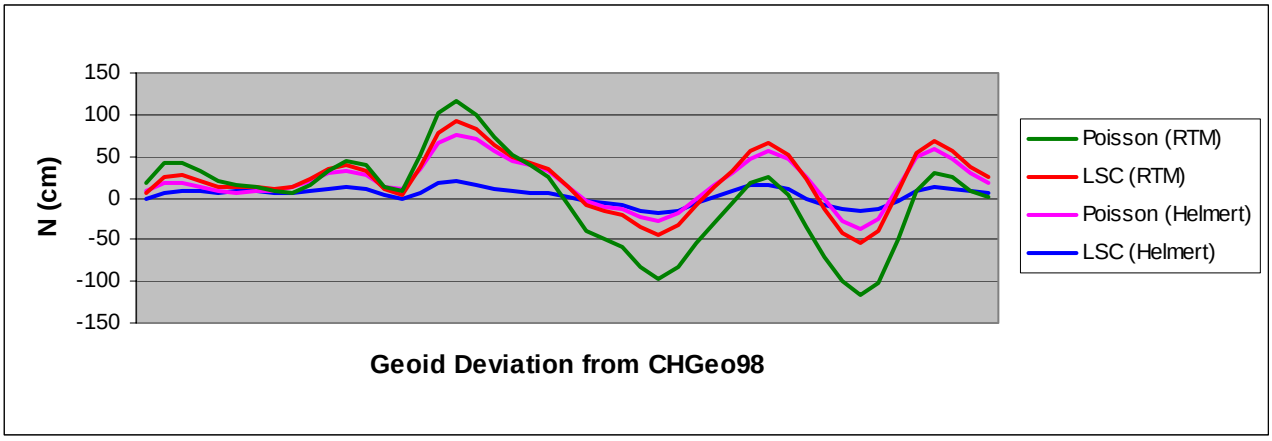


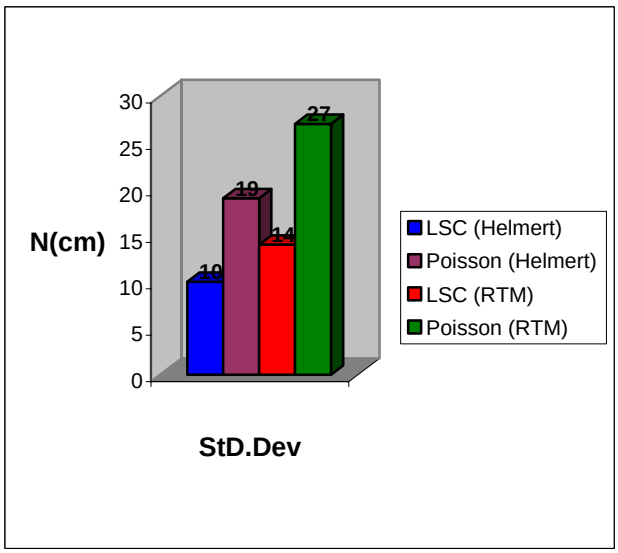


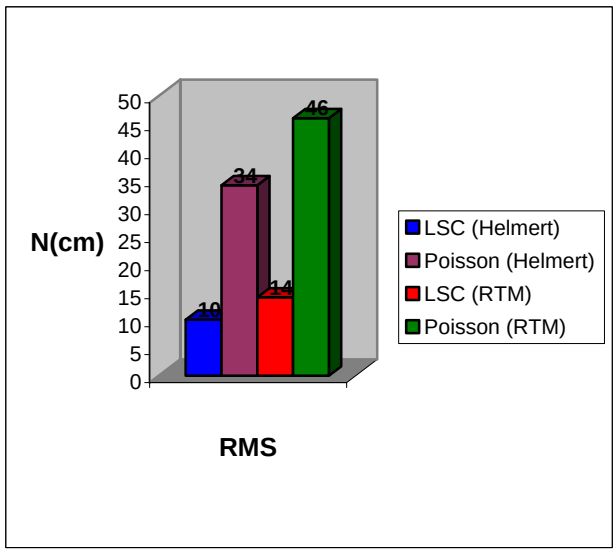

### 6.8.4 Results of geoid undulations after DC process in latitude φ=47°.00 ($7^\circ \le \lambda \le 9^\circ$)

In the northern part of Switzerland where the topography is smoother as in south, it is evidently that the Helmert terrain correction method and least-squares collocation offer better results comparing to other methods. The standard deviation is 5cm, which can be qualified as a promising accuracy for the geoid determination from airborne gravity data.

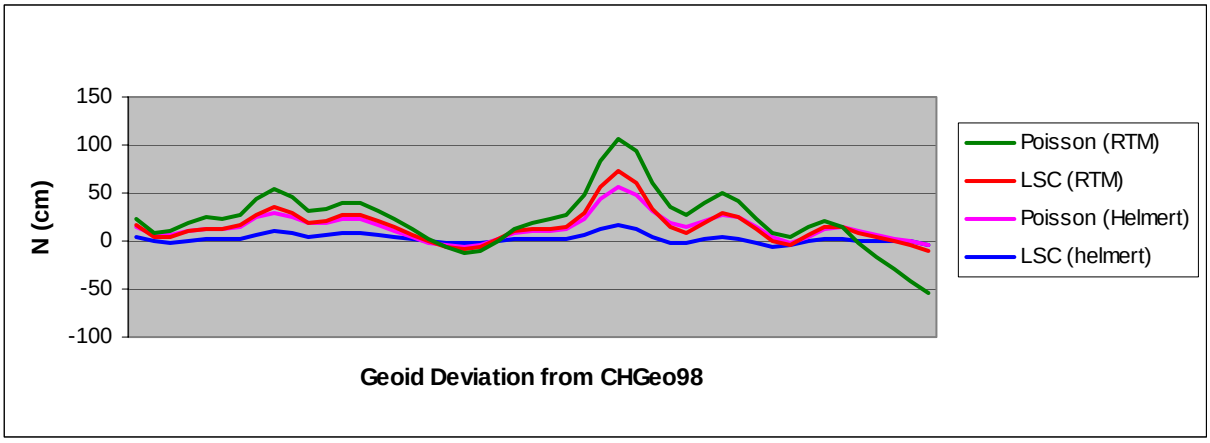


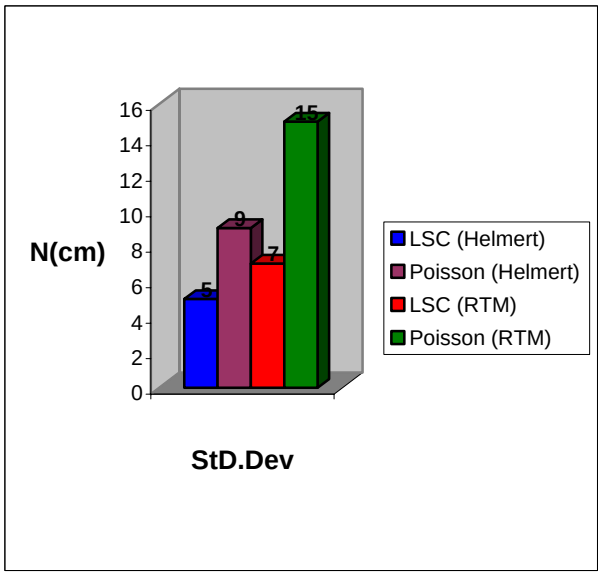


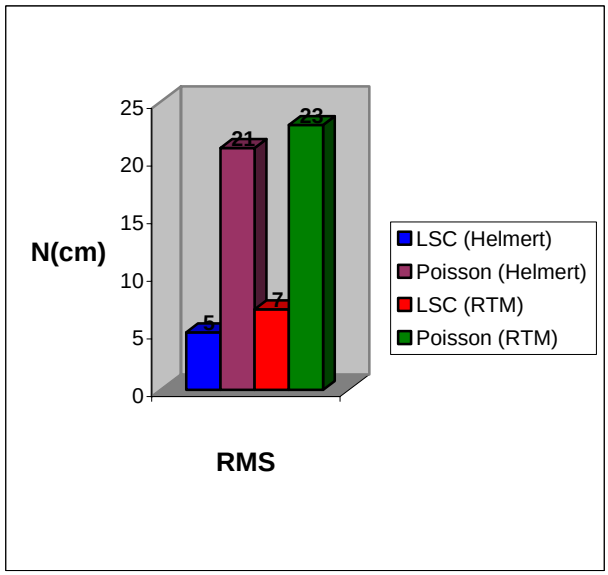

### 6.8.5 Results of geoid undulations after DC process in latitude φ=47°.25 ($7^\circ \le \lambda \le 9^\circ$)

In the northern profile at the latitude $\varphi=47°.25$ it is evidently proofed that for the flat areas, the least-squares collocation with Helmert's terrain correction technique gave the best results. The standard deviation of 5cm, shows the continuity of the accuracy followed from previous latitude. Otherwise, the Poisson integral method with the RTM terrain correction technique can be considered as unstable solution for areas with large topography and flight altitudes. Detailed description of the relationship between the geoid undulations computed from different methods are given in chapter 9.

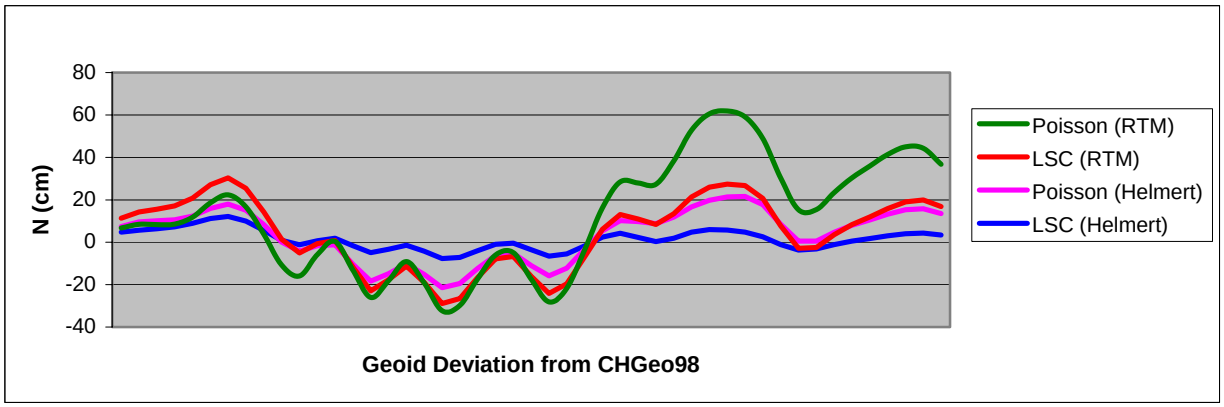


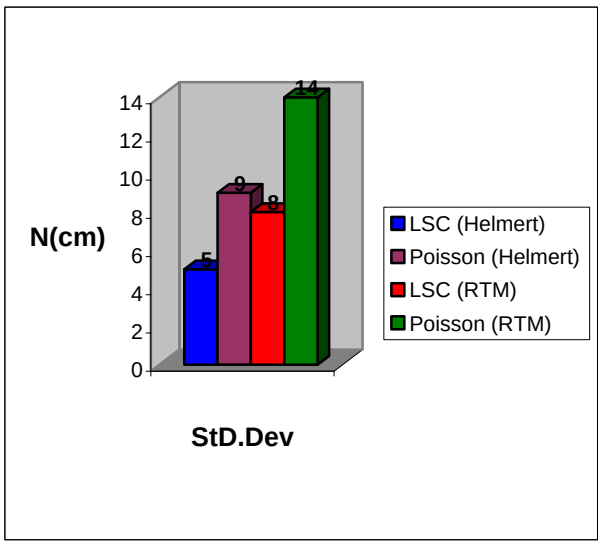


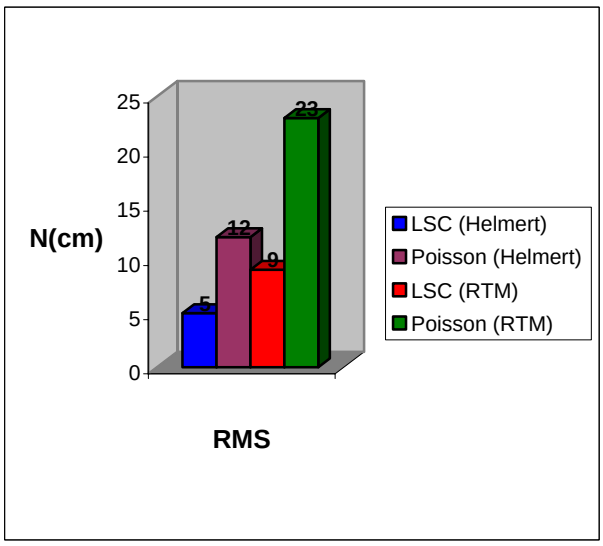

# 7 Conclusions and Recommendations

The general objective of the thesis was to analyze the downward continuation of airborne gravity data and its application to gravity field and geoid analysis. More explicitly it has been tried to answer the following questions (requirements): *a) Which is the most stable solution for the downward continuation of airborne gravity in large flight altitudes? and b) how the topography influences the downward continuation process?*

Besides most of the recent prevailing studies, which have treated downward continuation of gravity anomalies or disturbances as a poorly mathematical inversion or regularization problem, this thesis incorporates as well physical impacts in the solution of the problem (terrain correction).

The proposed strategy of the downward continuation process is divided in two parts. The first part treats the problem of the determination of disturbing potential at the flight altitude by Sequential Multipole Analysis (SMA). The second part includes continuation of the disturbing potential from the flight altitude to mean sea level by least-squares collocation with regularization. The advantages in performing this methods are:

i) Approximation of disturbing potential by potentials of radial multipoles is an exact technique for the determination of point potentials at the flight line and does not require grid data.

ii) The signal after determination of the disturbing potential (geoid) at the flight line is smoother (harmonic) as it can be a signal with gravity anomalies or disturbances.

iii) Possibility to use heterogeneous data for the stabilization of the downward continuation procedure, such as GPS/leveling and land gravity data.

iv) No spherical approximation of the geoid is needed.

The downward continuation output results at mean sea level are stored in the set of geoid undulations, which are computed by Bruns' formula. Its accuracy has been compared by geoid undulations of the geoid of Switzerland CHGeo98.

The impact of the topographical masses in gravity observation is analyzed by using two independent terrain correction methods. Analyzing results in chapter 6, it is evident that there is no unique method that can fulfills the given requirements.

The advantage of the combination of Sequential Multipole Analysis and least-squares collocation is the possibility to impose the land data, which stabilize the downward

continuation process. The land data (GPS/leveling points) is used as well for the improvement of the disturbing potential determined by sequential Multipole Analysis at the flight altitude.
The problem of instability in Poisson's integral method is because this method is based in the data at discrete points and needs very large extension of the data (grid) for the calculation of far-zone contribution and edge effects (about 2° in the East-West and 1° in the South-North direction). By gridding of the observed gravity values, a lot of information may be lost. One of the advantages of the SMA+LSC method is the volume of the data, that has been used (55448 points); otherwise for the Poisson method, the number of points is equal to 2160 (5'x5' grid). Other conclusions of the presented study are the terrain corrections. There are no unique terrain correction methods, which can be used for whole area. It is proven that in the rough topography, for a suitable downward continuation of airborne gravity data, it is essential and advantageous to use RTM reduction with Mean Elevation Surface. This is due to the fact that the impact of long-wave components of the gravity is small, together with the effect of large differences of DTM heights. In this study, the Residual Terrain Model (RTM) method gave very good results in south part of the test area comparing to the second Helmert's condensation method, and vice versa for the north part (smooth topography). For the development of an efficient strategy for the downward continuation of airborne gravity data, there are two aspects that should be taken into account; first, the *airborne survey strategy* and second, the *computation methodology*. The recommendations for the gravity surveys should be given to better flight planning and filtering.
It is very useful to arrange the filtering technique with the flight plan to eliminate the gaps, which come through filtering edge effects. The recommendations for the computation strategy of the downward continuation should be concentrated on these aspects; it is preferable to define the Geopotential (e.g. by SMA) at constant flight line and then to continue it to mean sea level. The reason is that the Geopotential is a harmonic function outside the Earth's surface; the surface for the downward continuation is smoother as it can be the surface with gravity anomalies or disturbances. It is preferable to use the insertion of GPS/leveling or geoid heights for the stabilization of the downward continuation process. These recommendations come from the analysis done in this study work and are successfully tested by combination of the Sequential Multipole Analysis (SMA) and least-squares collocation in Bjerhammar-Krarup model.

# 8 Bibliography

Abrikosov, O.A. On the stable determination of some Earth's radial density models. *Geodynamics, pp.11-17, (1999a).*

Abrikosov, O.A. The determination of the regularization parameter in the variational problem of data processing. *Geodynamics, pp.59-62, (1999b).*

Abrikosov, O.A. and Marchenko, D. AGF 4.2 Software, Analysis of the Gravity Field GFZ Version 4.2, *GeoForschungsZentrum Potsdam, ( 2001).*

Bastos, L. Cunha, S. Forsberg, R. Olesen, A. Gidskehaug, A. Timmen, L. Meyer, U . On the use of Airborne in Gravity Field Modeling; Experiences from the AGMASCO project. *Phys. Chem. Earth (A), Vol. 25, No. 1, pp. 1-7, (2000).*

Bian, S and Zhang, K. F. The Planar Solution of Geodetic Boundary Value Problem, *Manuscripta Geodaetica, Vol. 18, pp. 290-294, (1993).*

Childers, V. A. Bell, R. E. Brozena, J. M. Airborne Gravimetry: An investigation of filtering. *Geophysics, Vol. 64, No. 1, pp: 61-69, (1999).*

Forsberg, R. A study of Terrain Reductions, Density Anomalies and Geophysical Inversion Methods in Gravity Field Modeling. *Department of Geodetic Science and Surveying, Ohio State University, Ohio, Report No. 355, (1984)*

Forsberg, R. Terrain effects in Geoid Computations. - Lectures Notes. *International School for the Determination and Use of the Geoid. - International Geoid Service. DIIAR, Milan, Italy, (1994).*

Forsberg, R. and Brozena, J.M. Airborne geoid measurements in the arctic ocean. *Gravity, Geoid and Marine Geodesy IAG Symp. Proceed. vol. 117, pp. 139-146, Springer, (1997).*

Freeden, W. Schneider, F. Schreiner, M. Gradiometry - An Inverse Problem in Modern Satellite Geodesy. *In SIAM Symposium on Inverse Problems in Geophysical Applications. England, Louis, Rundell, editors, 179-239, (1997).*

Hein, G. Progress in airborne gravimetry: Solved, open and critical problems. *Proceedings of the IAG Symposium on Airborne Gravity Field Determination, IUGG XXI General assembly, Boulder, Colorado, July 2-14, (1995).*

Heiskanen, W.A. and Moritz, H. Physical Geodesy. *W.H. Freeman, San Francisco, (1967).*

Horn, R.A., and Johnson, C.R. Matrix Analysis. *Cambridge University Press: Cambridge, London, New York, New Rochelle, Melbourne, Sydney, (1986).*

Jekeli, C. and Kwon, J.H. Results of airborne vector (3-D) gravimetry. *Geophysic. Res. Lett., Vol. 26, No. 23, pp. 3533-3536, December 1st, (1999).*

Kearsley, A. H. W. Forsberg, R. Olesen, A. Bastos, L. Hehl, K. Meyer, U. Gidskehaug, A. Airborne gravimetry used in precise geoid computations by ring integration. *Journal of Geodesy, 72: pp. 600-605, (1998).*

Klees, R. Topics of boundary element methods. Geodetic Boundary Value Problems in View of the One Centimeter Geoid. *Volume 65 of Lecture Notes in Earth Sciences, pages 482-531. Springer, (1997).*

Klingelé, E. Cocard, M. Halliday, M. Kahle, H.-G. The Airborne Gravimetric Survey of Switzerland. *Matériaux pour la Géologie de la Suisse, Geophysique, No. 31,(1996).*

Krarup, T. A Contribution to the Mathematical Foundation of Physical Geodesy. *Danish Geod. Inst. Public., No 44, Copenhagen, (1969).*

Lelgemann, D. and Marchenko, A. On concepts for modeling the Earth's gravity field. *Deutsche Geodätische Kommission, Verlag der Bayerischen Akademie der Wissenschaften, Heft nr. 117, Reihe A, (2001).*

Lemoine, F.G. Kenyon, S.C. Factor, J.K. Trimmer, R.G. Pavlis, N.K. Chinn, D.S. Cox, C.M. Klosko, S.M. Luthcke, S.B. Torrence, M.H. Wang, Y.M. Williamson, R.G. Pavlis, E.C. Rapp, R.H. Olson, T.R. The Development of Joint NASA GSFC and the National Imagery and Mapping Agency (NIMA) Geopotential Model EGM96. *NASA Technical paper NASA/TP-1998-206861. Goddard Space Flight Center, Greenbelt, USA, (1998)*

Marchenko, A.N. Description of the Earth's gravity field by the system of potentials of non-central multipoles. *Kinematics and Physics of Celestial Bodies, Kiev, (1987).*

Marchenko, A.N. Abrikosov, O.A. Romanishin, P.O. Improvement of the Gravimetric Geoid in the Ukraine Area Using Absolute Gravity Data. *Proceed. of the Session G4 "Latest Developments in the Computation of Regional Geoids", XX General Assembly EGS, Hamburg, Germany, 1995, Rep. of Finnish Geod. Inst., No 7, 19-22, (1995).*

Marchenko, A. N. Parameterization of the Earth's gravity field. Point and line singularities. *Lviv Astronomical and Geodetic Society, (1998).*

Marti, U. CHGeo98 – Das neue Geoid der Schweiz. *Reporter 43, p. 4- 7, Leica geosystems AG, Herbrugg, Switzerland, (1999).*

Martinec, Z. Boundary-Value Problems for Gravimetric Determination of a Precise Geoid. *Lecture Notes in Earth Sciences; 73. Spinger Verlag, (1998).*

Martinec, Z. Stability investigations of a discrete downward continuation problem for geoid determination in the Canadian Rocky Mountains. *Journal of Geodesy, Vol. 70, (1996)*

Martinec, Z. and Matyska, C. On the solvability of the Stokes pseudo-boundary-value problem for geoid determination. *Journal of Geodesy, 71:103-112, (1997).*

Martinec, Z. and Vanicek, P. Direct topographical effect of Helmert's condensation for a spherical approximation of the geoid. *Manuscripta Geodaetica, 19: 257-268, (1994).*

Meyer, U. Boedecker, G. Pflug, H. Airborne Navigation and Gravimetry Ensemble & Laboratory (ANGEL). *GeoForschungsZentrum Potsdam Scientific Technical Report STR03/06, (2003).*

Moritz, H. Advanced Physical Geodesy, H. Wichmann, Karlsruhe (1980).

Moritz, H. Geodesist's Handbook, *IAG – International Association of Geodesy, (1992).*

Morozov, V.A. Regular Methods for Solution of Ill-posed Problems. *Nauka, Moscow, (1987).*

Nahavandchi, H. and Sjöberg, E. L. Two different views of topographical and downward-continuation corrections in the Stokes-Helmert approach to geoid computation. *Journal of Geodesy, Vol. 16, (2001).*

Neyman, Yu.M. Variational Method of Physical Geodesy. *Nedra, Moscow, (1979).*

NIMA Report No. TR8350.2, World Geodetic System 1984 – Its definition and Relationships with local Geodetic systems. *Department of Defense, USA, (2000).*

Novak, P. Kern, M. Schwarz, K.-P. Heck, B. On the determination of the gravimetric geoid from airborne gravity. *University of Calgary Tech. Rep. 30013, Department of Geomatics Engineering. (2001).*

Novak, P. Kern, M. Schwarz, K. P. Sideris, M. G. Heck, B. Ferguson, S. Hammada, Y. Wei, M. On geoid determination from airborne gravity. *Journal of Geodesy, 76:510-522. (2003).*

Salychev, O. Inertial Systems in Navigation and Geophysics. *Bauman MSTU Press, Moscow, (1998)*

Sanso, F. and Rummel, R. Geodetic Boundary Value Problems in View of the One Centimeter Geoid. *Lecture Notes in Earth Sciences, 65, Springer, Berlin, (1997).*

Schwarz, K.-P. and Li, Z. An introduction to airborne gravimetry and its boundary value problems. Geodetic boundary value problems in view of the one centimeter geoid. *Lecture Notes in Earth Sciences, pp. 312-355, Springer, (1997).*

Sünkel, H. Mathematical and Numerical Techniques in Physical Geodesy. *Lecture Notes in Earth Sciences Vol. No. 7, Springer, (1997).*

Tikhonov, A.N. and Arsenin, V. Y. Methods of Solution of Ill-posed Problems. *Nauka, Moscow, (1986) .*

Vanicek, P. and Janak, J. The UNB Technique for Precise Geoid Determination. *CGU, Banff, Alberta, May 26, (2000).*

Vanicek, P. Sun, W. Ong, P. Martinec, Z. Najafi, M. Vajda, P. Hostter, B. Downward continuation of Helmert's gravity. *Journal of Geodesy, 71:21-34, (1996).*

Vanicek, P. and Martinec, Z. The Stokes-Helmert Scheme for the Evaluation of Precise Geoid. *Manuscripta Geodaetica, 19, 119-128, (1994).*

Vanicek, P. Novak, P. Martinec, Z. Geoid, topography, and the Bouguer plate or shell. *Journal of Geodesy, Vol. 75, pp.210-215, (2001)*

Wei, M. and Schwarz, K. P. Flight test results from a strap-down airborne gravity system. *Journal of Geodesy, Vol. 72, No. 6, pp. 323-332 (1998).*

# 9 Annexes

*Ann. 1 Geoid undulation results after downward continuation of disturbing potential using RTM reduction technique for five selected profiles in constant latitudes*

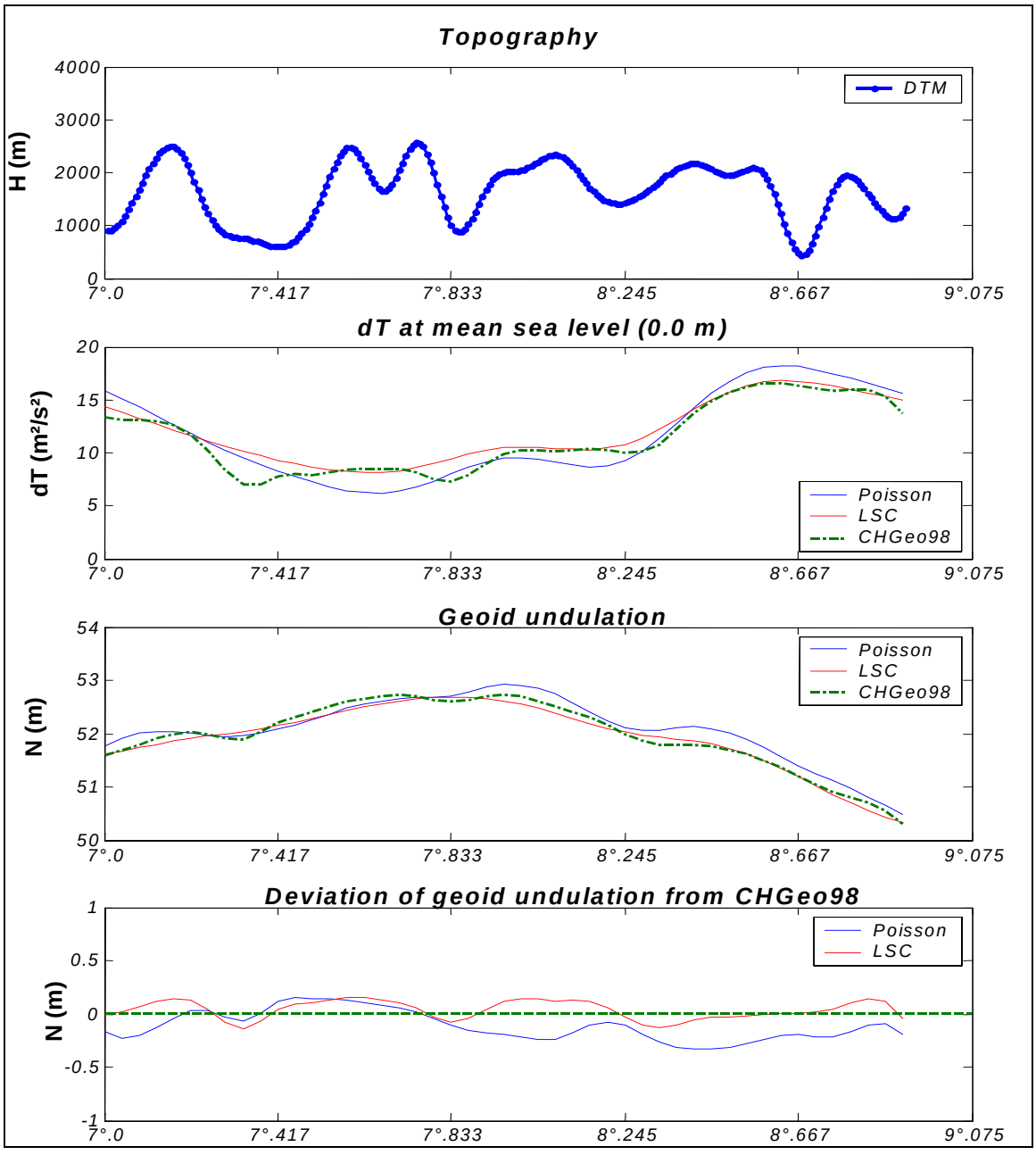


*Profile in latitude 46°.25*

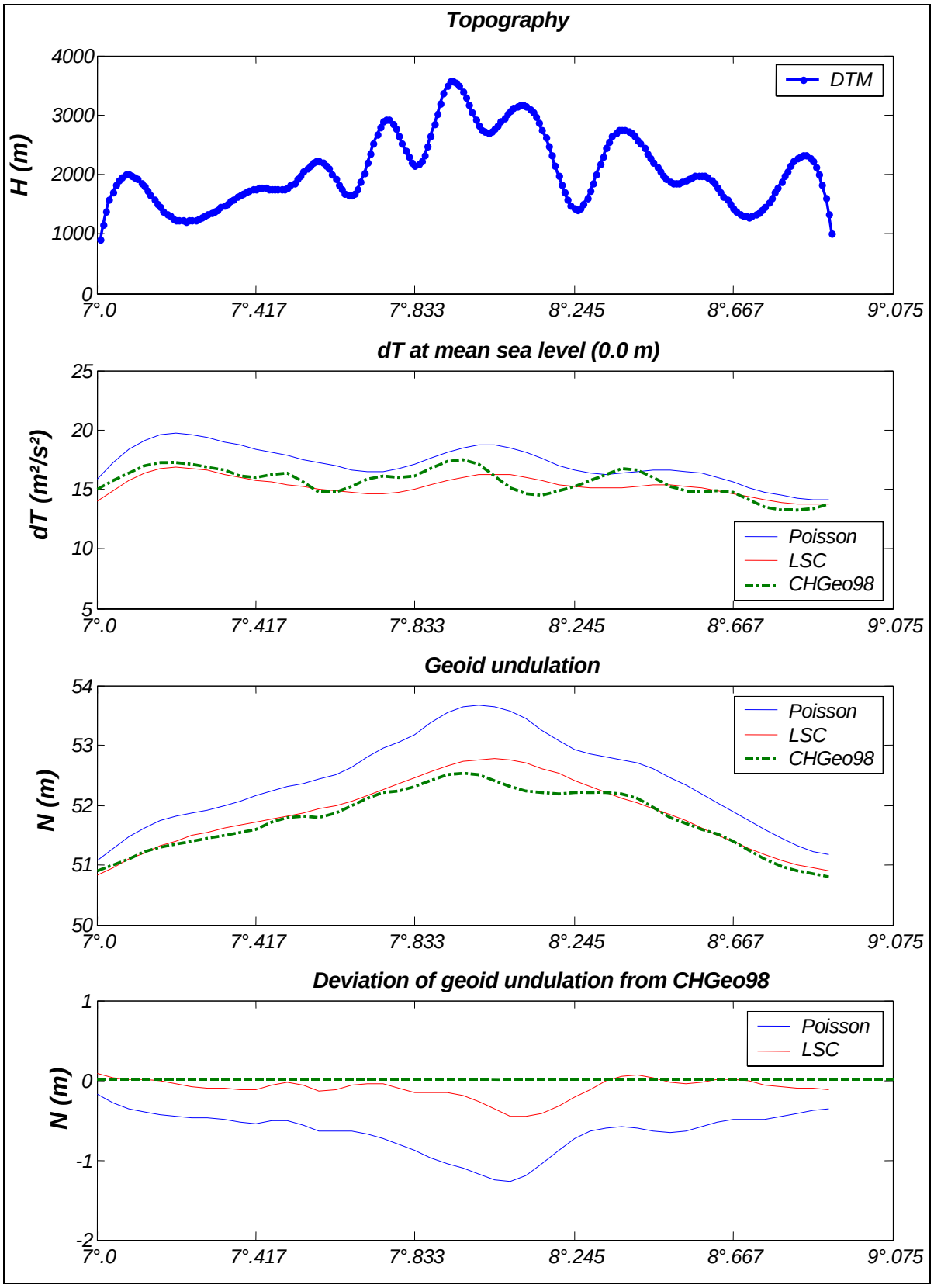


*Profile in latitude 46°.50*

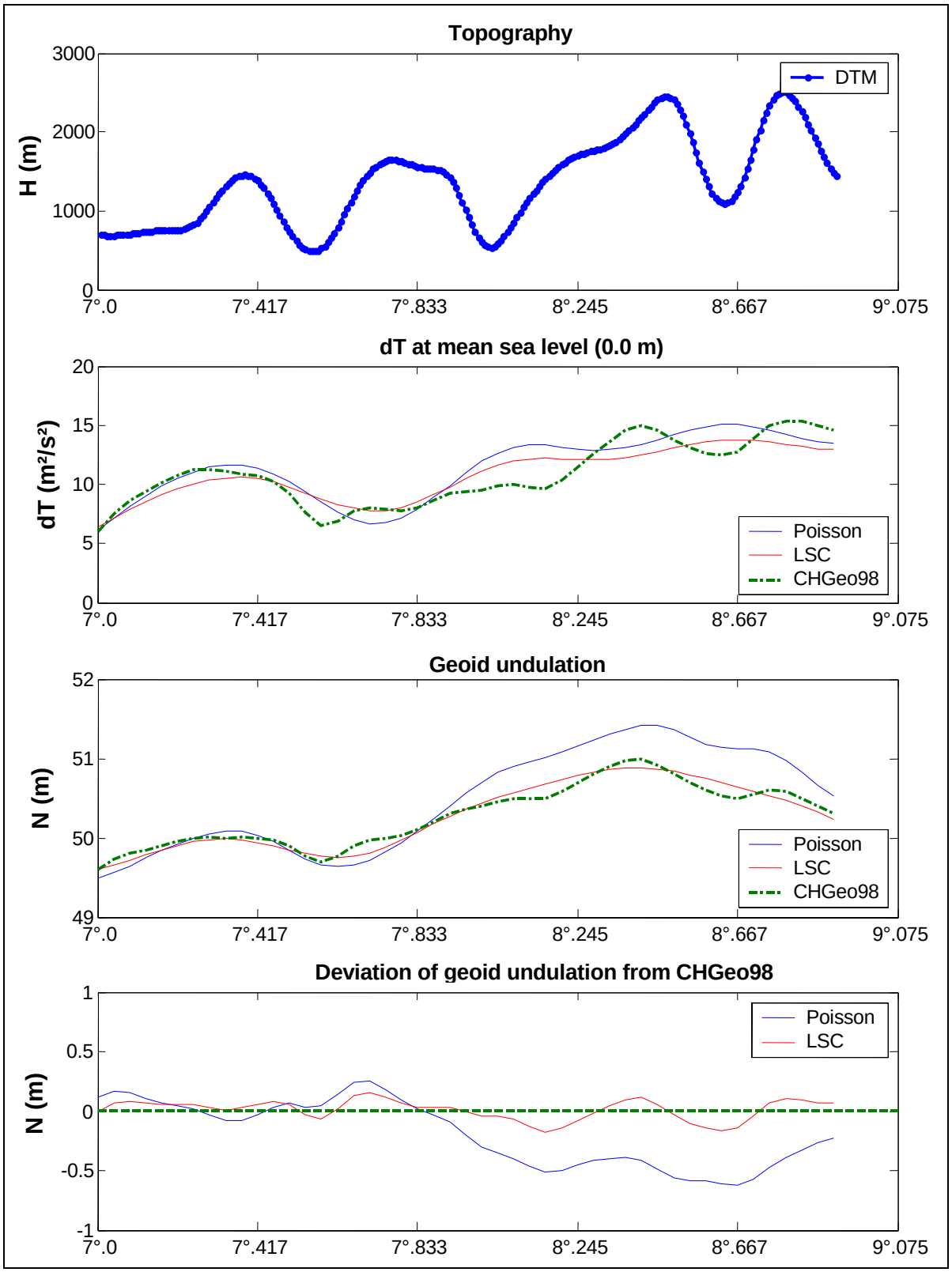


*Profile in latitude 46°.75*

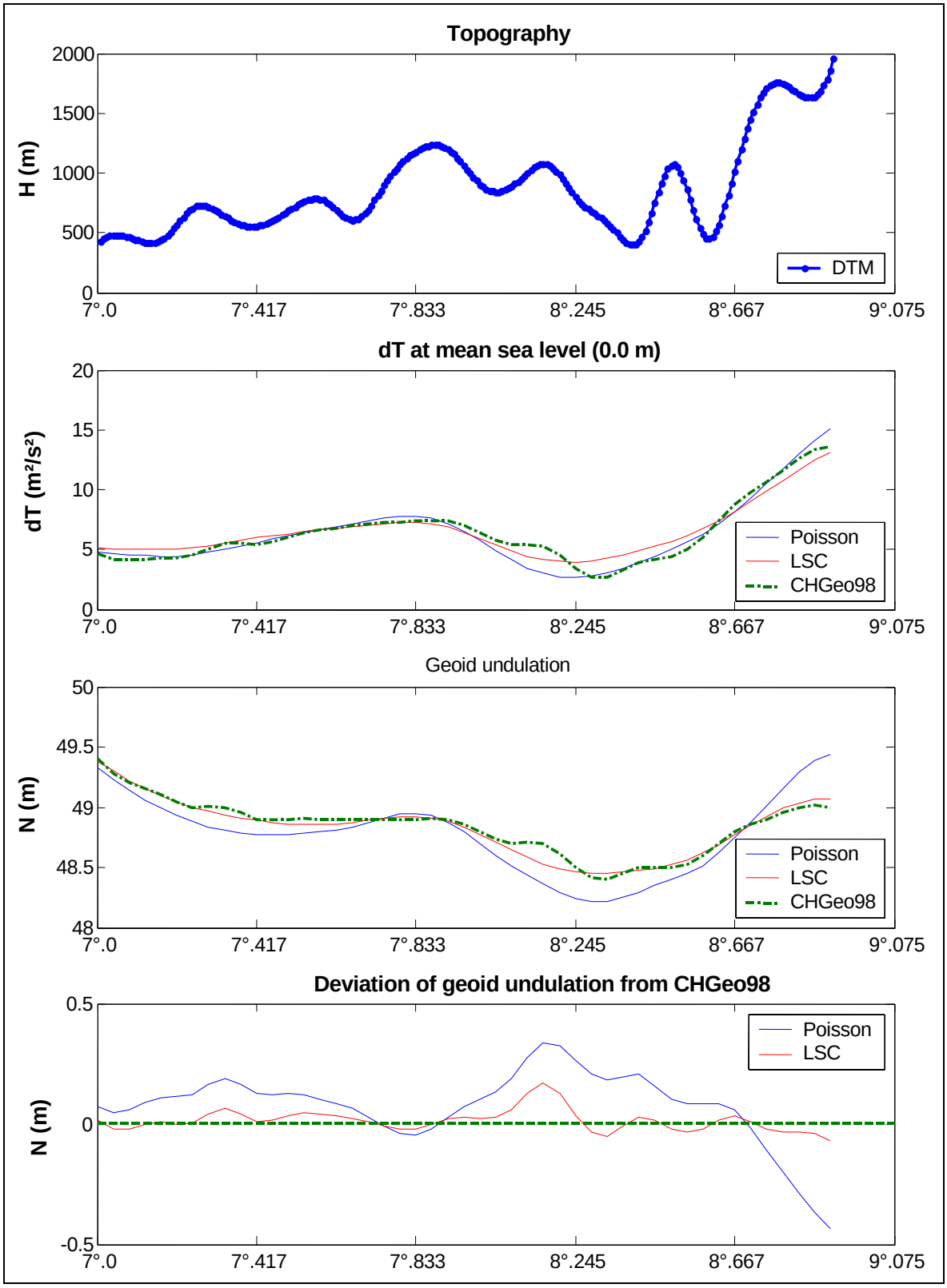


*Profile in latitude 47°.00*

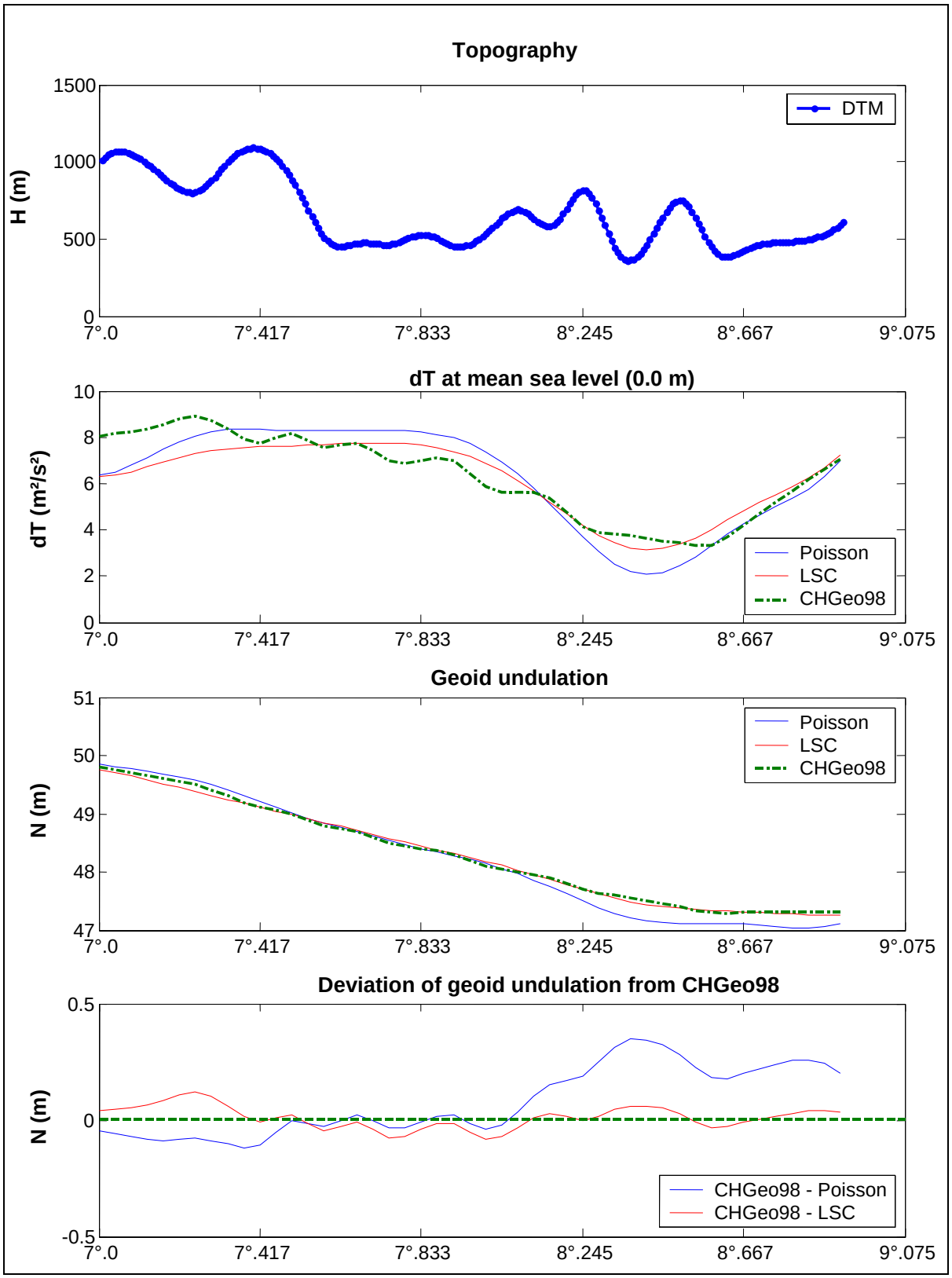


*Profile in latitude 47°.25*

*Ann. 2 Geoid undulation results after downward continuation of disturbing potential using Helmert's reduction technique for five selected profiles in constant latitudes*

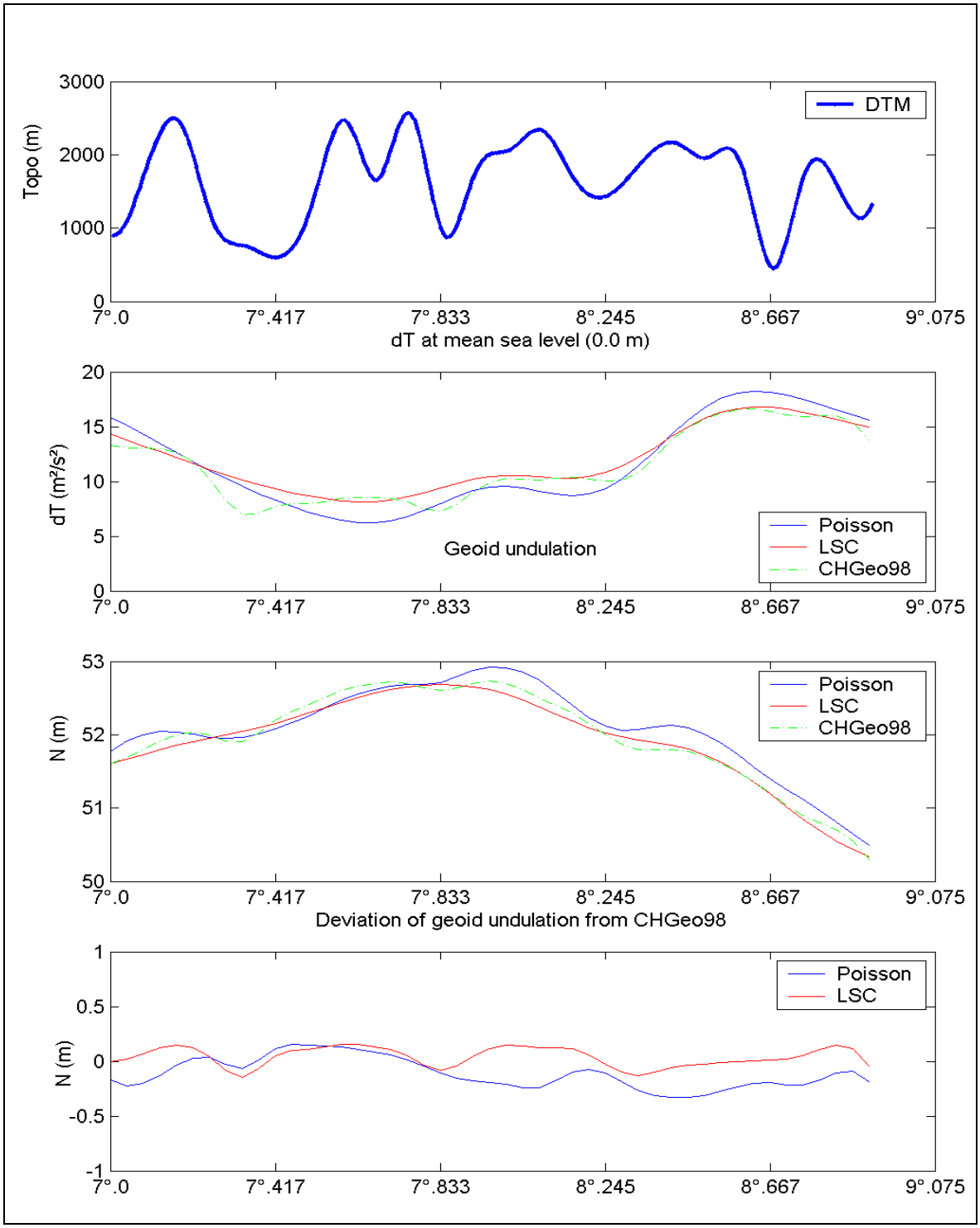


*Profile in latitude 46°.25*

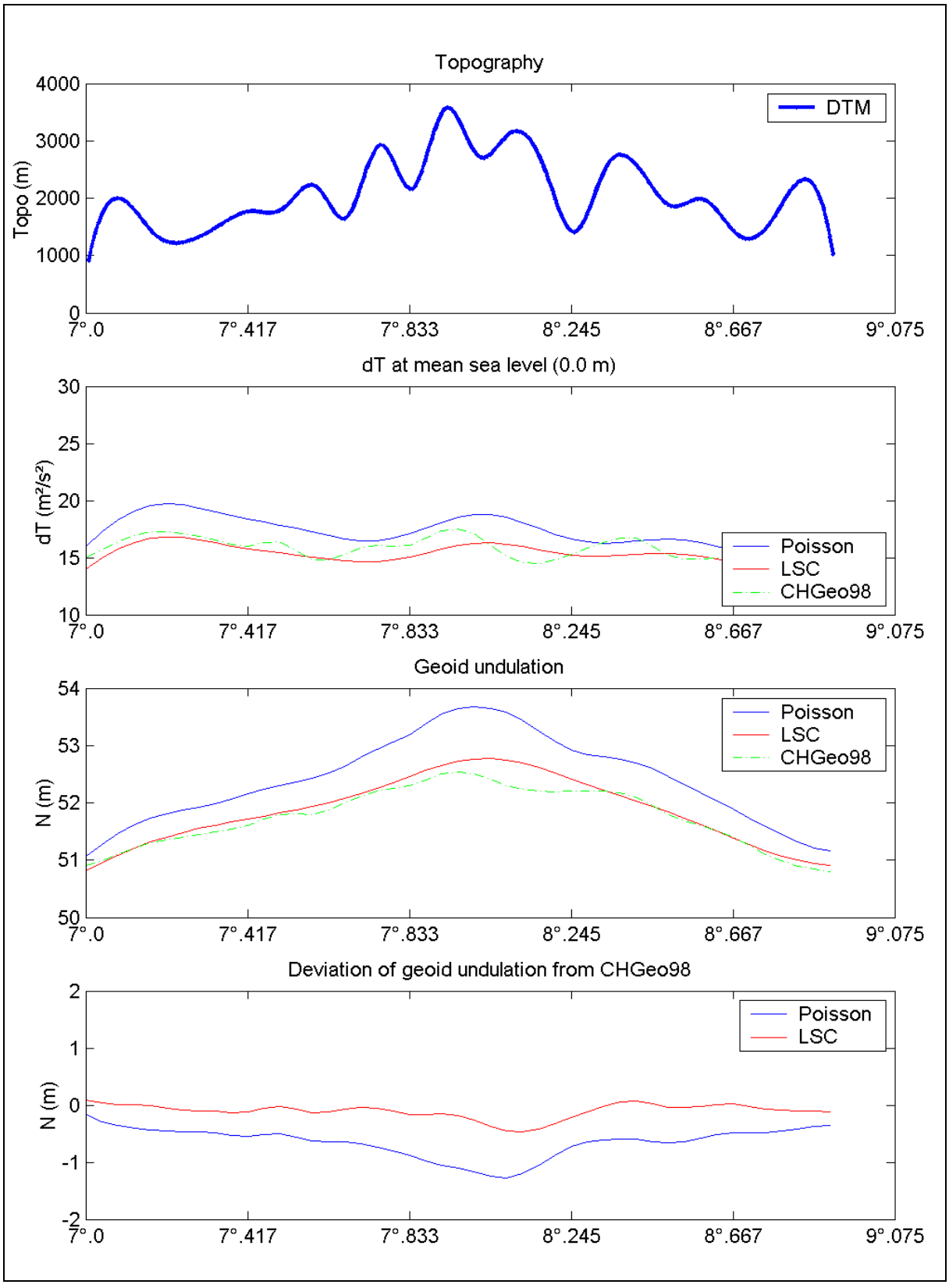


*Profile in latitude 46°.50*

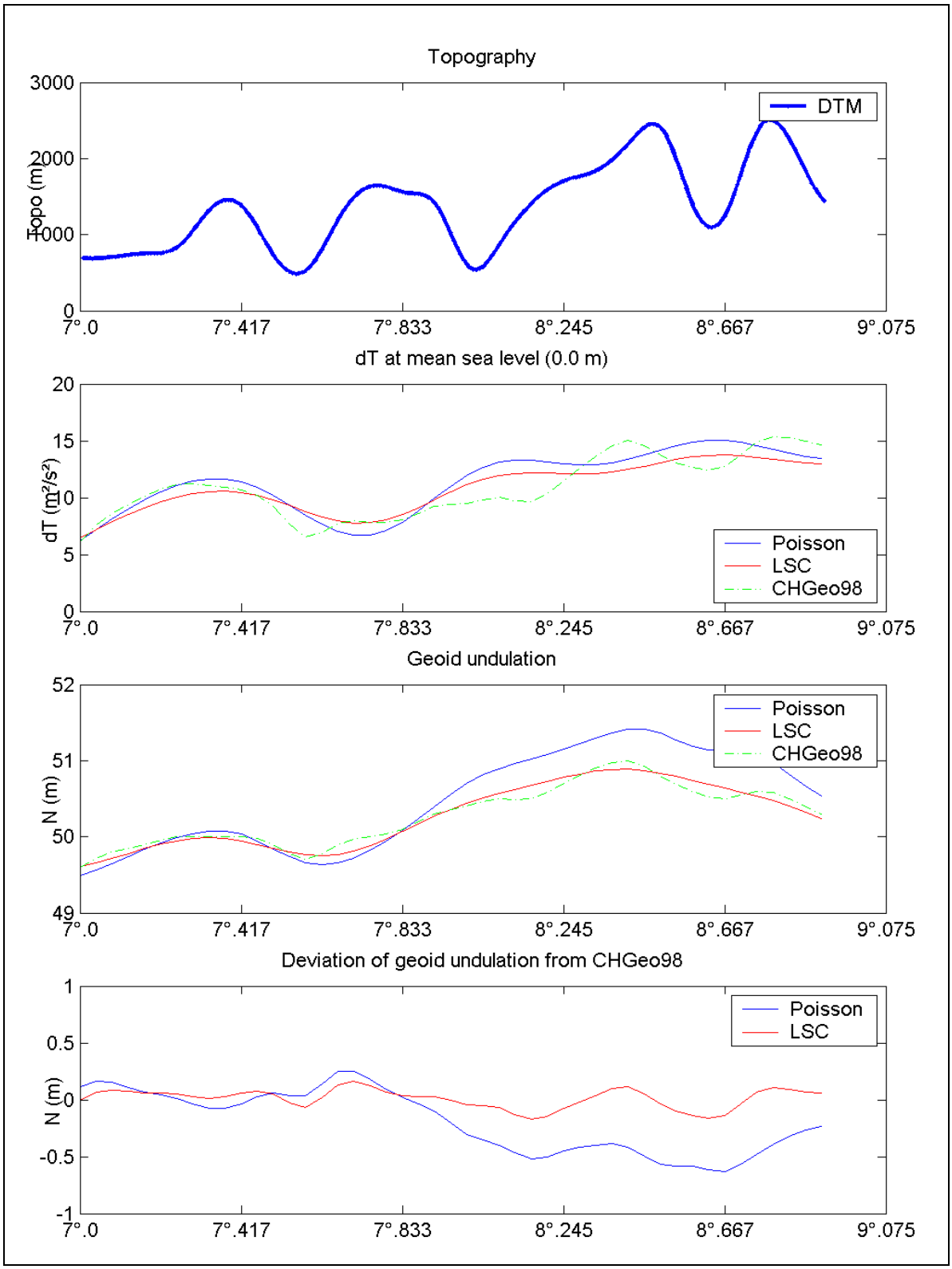


*Profile in latitude 46°.75*

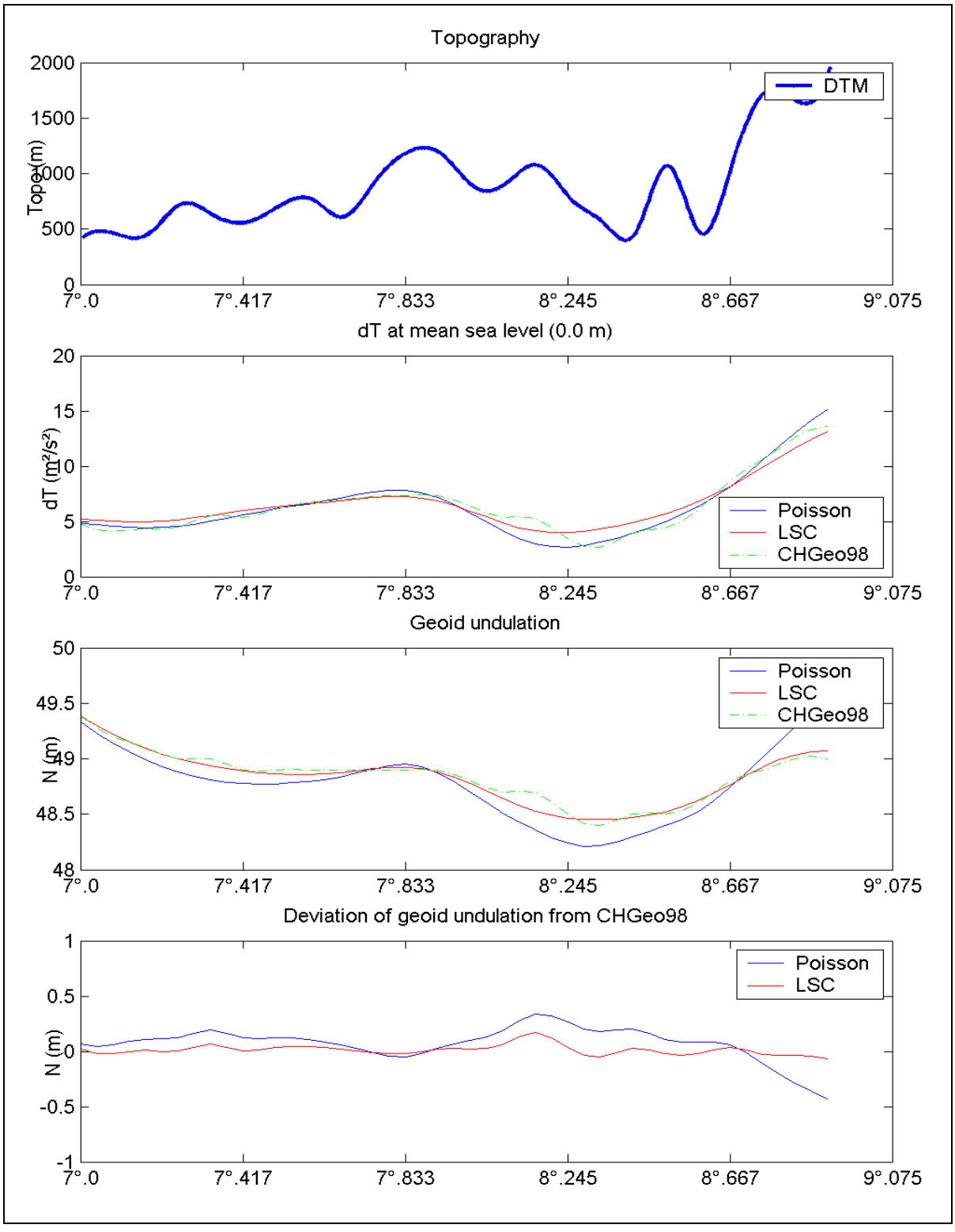


*Profile in latitude 47°.00*

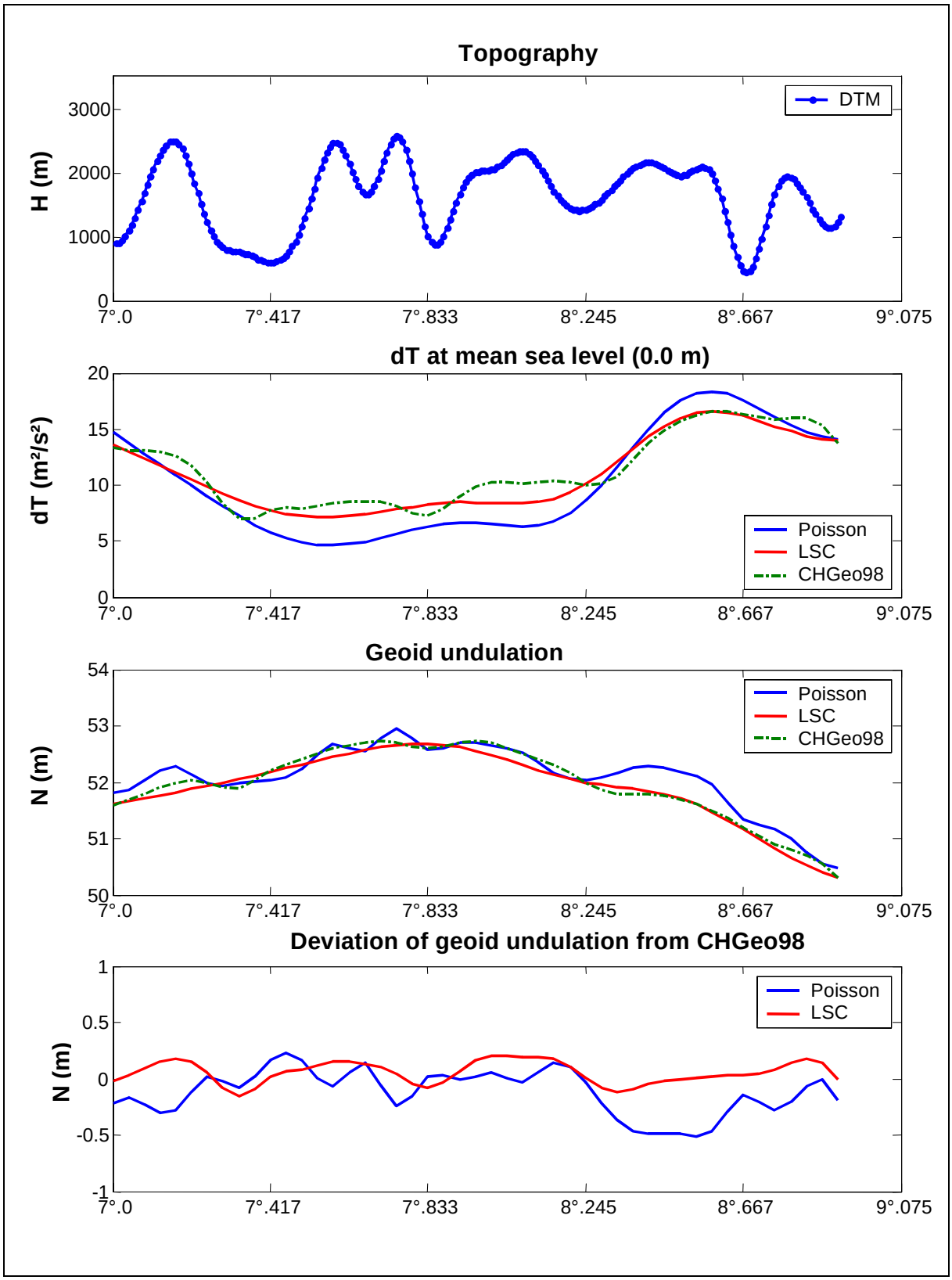


*Profile in latitude 47°.25*

# Curriculum Vitae

**Personal data**

| | |
|---|---|
| Surname: | Ameti |
| First Name: | Perparim |
| Place of Birth: | Smira, Kosova |
| Date of Birth: | February 16th, 1973 |

**Education**

| | |
|---|---|
| 1979 – 1987 | Primary school, Smira, Kosova |
| 1987 – 1991 | High geodetic school, Gjakova, Kosova |
| 1991 – 1997 | Study of Geodesy, University of Zagreb, Croatia |
| 1999 – 2000 | Study of Geoinformatics, Mainz University of Applied Sciences, Mainz |

**Research**

| | |
|---|---|
| 2000 – 2004 | Doktorand at GeoForschungsZentrum Potsdam |
| Since 2004 | Doktorand at Institute of Physical Geodesy, TU Darmstadt |